AN ABSTRACT OF THE THESIS OF

Tara Lin Couch for the degree of Doctor of Philosophy in Chemistry presented on September 13, 1996. Title: The Photodebromination of Polybromobenzenes.

Abstract approved: Redacted for Privacy

Peter K. Freeman

The photodebromination of a series of polybromobenzenes has been studied at 254 nm to determine the complete mechanistic description of the photolytic removal of bromine substituents. Photolyses of bromobenzene (**BB**), 1,2,4-tribromobenzene (**124TrBB**), and 1,2,3,5-tetrabromobenzene (**1235TBB**) were carried out directly and with the presence of triethylamine and sodium borohydride as electron donors. Irradiations lead to clean reactions that result in only the aryl debrominated products. Direct photolysis Stern-Volmer plots of the inverse product quantum yield against the inverse concentration of **BB**, **124TrBB**, and **1235TBB** are linear demonstrating that excimers are the product determining intermediates. Triplet quenching studies with oxygen, fumaronitrile, and isoprene were used to determine that the excimers were of singlet origin. The existence of the singlet excimers was further confirmed by fluorescence quenching. When the electron donors are present, an exciplex may take over or compete with the excimer as the product determining intermediate. Studies on **BB** and **124TrBB** in the presence of both triethylamine and sodium borohydride demonstrate that sole singlet exciplexes are responsible for the photodebromination.

However, photolysis of **1235TBB** proceeds through both a singlet excimer and a singlet exciplex when triethylamine or sodium borohydride are present, depending on the relative concentration of **1235TBB** to the electron donor.

To investigate the nature of the product determining intermediates, lithium 4-4'-di-*tert*-butylbiphenyl was used to chemically reduce **124TrBB** by way of a well established electron transfer reaction. The reduction produces a charge separated aryl bromide radical anion. Regiochemical comparisons of the reduction with donor assisted photodebrominations suggest that the exciplex does produce this completely charge separated species. Negative chemical ionization mass spectrometry (NCIMS) was used to determine that the free aryl bromide radical anion then fragments to produce an aryl radical and bromide ion.

Computational methods were employed to ascertain why singlet reactivity is so prevalent in polybromobenzenes which would normally be assumed to undergo triplet reactivity because of the heavy atom effect. Gaussian RCIS/6-31G* calculations predict that a lack of symmetry conservation in the intersystem crossing transition prevents formation of the triplet state.

The Photodebromination of Polybromobenzenes

by

Tara Lin Couch

A THESIS

submitted to

Oregon State University

in partial fulfillment of
the requirements for the
degree of

Doctor of Philosophy

Completed September 13, 1996
Commencement June 1997

Doctor of Philosophy thesis of Tara Lin Couch presented on September 13, 1996

APPROVED:

Redacted for Privacy

Major Professor, representing Chemistry

Redacted for Privacy

Chair of Department of Chemistry

Redacted for Privacy

Dean of Graduate School

I understand that my thesis will become part of the permanent collection of Oregon State University libraries. My signature below authorizes release of my thesis to any reader upon request.

Redacted for Privacy

Tara Lin Couch, Author

ACKNOWLEDGEMENTS

I wish to thank my major professor, Dr. Peter K. Freeman, for providing me with such a diverse, interesting, and constantly surprising research topic. His friendly advice and guidance are also greatly appreciated. I must also thank Dr. Gerald J. Gleicher for his many ideas and suggestions my first three years as a graduate student. Special thanks to Dr. Max L. Deinzer for his insightful discussions pertaining to mass spectrometry. Synthetic advice from Dr. Scott Truksa is greatfully acknowledged and support from my labmates, Dr. Christian Haugen, Sharon Maley, Jim Pugh, and Jelena Dacres is appreciated.

Finally, I thank my wonderful husband, Shiloh, for his unwavering faith and support in me throughout my graduate career.

Funding for the work in this thesis was provided by the National Institute of Environmental Health Sciences and the N. L. Tartar Research Foundation.

CONTRIBUTION OF AUTHORS

Dr. Peter K. Freeman was involved in project ideas, interpretation of results, and the writing of this thesis. All negative chemical ionization mass spectrometry studies were performed in the laboratory of Dr. Max L. Deinzer.

TABLE OF CONTENTS

TABLE OF CONTENTS (Continued)

TABLE OF CONTENTS (Continued)

LIST OF FIGURES

LIST OF FIGURES (Continued)

LIST OF FIGURES (Continued)

LIST OF TABLES

LIST OF APPENDICES

LIST OF SCHEMES

This thesis is dedicated to my loving parents, Larry and Karen Kasheimer

The Photodebromination of Polybromobenzenes

Chapter 1

Introduction

Importance and Application of Study

The chemistry, and particularly the photochemistry, of halogenated aromatic compounds is currently a topic of great interest. These compounds are widely used for a variety of agricultural and industrial purposes and are environmentally significant due to their toxicity and persistence.[1,2,3] The nature of this persistence is primarily due to the halogen presence. Microorganisms, which can otherwise degrade organic compounds, are prevented from doing so because the large halogens sterically hinder their access.[4] Thus, once ingested, polyhaloaromatic compounds simply accumulate within the microorganism due to their solubility in fats. These microorganisms are then digested by larger organisms which are in turn eaten by small animals. In this manner, toxic halogenated aromatic compounds reach their highest concentrations at the top of the food chain. The entire process is known as biomagnification[5] and explains why the presence of halogenated aromatic compounds in the environment is a concern to human health.

The most common disposal technique for these compounds is high temperature incineration. However, incineration leads to unwanted polymerization and direct release into the environment.[6,7] The aromatic skeleton and occupied p orbitals of the halogen in polyhaloaromatics serve as an active chromophore which absorbs electromagnetic radiation just within the visible region of the spectrum. Although the absorption is not

high ($\epsilon_\lambda < 10^3$ $M^{-1}cm^{-1}$), it is sufficient to cause excitation upon exposure to the sun. This feature establishes the possibility of photodegradation as an alternative method of waste disposal which would use the sun's abundant energy as a resource. Prior to any practical application, a complete understanding of the photodegradation mechanism must be obtained. This research is dedicated to developing this knowledge by investigating a series of brominated benzenes as model compounds. Initially, 1,2,4-tribromobenzene was chosen for its regiochemical potential and commercial availability, the study was then expanded to include 1,2,3,5-tetrabromobenzene also with regiochemical potential but which was synthesized, and finally bromobenzene was added for its application as a standard polybromobenzene.

Process of Light Absorption

Upon irradiation the aryl bromide, **ArBr**, absorbs a photon and is promoted to an excited state. It may dissipate this extra energy through several types of deactivation processes, depicted in a Jablonski diagram, Figure 1.1. Depending on the energy of the light absorbed, the molecule is promoted into a particular vibrational level of the singlet excited state, S_n (where n = 1,2,3, ...). From here it may undergo internal conversion, IC, to another singlet state of same multiplicity but lower energy. This non-radiative process occurs when there is an overlap in the potential energy curves, or wells, of the two electronic states and for organic compounds generally has a rate of 10^{12} s^{-1}.[8] Radiative deactivation from the singlet is referred to as fluorescence. Typical fluorescence rates range from 10^6 to 10^{10} s^{-1} for organic compounds. The fluorescence quantum yield, Φ_f, is

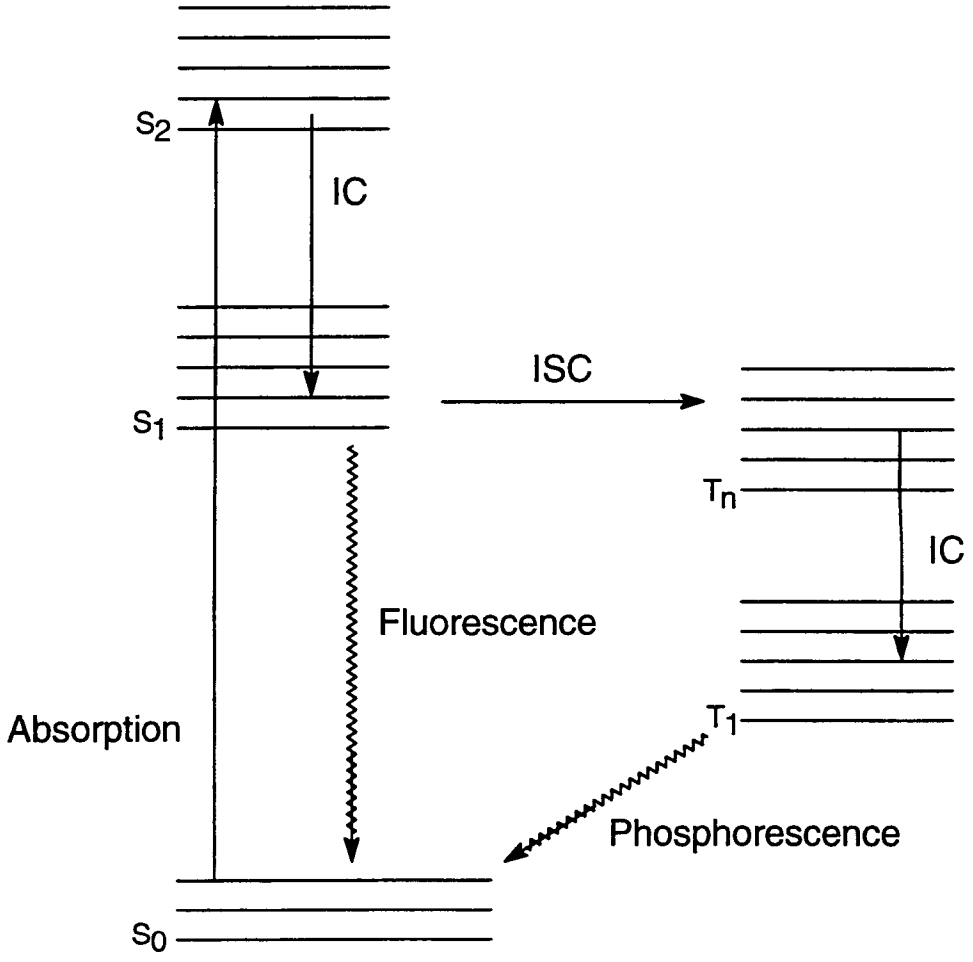

Figure 1.1. Jablonski diagram depicting the process of light absorption.

often used to describe the efficiency of this radiative decay. It is defined by equation 1.1 and varies between 0 and 1, depending on the rates of fluorescence, internal conversion, and intersystem crossing, k_f, k_{ic}, k_{isc}, respectively, assuming no bimolecular reactions take place.

$$\Phi_f = \frac{k_f}{k_f + k_{ic} + k_{isc}} \qquad \textbf{(1.1)}$$

Intersystem crossing, ISC, is another form of non-radiative decay. However, ISC involves a crossover between electronic states of differing multiplicity which results in a triplet excited state, T_n (where n = 1,2,3, ...). The S → T transition requires a change in spin orientation that originates from two unpaired electrons of opposite spin (electron spin quantum numbers, m_s = ½ and -½) in the singlet state, (↑) and (↓), and results in two unpaired electrons of the same spin, (↑) and (↑), in the triplet state. Non-radiative decay from the triplet may also occur via IC. Phosphorescence is the radiative deactivation from the triplet. Its quantum yield, Φ_p, given in equation 1.2 ranges from 0 to 1 and is dependent on the efficiency of intersystem crossing, ϕ_{isc}, expressed as the first term of the equation, as well as the rates of phosphorescence and triplet internal conversion,

$$\Phi_p = \left(\frac{k_{isc}}{k_f + k_{ic} + k_{isc}}\right)\left(\frac{k_p}{k_p + k_{tic}}\right) \qquad \textbf{(1.2)}$$

k_p and k_{tic}, respectively, assuming no bimolecular reactions.

Strictly speaking the ISC process is spin forbidden. The reason it occurs at all is because of spin orbit coupling, SOC. SOC is the coupling interaction between the magnetic moment of a spinning electron and the orbital magnetic field of a charged electron.[9] The extent of coupling is determined by several factors[10] including, the energy gap between the singlet and triplet state, the wavefunctions of those states, and the Hamiltonian operator, H_{SO}, which all will be discussed in greater detail in Chapter 4 of this thesis. The Hamiltonian is dependent on the spin-orbital coupling constant, ξ, and dot product of the orbital angular momentum and spin angular momentum operators, L and S, respectively.[11] Since ξ is proportional to Z^4, where Z is atomic number, H_{SO} is also dependent on Z^4. Therefore, the presence of heavy atoms strongly enhances SOC, ISC, and consequently increases triplet reactivity. This phenomena is known as the heavy atom effect and may arise from the presence of heavy atoms within the molecule of interest; the internal heavy atom effect, or from heavy atoms present in the solvent or other additives; the external heavy atom effect. Polyhaloaromatic compounds normally exhibit very high triplet reactivity because of the existence of the numerous internal heavy atoms.

Besides undergoing radiative and non-radiative deactivation upon excitation, excess energy can be dissipated by quenching and bond cleavage. Quenching occurs when the photoexcited state is deactivated by transferring its energy to another molecule.[12] If this is to effectively take place, the quencher must be present in significant concentrations, but not so high as to absorb the majority of the radiation, and spin must be conserved in the quenching process. For example, quenching of a triplet substrate with a

singlet state quencher will demote the triplet substrate to the ground state, S_0, and promote the quencher to a T_1 excited state. Because of this, the T_1 state of the quencher must be of lower energy than the triplet state of the substrate. The weakest bond in a polybromoaromatic compound is the aromatic C-Br bond which has a bond dissociation energy of 80-81 kcal/mol.[13,14] Direct homolytic cleavage of the C-Br bond is therefore possible from the lowest vibrational level of the singlet state, S_1, and the lowest vibrational level of the triplet state, T_1. This possibility is examined in Chapter 2 where the energetic and physical properties of bromobenzene, 1,2,4-tribromobenzene, and 1,2,3,5-tetrabromobenzene are measured.

Photolytic removal of the bromine substituents may also be possible through a reactive intermediate. Upon direct photolysis, an excimer can aid in photodebromination, and if a sufficient electron donor is employed an exciplex can also contribute. As with the quencher, the donor must possess an energy level lower than that of the aryl bromide excited species and must not absorb a significant amount of incident radiation. Exciplex formation also depends on redox potentials and coulombic forces. Both intermediates are derived from an excited state of the aryl bromide. An excimer is an "excited dimer" formed between an excited state aryl bromide and a ground state aryl bromide. The exciplex is an "excited complex" resulting from an excited state aryl bromide and a ground state electron donor. Although the exciplex forms a complete charge separation, the extent of charge distribution within an excimer is not well understood and varies depending on the substrate.

A complete picture of all possible deactivation pathways for the photolysis of an aryl bromide is given in Scheme 1.1. Designations for singlet and triplet excited states are **ArBr**^{*1} and **ArBr**^{*3}, respectively, radiative decays are illustrated by wavy lines, and reactive intermediates are shown in italic. The scheme illustrates that there are six competing processes from each excited state, but that debrominated products are only formed from half of these. The latter can be monitored by the product quantum yield, $\Phi_{products}$, which is a measure of photon usage defined as the moles of products formed over the intensity of the absorbed incident radiation, I^0. A chemical actinometer is used to measure I^0 by employing a photochemical reaction which has a well established quantum yield and is easily reproducible.[15] By running this reaction simultaneously and determining its product formation, I^0 can be calculated from equation 1.3, where n_B is the moles of actinometer products, Φ_B is the actinometer quantum yield, t is the irradiation time, and the term in parentheses is the fraction of light absorbed.

$$I^0 = \frac{n_B}{\Phi_B t(1 - 10^{-A})} \qquad \textbf{(1.3)}$$

In order to limit variation in the intensity, the fraction of light absorbed is kept as close to 100%, as possible. This is accomplished by ensuring that both the actinometer and photolysis samples have an absorbance, $A \geq 2$ at the wavelength of excitation. Experiments in this thesis have been constructed to determine which of the Scheme 1.1 pathways are important and why, and reaction rates have been calculated whenever possible for each polybromobenzene.

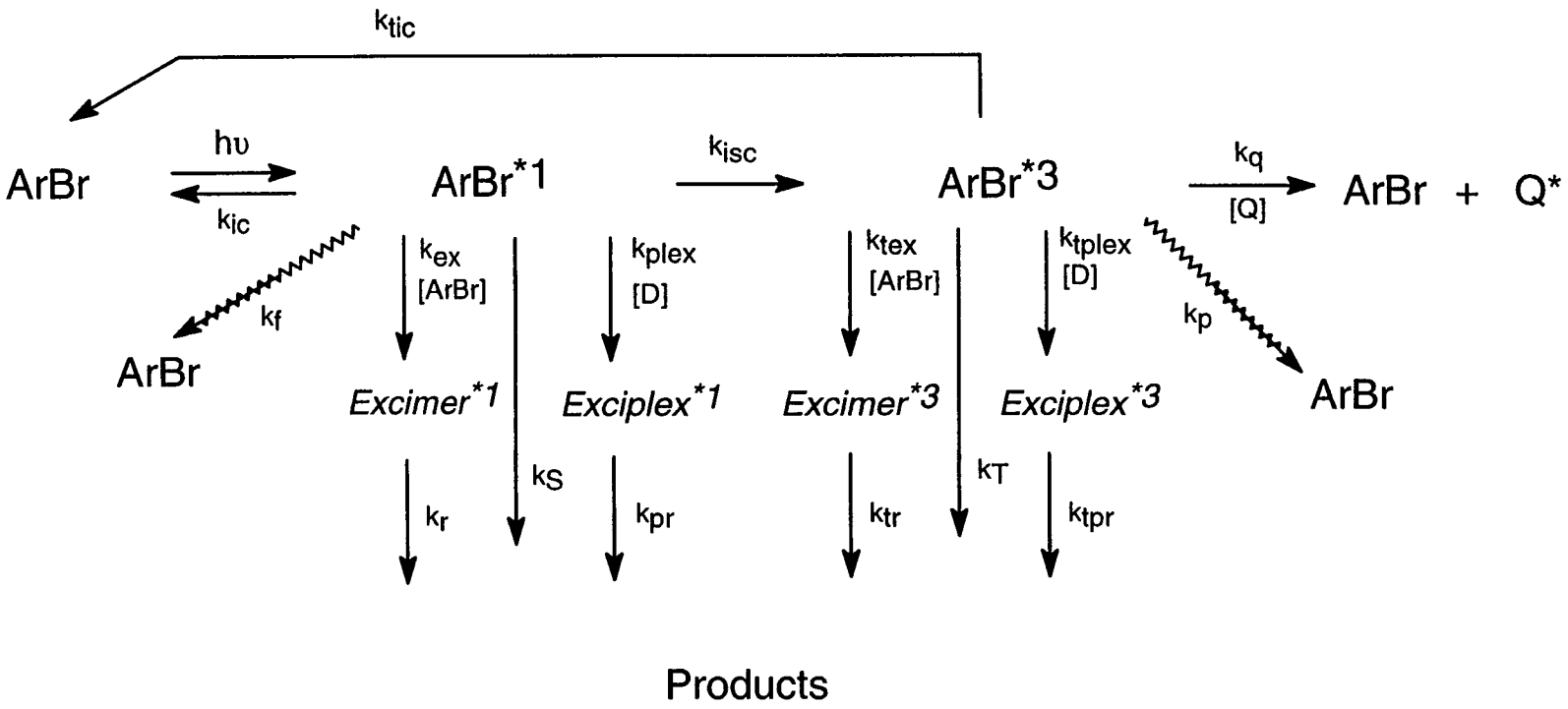

Scheme 1.1. Polybromobenzene deactivation pathways upon photolysis.

Reactive Intermediates

The type of reactive intermediate, either excimer or exciplex, is determined by careful kinetic analyses of the appropriate corresponding mechanistic photodebromination schemes. An excimer intermediate may be formed and interpreted by direct degassed photolyses on each polybromobenzene with various concentrations of **ArBr**. The kinetic analysis of this mechanism predicts a non-linear Stern-Volmer plot of the inverse product quantum yield, $1/\Phi_{products}$, against the inverse polybromobenzene concentration, 1/[**ArBr**], if all product forming pathways compete. However, participation of an excimer intermediate is confirmed if $1/\Phi_{products}$ is a function of [**ArBr**]. Mathematical derivations of the entire kinetic process and its implications to the contributing photodebromination pathways are discussed in detail in Chapter 2 of this thesis. To test for an exciplex, the photolysis is performed with constant **ArBr** concentration, but varying donor concentrations, [D]. This kinetic analysis is much more complicated since competition between excimer and exciplex intermediates may also exist. A Stern-Volmer plot of $1/\Phi_{products}$ vs. 1/ [D] is again non-linear if more than one of the product forming deactivation pathways is in progress. If one of these competing pathways is indeed an exciplex, $1/\Phi_{products}$ will be a function of the donor concentration. Chapter 3 deals with this kinetic analysis.

Quenching studies are needed to determine the excited state multiplicity of the reactive intermediates. Stern-Volmer plots only predict their presence. As illustrated in Scheme 1.1, the addition of a triplet quencher provides the triplet state with an alternative non-product forming pathway. Oxygen is an extremely effective triplet quencher, which

at sufficient concentrations will quench out all other triplet deactivation pathways.[16] The involvement of a triplet species can therefore be determined by comparing degassed and aerated photodebromination reactions. Aerated photolysis products can only originate from singlet species and a substantial decrease in the product quantum yield will be observed if a triplet species had been responsible for products under degassed conditions. A quantitative measure of the extent of triplet reactivity can be made by accurately varying the concentration of a chemical triplet quencher. If the reaction proceeds through a triplet species alone, equation 1.4 is predicted from a kinetic analysis of the reaction scheme. In the expression, $\Phi_{products}$ and $\Phi^0_{products}$ represent the product quantum yields with and without quencher, respectively, k_q is the rate constant of triplet quenching, and τ_p is the lifetime of the aryl bromide triplet.

$$\frac{\Phi^0_{products}}{\Phi_{products}} = 1 + \tau_p k_q [Q] \qquad \textbf{(1.4)}$$

A plot of the product quantum yield ratio, $\Phi^0_{products} / \Phi_{products}$, against the concentration of quencher, [Q], will be linear, according to the equation, if there is complete triplet reactivity. However, if there is also participation from a singlet species the resulting plot will be nonlinear. Sole singlet derived product formation can be concluded from a flat horizontal line, where $\Phi^0_{products} / \Phi_{products} = 1$.

Radiative quenching is a technique that can be used to identify both an excimer and an exciplex intermediate and their corresponding reactive states. The luminescence of a molecule is monitored by viewing the emission at a 90° angle from that of the

incident light. By definition, the lifetime of this emission is inversely proportional to its rate as shown in equation 1.5, where τ^0_f and τ^0_p are radiative lifetimes of fluorescence

$$\tau_f^0 = \frac{1}{k_f} \qquad \tau_p^0 = \frac{1}{k_p} \qquad \textbf{(1.5)}$$

and phosphorescence, respectively. The large difference between the rates is exploited in order to distinguish fluorescence from phosphorescence.[17] The latter is separated by imposing a delay after the initial flash of the excitation beam. Furthermore, upon initiation of the phosphorescence measurement the dark current is measured. This value is stored and then subtracted from the signal to correct for any lingering fluorescence. To measure fluorescence, the signal is collected immediately following the excitation pulse for a set length of time. The dark current signal is taken after this and subtracted off the original signal, this time to correct for any residual phosphorescence. A decrease in the luminescence signal with increasing concentrations of **ArBr** is evidence of self quenching, or in other words excimer formation. At increased concentrations there is a greater probability of excited state **ArBr** reacting with the ground state to form an excimer. When this happens, the efficiency of fluorescence is necessarily decreased since it is in direct competition with the excimer process. Fluorescence self quenching is a result of singlet state excimer formation and phosphorescence self quenching corresponds to triplet state excimer formation. Increasing concentrations of an electron donor have the same effect if an exciplex intermediate is formed.

The choice of solvent plays a key role in establishing the unique nature of the transition state and reactive intermediate.[18] Solvent reorganization corresponds to the

orientational changes of solvent molecules that surround reactants during the course of a reaction. Linear solvation energy parameters[19] have been used by Freeman et al.[20] in prior excimer intermediate studies to predict the importance of particular solvent properties. It was found that the solvent cohesive energy density and solvent nucleophilic assistance were significant factors with the former being of greatest importance for 4-bromobiphenyl excimer formation. Polar, aprotic solvents are known to enhance nucleophilic assistance. Polar solvents promote the solubility of ionic compounds and aprotic solvents prevent solvation by H-bonding. Acetonitrile is a polar aprotic solvent which had the largest cohesive energy density among the organic solvents investigated by Freeman et al. Therefore, to enhance excimer and exciplex formation acetonitrile was used in the photodebromination reactions of bromobenzene, 1,2,4-tribromobenzene, and 1,2,3,5-tetrabromobenzene discussed in this thesis.

The characteristic charge separation within the exciplex intermediate is expected to result in an unemcumbered radical anion. Given this scenario, a specific regiochemical outcome will be observed for the photodebromination of the polybromobenzenes with an electron donor present. Non-photochemical generation of a radical anion has been developed by Freeman and Hutchinson[21] using 4-4'-di-*tert*-butylbiphenyl. A comparison of regiochemistry between the photodebromination and the chemical reduction of 1,2,4-tribromobenzene with this agent offers an informative tool for probing the environment of the radical anion within the exciplex. It is also used to investigate the characteristic nature of the excimer intermediate as well. A complete reversal of regiochemistry has been exhibited by pentachlorobenzene, 1,2,3,5-tetrachlorobenzene, and 1,4,6,7-

tetrachloronaphthalene when triethylamine, serving as the electron donor, is not present.[22,23] These excimers are therefore believed to be quite different from their exciplex counterparts which illustrate free aryl radical anion properties.

The electron transfer reaction of a donor assisted photodebromination is simulated in the gas phase by negative chemical ionization mass spectrometry, NCIMS, to determine the mode of C-Br bond fission. NCIMS is a soft ionization technique that leads to valuable structural and fragmentation information due to the low energy of the electrons used. The technique is very well suited for brominated benzene compounds because of their high electron affinity and ability to stabilize additional negative charge. The polybromobenzene captures an electron, with the aid of a buffer gas, in this case methane, and forms the aryl radical anion known as the parent. The parent then has two possible modes of bond fission, cleavage resulting in the formation of an aryl radical anion and a bromide ion, or cleavage which produces an aryl carbanion and a bromine atom. In NCIMS only negative ions are detected so polybromobenzene fragmentation produces only parent ion, carbanion, and bromide ion. Chapter 5 discusses the ramifications of the NCIMS results.

References

1. Buser, H. R. *Anal. Chem.*, **1986**, *58*, 2913-2919.

2. Watanabe, I.; Kashimoto, T.; Tatsukawa, R. *Bull. Environ. Contam. Toxicol.*, **1986**, *36*, 778-784.

3. Watanabe, I.; Tatsukawa, R. *Bull. Environ. Contam. Toxicol.*, **1987**, *39*, 953-959.

4. Freedman, B. *Environmental Ecology: The Impacts of Pollution and Other Stresses on Ecosystem Structure and Function*, **1989**, Academic Press, Inc., New York, NY, pp. 147-158.

5. Libes, S. M. *An Introduction to Marine Biogeochemistry*, **1992**, John Wiley & Sons, Inc., New York, NY, pp. 599.

6. Bieniek, D.; Bahadir, M.; Korte, F. *Heterocycles*, **1989**, *28*, 719-722.

7. Klusmeier, W.; Vogler, P.; Ohrbach, K.-H.; Weber, H.; Kettrup, A. *J. Anal. App. Pyrolysis*, **1988**, *13*, 277-285.

8. Ingle, J. D. Jr.; Crouch, S. R. *Spectrochemical Analysis*, **1988**, Prentice-Hall, Inc., Englewood Cliffs, NJ, pp. 339.

9. Barltrop, J. A.; Coyle, J. D. *Excited States in Organic Chemistry*, **1975**, John Wiley & Sons, Ltd., Great Britain, pp. 21.

10. Turro, N. J. *Modern Molecular Photochemistry*, **1978**, The Benjamin / Cummings Publishing Company, Inc., Menlo Park, CA, pp. 185.

11. Barltrop, J. A.; Coyle, J. D. *Excited States in Organic Chemistry*, **1975**, John Wiley & Sons, Ltd., Great Britain, pp. 21.

12. Carey, F. A.; Sundberg, R. J. *Advanced Organic Chemistry. Part A: Structure and Mechanisms*, 3rd Ed., **1990**, Plenum Press, New York, NY, pp. 732.

13. McMillen, D. F.; Golden, D. M. *Ann. Rev. Phys. Chem.*, **1982**, *33*, 493.

14. Benson, S. W. *Thermochemical Kinetics*, **1968**, Wiley, New York, NY, pp. 215.

15. Calvert, J. G.; Pitts, J. N. *Photochemistry*, **1966**, John Wiley & Sons, New York, NY, pp. 781.

16. Barltrop, J. A.; Coyle, J. D. *Excited States in Organic Chemistry*, **1975**, John Wiley & Sons, Ltd., Great Britain, pp. 101.

17. Perkin Elmer Model LS 50B Luminescence Spectrometer Owner's Manual, Chapter 8.

18. Kavarnos, G. J. *Fundamentals of Photoinduced Electron Transfer*, **1993**, VCH Publishers, Inc., New York, NY, pp. 314.

19. Abraham, M. H.; Doherty, R. U.; Kamlet, M. J.; Harris, J. M.; Taft, R. W. *Ibid.*, **1987**, 1097-1101, 913-920.

20. Freeman, P. K.; Jang, J.-S.; Ramnath, N. *J. Org. Chem.*, **1991**, *56*, 6072-6079.

21. Freeman, P. K.; Hutchinson, L. L. *J. Org. Chem.*, **1980**, *45*, 1924-1930.

22. Freeman, P. K.; Ramnath, N. *J. Org. Chem.*, **1991**, *56*, 3646-3651.

23. Freeman, P. K.; Clapp, G. E.; Stevenson, B. K. *Tetrahedron Letters*, **1991**, *32*, 5705-5708.

Chapter 2

Photodebromination of Polybromobenzenes

Tara Lin Couch and Peter K. Freeman*

Department of Chemistry
Oregon State University
Corvallis, OR 97331

Introduction

Polybrominated aromatic compounds are common, toxic, and persistent environmental pollutants which are commercially important due to their widespread use in fire retardants.[1] Disposal of products containing brominated aromatic compounds is usually accomplished by high-temperature incineration. However, incineration leads to their release into the environment.[2,3] Since many of the polybrominated compounds absorb in the sunlight range, photodegradation would be an excellent remediation alternative. A complete understanding of the mechanisms involved in the photodegradation process is therefore essential. In this study, a detailed mechanistic description of the photolytic removal of bromine substituents has been formulated from a series of simple polybrominated benzenes.

Results and Discussion

The photochemistry of polychloroarenes has been investigated extensively.[4,5,6,7] It has been concluded that the mechanism of photodechlorination proceeds primarily through a triplet excimer intermediate. This is in agreement with the heavy atom effect which states that the probability of a singlet to triplet transition, $S \rightarrow T$, is dependent on the nuclear charge to the fourth power (Z^4).[8] When heavy atoms are present, as in the case of polychloroarenes, this transition is significantly enhanced. It is reflected in a high intersystem crossing rate, and reaction from the triplet state is most likely. It was therefore expected that the photodebromination of polybromoarenes would be no different, and would also proceed through a triplet excimer intermediate. Indeed, this was

evident with 4-bromobiphenyl.[9] However, as will be shown, photodebromination of polybromobenzenes provide a surprise and instead proceed through a singlet excimer intermediate.

Degassed Photolysis:

Irradiation of degassed solutions of bromobenzene (**BB**), 1,2,4-tribromobenzene (**124TrBB**), and 1,2,3,5-tetrabromobenzene (**1235TBB**) at 254 nm in acetonitrile leads to the various corresponding debromination products, Figure 2.1. The observed product regiochemistry is consistent with steric strain relief tendencies. When bromine substituents are in an *ortho* orientation their large electron clouds are forced to overlap causing strong repulsive interactions. The magnitude of this strain has been calculated to be 2.391 kcal/mol by comparing ground state energies of HF/6-31G* geometry optimized structures of *ortho*-dibromobenzene and *para*-dibromobenzene. For this reason, the product pathway that removes the greatest amount of strain, or *ortho* interaction, is greatly favored. Thus photodebromination of **1235TBB** leads to predominantly 1,3,5-tribromobenzene (49.1%) where two such interactions are relieved, and 1,2,4-tribromobenzene (46.2%) which removes one *ortho* interaction. Similarly, **124TrBB** results in *para*-dibromobenzene (50.2%) and *meta*-dibromobenzene (49.8%) which both completely eliminate the original strain.

The photodebromination process of the polybromobenzenes (**ArBr**) is depicted in Scheme 2.1. Debromination products may be formed by direct homolytic cleavage from the excited states or fragmentation may be facilitated by reaction via an excimer

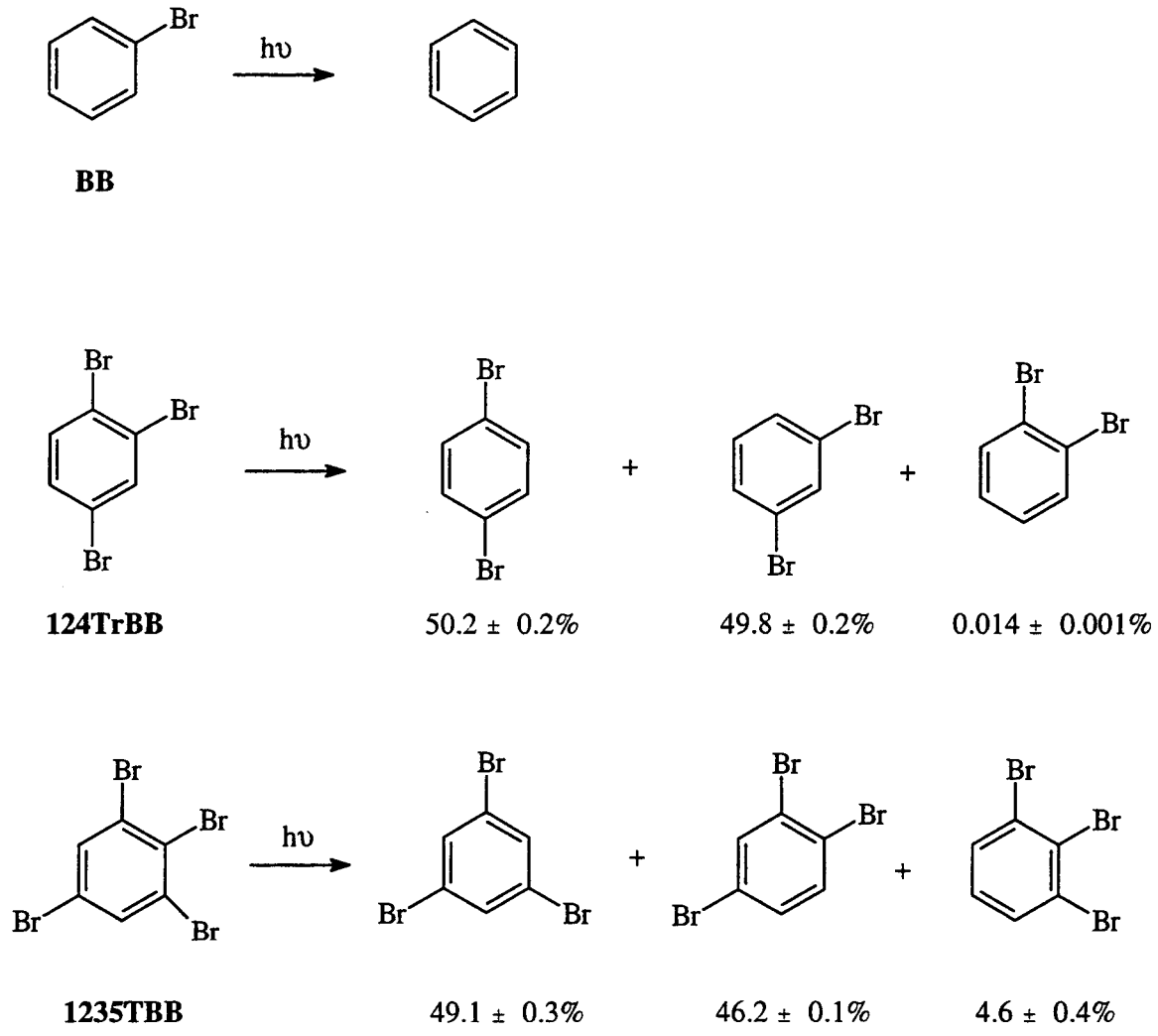

Figure 2.1. Products and regiochemical outcome of bromobenzene, 1,2,4-tribromobenzene, and 1,2,3,5-tetrabromobenzene photodebromination in acetonitrile at 254 nm.

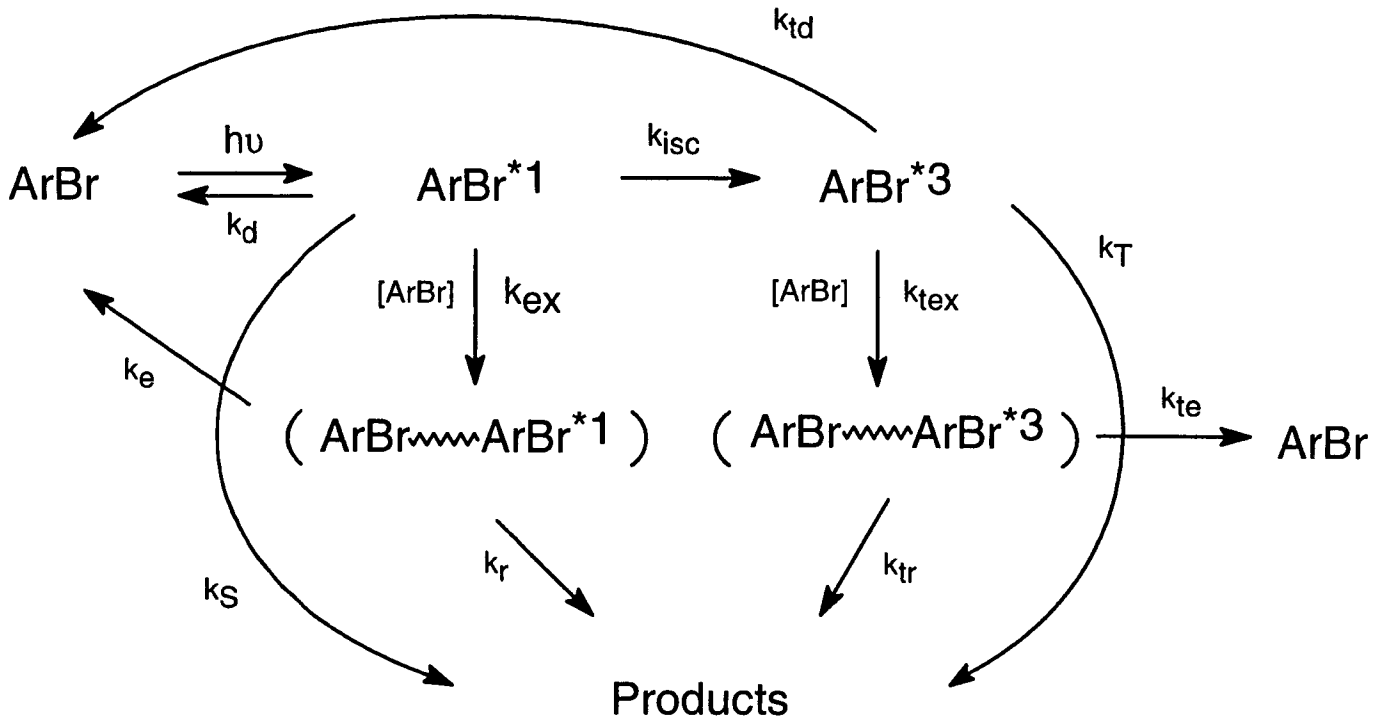

Scheme 2.1. Complete polybromobenzene photodebromination mechanism.

intermediate. The latter is an excited dimer composed of an excited state and ground state polybromobenzene. The excimer develops a partial charge separation and extends the moieties lifetime[10] allowing for the absorption of additional energy which aids in the debromination. A polar aprotic solvent, such as acetonitrile, enhances excimer formation by promoting the solubility of polar compounds.[11] These conditions allow the anion to more freely react, promoting its nucleophilicity.[12]

According to Scheme 2.1, the absorption of 254 nm light, 113 kcal/mol, promotes the polybromobenzenes to a singlet excited state, **ArBr**^{*1}. From here it may undergo singlet decay, k_d, which includes non-radiative internal conversion or radiative fluorescence. The excited singlet may also intersystem cross, k_{isc}, to the excited triplet state, **ArBr**^{*3}, where triplet decay, k_{td}, encompassing phosphorescence or non-radiative internal conversion can occur. As mentioned previously, direct homolytic cleavage from either excited state, k_S from the singlet or k_T from the triplet, would create debromination products. Also potentially resulting in products are the excimer intermediates, k_r and k_{tr}. The singlet excimer is formed, k_{ex}, from an excited singlet and a ground state **ArBr**. The dimer can deactivate, k_e, by falling apart and experiencing non-radiative decay and/or fluorescence or vice versa. Once formed, k_{tex}, the triplet state excimer may also deactivate in the same manner, k_{te}.

Direct homolytic cleavage of an aromatic C-Br bond requires 80-81 kcal/mol.[13,14] The lowest lying triplet states, E_T, of the polybromobenzenes listed in Table 2.1, do not have energy in excess of this, although in the case of bromobenzene it is quite close. However, the first excited singlet states, E_S[15], of **BB**, **124TrBB**, and **1235TBB** also listed

Table 2.1. Photophysical Properties of Polybromobenzenes.

Compound	E_T * (kcal/mol)	E_S [C] (kcal/mol)	τ_p^0 (ms)	τ_f^{0} [E] (ps)	Φ_p [C]	Φ_f [C]
BB 1.00×10^{-5} M	76[B], 80[C], 80[D]	102	0.119[C], 0.120[D]	53.2	0.10	0.96
124TrBB $\sim 3 \times 10^{-3}$ M [A] 1.05×10^{-6} M [B,C] 1.00×10^{-4} M [D]	74[A], 70[B], 72[C], 72[D]	92.3	0.30[A], 0.115[C], 0.117[D]	32.8	0.12	0.52
1235TBB $\sim 3 \times 10^{-3}$ M [A] 9.75×10^{-7} M [B,C] 1.10×10^{-4} M [D]	68[A], 72[B], 72[C], 72[D]	98.0	0.31[A], 0.114[C], 0.117[D]	15.3	0.05	0.94

[A] In EPA (5:5:2, Ether: Isopentane: Ethanol) at 77°K.
[B] In ethanol at 77°K.
[C] In ethanol at room temperature.
[D] In acetonitrile at room temperature.
[E] Approximated from absorbance spectra in ethanol. Turro, N. J. *Modern Molecular Photochemistry*, **1978**, The Benjamin / Cummings Publishing Co., Inc., Menlo Park, CA, pp. 86-91.
* Determined from 0-0 band of phosphorescence emission spectra under various conditions.

in Table 2.1 and determined from the intersection of absorbance and fluorescence emission spectra as mirror images, Figures 2.2, 2.3, and 2.4, respectively, do possess sufficient energy. For this reason, the possibility of direct homolytic cleavage from the triplet state, k_T, is disregarded for the initial hypothesis, but direct homolytic cleavage from the singlet state, k_S, is left as a feasible route to product formation. This leaves three possible competing pathways which may be responsible for the photodebromination products. To elucidate which mechanism(s) are involved three conditions may be considered; complete mathematical derivations are shown in Appendix A. In case ①, the intersystem crossing term, k_{isc}, is high as anticipated based on the heavy atom effect. Direct homolytic cleavage from the singlet excited state, k_s, and formation of a singlet excimer, k_{ex}, will then be negligible by comparison. The steady-state approximation (SSA) states that for reactive, unstable species, such as excited states, the rate of consumption equals the rate of formation.[16] A quantum yield is a measure of the efficiency of photon usage. The product quantum yield, $\Phi_{products}$, is defined as the rate of product formation, d[products]/dt, over the intensity of incident radiation, I^0. A kinetic analysis of Scheme 2.1 under these conditions using the SSA and the definition of the product quantum yield results in equation 2.1. In this equation, F is the efficiency of product formation from the triplet excimer and ϕ_{isc} is the quantum efficiency of intersystem crossing, which would approach unity.

$$\frac{1}{\Phi_{products}} = \frac{k_{td}}{F\phi_{isc}k_{tex}[ArBr]} + \frac{1}{F\phi_{isc}} \qquad \textbf{(2.1)}$$

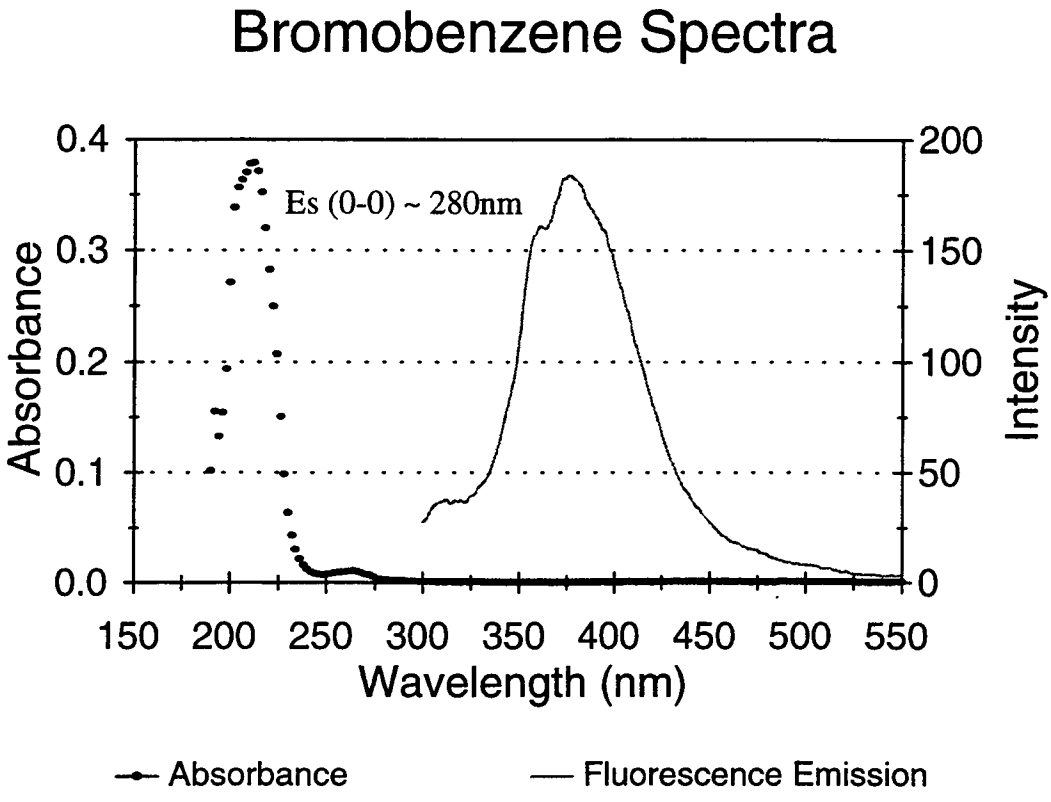

Figure 2.2. Spectroscopy of 2.00×10^{-5} M (fluorescence) and 5.00×10^{-5} M (absorbance) bromobenzene in ethanol at room temperature used to determine the lowest lying singlet excited state energy, where the fluorescence emission baseline is normalized to the absorbance baseline.

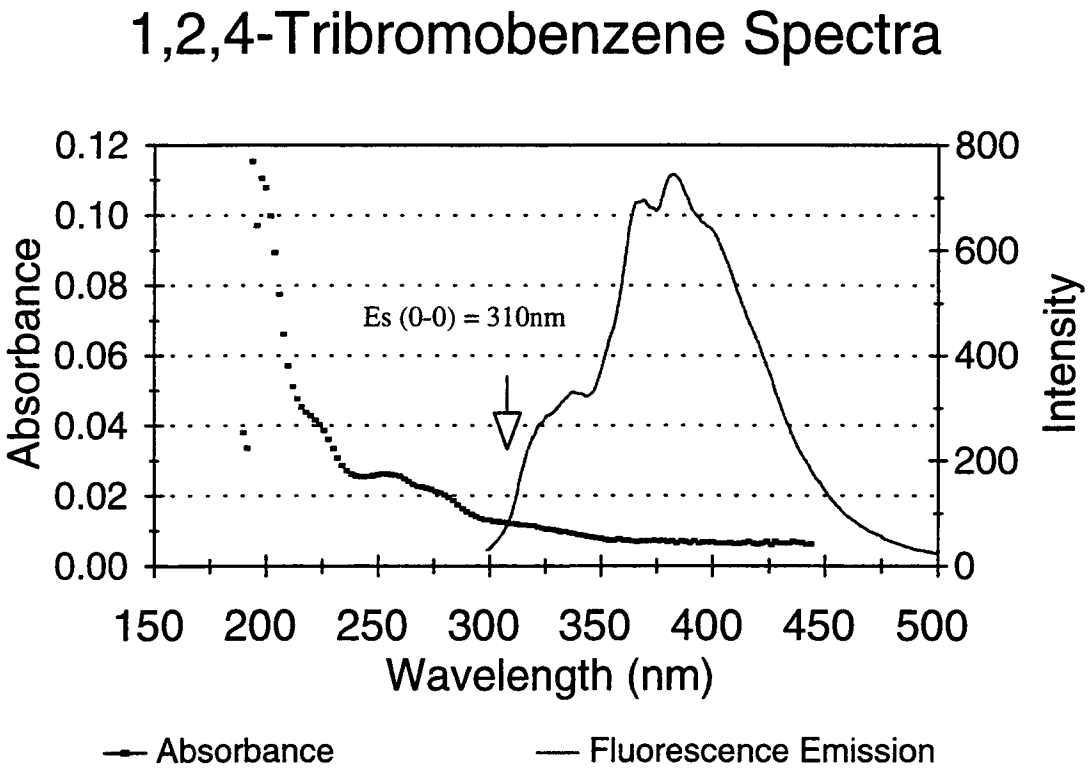

Figure 2.3. Spectroscopy of 1.05×10^{-6} M 1,2,4-tribromobenzene in ethanol at room temperature used to determine the lowest lying singlet excited state energy.

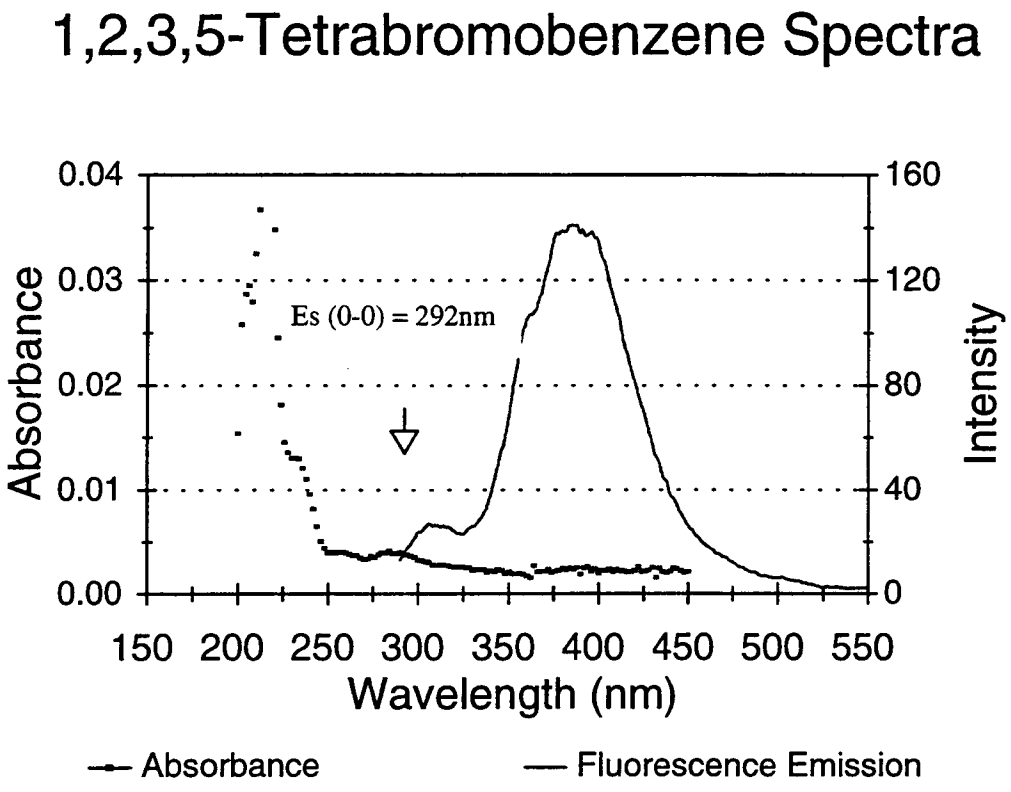

Figure 2.4. Spectroscopy of 9.75×10^{-7} M 1,2,3,5-tetrabromobenzene in ethanol at room temperature used to determine the lowest lying singlet excited state energy.

A Stern-Volmer plot of the inverse of the experimentally determined product quantum yield, $1/\Phi_{products}$, versus the inverse of the aryl bromide concentration, 1/[**ArBr**], will be linear if a bimolecular triplet excimer process is at work. In case ②, the intersystem crossing term is low. Now triplet formation is minimal and all pathways from it, in particular k_{tex}, are negligible. A kinetic analysis with this hypothesis using the SSA results in equation 2.2, where F_s is the formation of products from the singlet excimer.

$$\frac{1}{\Phi_{products}} = \frac{k_d + k_{isc} + k_s + k_{ex}[ArBr]}{k_s + F_s k_{ex}[ArBr]} \qquad \textbf{(2.2)}$$

In this Stern-Volmer plot, two regions of the graph should be evident. One region dependent on the concentration of aryl bromide, due to singlet excimer formation, and another independent portion characteristic of direct homolytic cleavage from the singlet. Finally, in case ③, the intersystem crossing rate could be intermediatary, that is not exceedingly high or low. In this case a linear Stern-Volmer relationship does not drop out and instead a plot of the inverse product quantum yield against the inverse polybromobenzene concentration will be non-linear as a result of the competition between singlet and triplet excimer intermediates.

Photolysis experiments have been conducted on **BB**, **124TrBB**, and **1235TBB** in degassed acetonitrile solutions. Several solutions of various polybromobenzene concentrations were prepared in duplicate with an internal standard, degassed, and photolyzed to obtain an extent of reaction of approximately 28%. The appearance of products and disappearance of the initial polybromobenzenes were quantified by gas

chromatography. Azoxybenzene actinometry solutions,[17] photolyzed with the samples, were analyzed spectrophotometrically to determine the intensity of the incident radiation of the experiment. Product quantum yields were then calculated and plotted against the corresponding inverse concentration of intitial polybromobenzene. All three resulting graphs for **BB**, **124TrBB**, and **1235TBB**, Figures 2.5, 2.6, and 2.7, respectively, exhibit linear relationships with good correlation coefficients, 0.961, 0.996, and 0.997, respectively. This observed linearity rules out case ③ because of its quadratic nature, but is consistent with case ① and ②. The mechanisms of the photodebromination for **BB**, **124TrBB**, and **1235TBB** must therefore proceed through either triplet excimer intermediates or singlet excimer intermediates.

Aerated Photolysis:

In order to determine the multiplicity of the excited state excimer intermediate, photolysis experiments on **BB**, **124TrBB**, and **1235TBB** were performed in aerated solutions. Oxygen is an extremely effective triplet quencher which quickly quenches any triplet moiety that is formed.[18,19] A mechanistic description of the effect of a triplet quencher is shown in Scheme 2.2.

Direct homolytic cleavage from the triplet excited state has again been eliminated for energetic reasons and direct homolytic cleavage from the singlet excited state has also been removed based on the degassed photolysis results discussed above. The presence of a triplet quencher, Q, allows the triplet excited state another non-product forming pathway. The excitation energy of the triplet is transferred to the quencher,

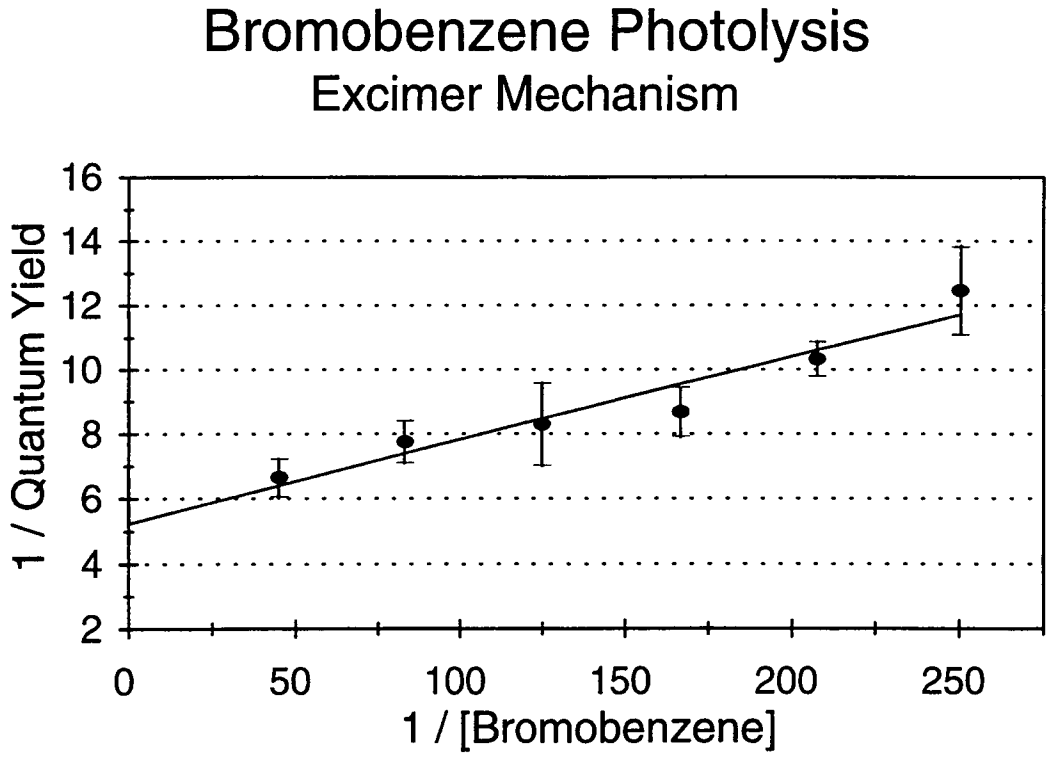

Figure 2.5. Degassed photolysis of bromobenzene at 254 nm in acetonitrile.

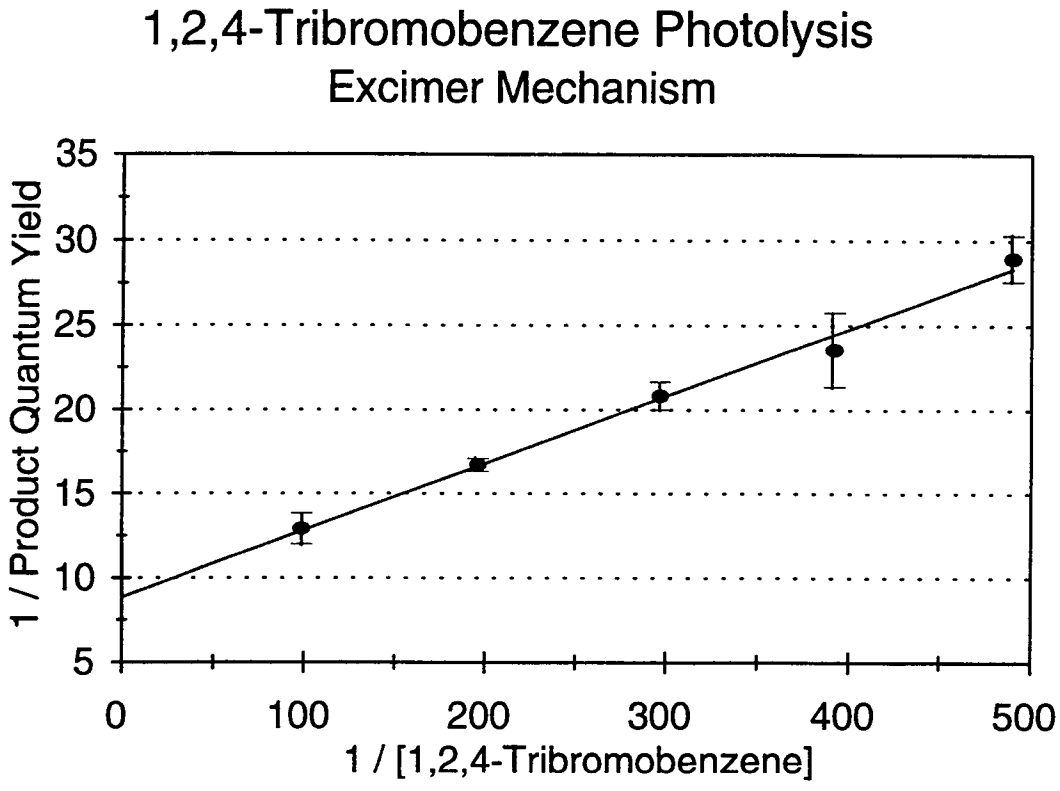

Figure 2.6. Degassed photolysis of 1,2,4-tribromobenzene at 254 nm in acetonitrile.

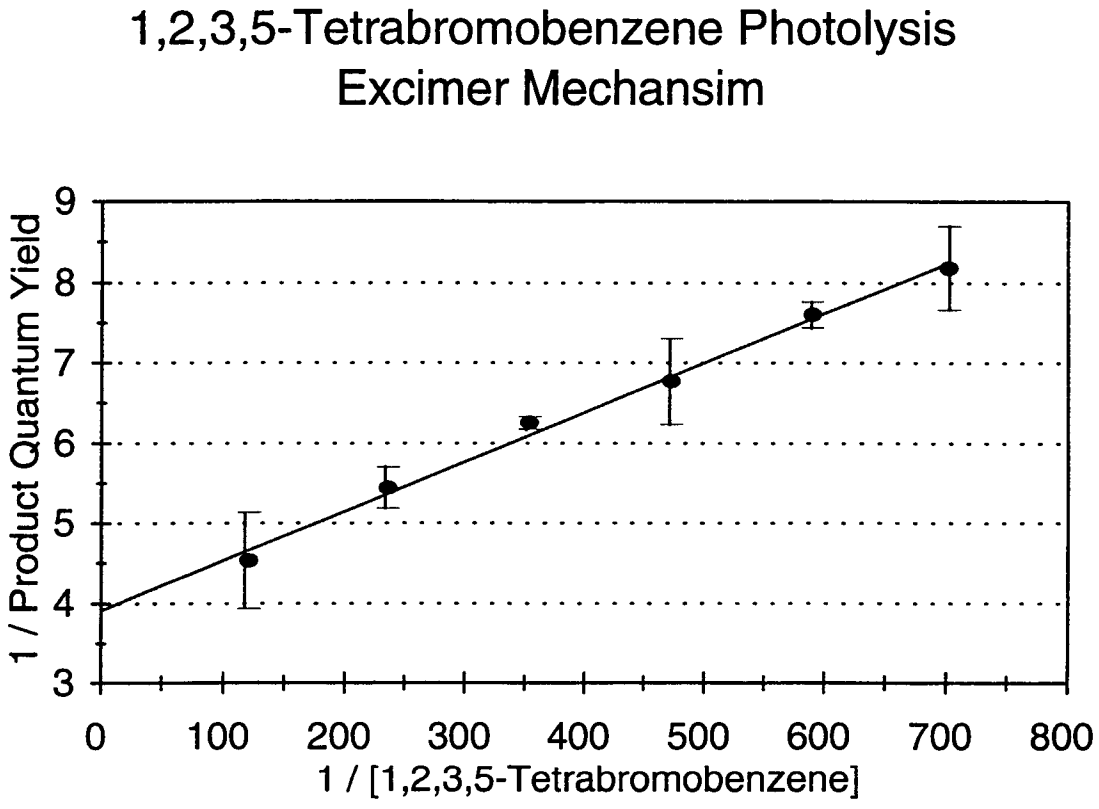

Figure 2.7. Degassed photolysis of 1,2,3,5-tetrabromobenzene at 254 nm in acetonitrile.

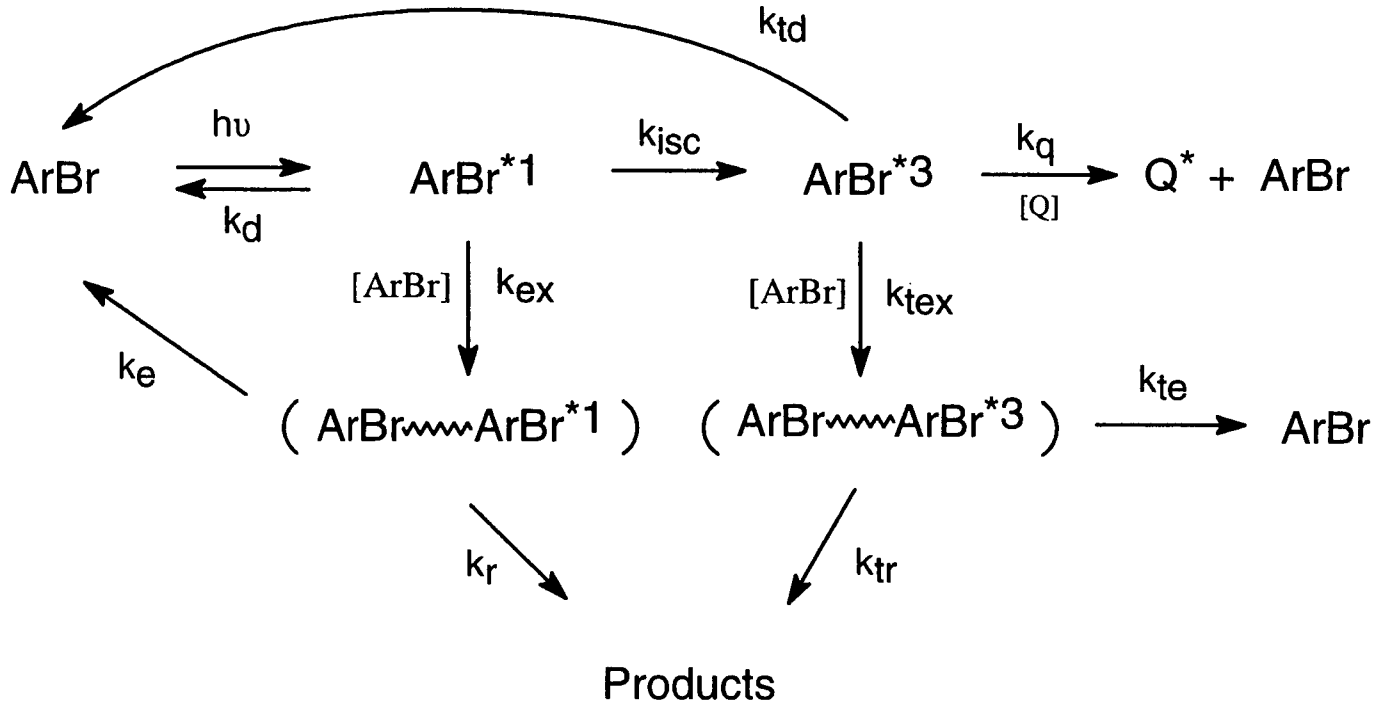

Scheme 2.2. Triplet quenching mechanism of polybromobenzenes.

resulting in an excited quencher, Q^*, and a ground state aryl bromide, **ArBr**. The quenching rate constant, k_q, is dependent on the characteristics of the quencher. When oxygen is the quencher, $Q = O_2$, and the rate of quenching is diffusion controlled.[20,21] Nondegassed acetonitrile has an oxygen content of 9.1×10^{-3} M at 24 °C and 1 atm of air,[22,23] sufficient enough to eliminate the possibility of triplet excimer formation, Appendix B. Product formation from the photodebromination is therefore, reduced to proceeding solely through the singlet excimer intermediate, which corresponds to the simplified version of case ② discussed above. Kinetic analysis of this isolated product formation mechanism using the SSA, Appendix B, results in equation 2.3.

$$\frac{1}{\Phi_{products}} = \frac{k_d + k_{isc}}{F_s k_{ex}[ArBr]} + \frac{1}{F_s} \qquad \textbf{(2.3)}$$

A linear Stern-Volmer plot of $1/\Phi_{products}$ versus 1/[**ArBr**] would support this bimolecular singlet reaction mechanism and lead to the conclusion that no direct singlet homolytic cleavage occurs.

The aerated experiments of **BB**, **124TrBB**, and **1235TBB** were conducted at similar polybromobenzene concentration ranges as those performed in the degassed photolyses. All solutions were prepared in duplicate with an internal standard and photolyzed to an approximate 16% conversion with no prior degassing procedure. Again, the appearance of products and disappearance of the initial polybromobenzenes were analyzed by gas chromatography, and the incident radiation was determined by azoxybenzene actinometry. The inverse of the product quantum yields were then

calculated and plotted against the corresponding inverse of the initial polybromobenzene concentrations. The generated Stern-Volmer plots of **BB**, **124TrBB**, and **1235TBB** were all observed to be linear with good correlation coefficients, 0.978, 0.992, and 0.989, as illustrated in Figures 2.8, 2.9, and 2.10, respectively. These results verify a singlet excimer mechanism for all three polybromobenzenes studied and validate equation 2.3. In the linear expression, the slope is represented as $(k_d + k_{isc}) / F_S k_{ex}$ and $1/ F_S$ is the intercept. Dividing the intercept by the slope cancels out the F_S term, and results in $k_{ex} / (k_d + k_{isc})$.

Experimentally determined intercept to slope ratios for aerated and degassed photolyses of **BB**, **124TrBB**, and **1235TBB** are shown in Table 2.2. The ratio values obtained in the degassed photolysis experiments are similar to those obtained in the aerated photolysis experiments. Because the triplet excimer intermediate is expected to be effectively quenched in aerated solutions, the prevailing mechanism for both degassed and aerated photolyses must be that of the singlet excimer intermediate.

Based on this conclusion, equation 2.3 is the correct Stern-Volmer respresentation of both degassed and aerated photodebromination of **BB**, **124TrBB**, and **1235TBB**. The intercept to slope ratio is $k_{ex} / (k_d + k_{isc})$ which is the same as $k_{ex}\tau_f$. Singlet lifetimes, τ_f, are obtained by taking the product of the radiative singlet lifetimes, τ_f^0, and the fluorescence quantum yields, Φ_f. The rates of singlet excimer formation, k_{ex}, were then calculated in both degassed and aerated solutions for all three aryl bromides. However, if the radiative singlet lifetimes given in Table 2.1 are utilized, excimer formations rates are calculated to be in excess of the rate of diffusion. According to the Smoluchowski

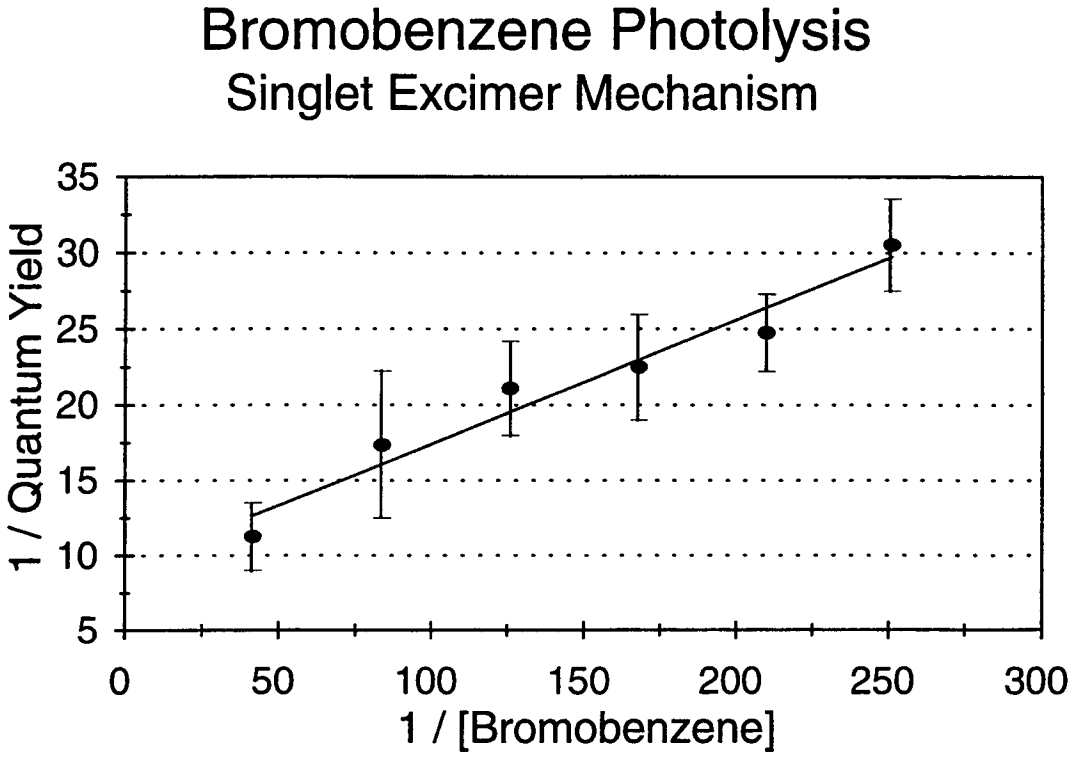

Figure 2.8. Aerated photolysis of bromobenzene at 254 nm in acetonitrile.

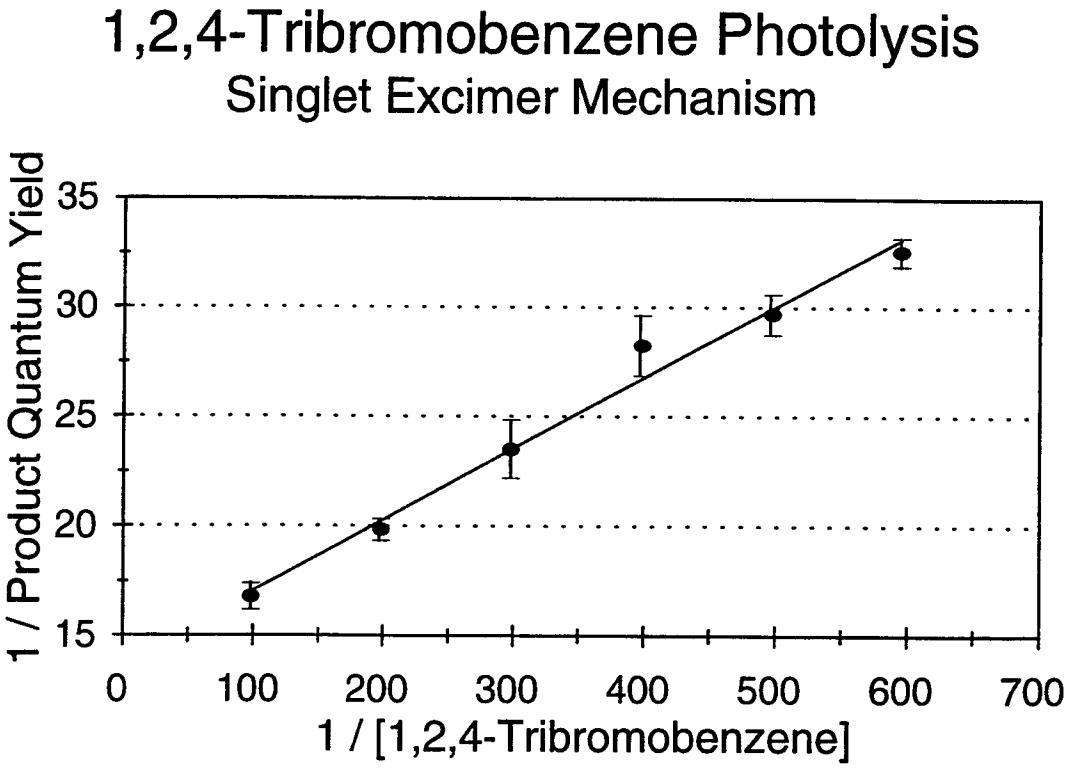

Figure 2.9. Aerated photolysis of 1,2,4-tribromobenzene at 254 nm in acetonitrile.

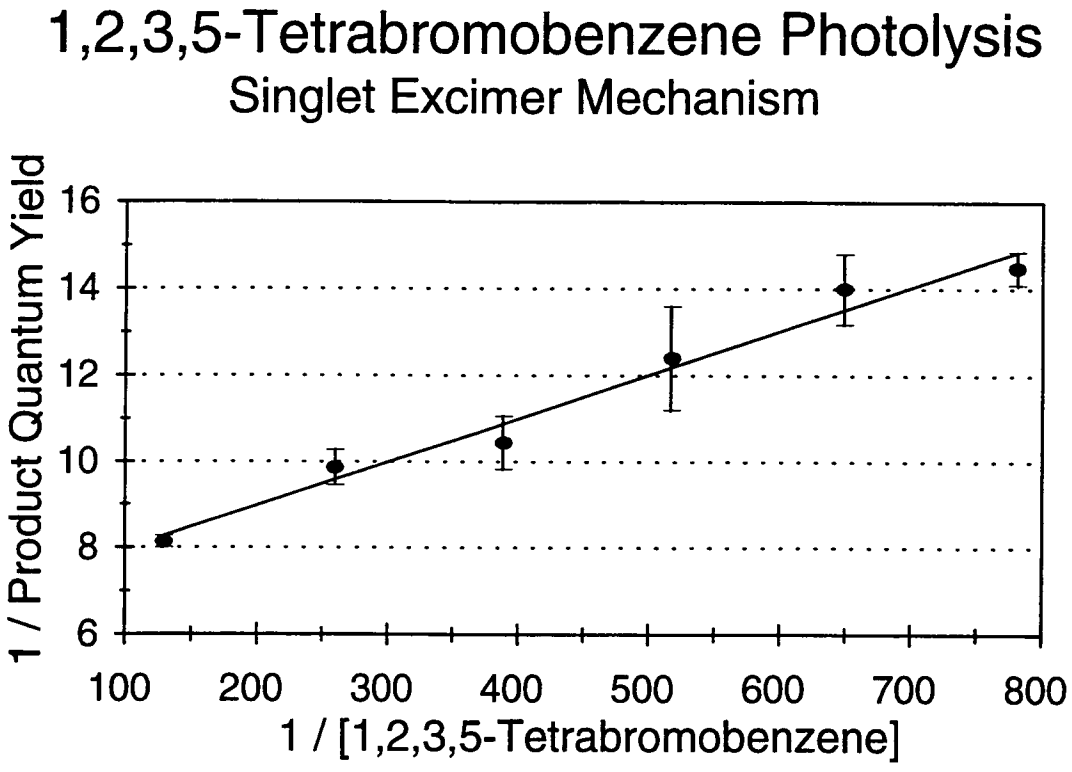

Figure 2.10. Aerated photolysis of 1,2,3,5-tetrabromobenzene at 254 nm in acetonitrile.

Table 2.2. Comparison of excited state excimer mechanisms of the photodebromination of polybromobenzenes in degassed and aerated acetonitrile solutions using intercept to slope ratioing.

Compound	Intercept / Slope		k_{ex} (s^{-1}) *Degassed*	k_{ex} (s^{-1}) *Aerated*
	Degassed Photolysis	Aerated Photolysis		
BB	204 ± 39	113 ± 29	4.3×10^{10}	2.4×10^{10}
124TrBB	222 ± 19	424 ± 36	8.5×10^{10}	1.6×10^{11}
1235TBB	633 ± 26	688 ± 67	1.3×10^{11}	1.5×10^{11}

Propagation of errors preformed on linear regression output obtained within Quattro Pro for Windows Version 5.00.

equation,[24] the rate of diffusion in acetonitrile at 25 °C is $1.9 \times 10^{10}\ M^{-1} s^{-1}$ assuming a viscosity of 0.345 cP. Therefore, direct measurement of the fluorescence lifetimes of **BB**, **124TrBB**, and **1235TBB** were attempted using a pulsed laser at 266 nm, which is capable of obtaining lifetimes of up to approximately 5 ns.[25] Unfortunately, none of the singlet lifetimes were measurable, leading to the conclusion that the lifetimes must be at or faster than 5 ns. When this value is used for the radiative singlet lifetimes, more reasonable excimer formation rate constants are predicted, Table 2.2. It is apparent, then, that the rate of singlet excimer formation, k_{ex}, is diffusion controlled.

Triplet Quenching:

The extent of excited triplet state participation in a photochemical reaction can also be investigated more quantitatively by varying the concentration of a chemical triplet quencher, Scheme 2.2. In the polybromobenzene photodebromination experiments discussed above, the oxygen triplet quencher was either totally removed by degassing all solutions or it was present at a constant level where it completely quenched all other triplet reactive pathways. If the concentration of the quencher is varied from a concentration of zero to high concentrations, both extremes and everything in between are examined.

A kinetic analysis, employing the SSA, was applied to Scheme 2.2 to determine the product quantum yield with, $\Phi_{products}$, and without a triplet quencher, $\Phi^0_{products}$, Appendix C. A ratio of the resulting expressions creates a complicated, non-linear equation. However, a consideration of the limiting cases simplifies it into understandable

terms. If the reaction proceeds solely through a triplet excited state, equation 2.4 governs the reaction.

$$\frac{\Phi^0}{\Phi} = 1 + \frac{k_q[Q]}{k_{td} + k_{tex}[ArBr]} \qquad \textbf{(2.4)}$$

The equation represents a linear expression when the quantum yield ratio, Φ^0/Φ, is plotted against the concentration of the quencher, [Q]. If the other extreme is considered, where the reaction proceeds only through a singlet excited state, the quantum yield is not dependent on the quencher. Therefore, $\Phi = \Phi^0$, and $\Phi^0/\Phi = 1$. A photochemical reaction that has both a reactive singlet excited state and a reactive triplet excited state, will have a region of Φ^0/Φ dependent on the quencher concentration and one independent of quencher. This would result in a Stern-Volmer plot that exhibits a "roll-over" point in the graph, where the linearity flattens into a straight horizontal line.

As illustrated in Scheme 2.2, the ground state of the quencher reacts with the excited triplet state of the aryl bromide. Experimentally then, conditions must be set up such that **ArBr** absorbs the vast majority of the incident radiation and that its concentration lies within the range of known excimer formation. To accomplish this, the molar extinction coefficients at the wavelength of excitation, ϵ_λ, for the three polybromobenzenes and all potential quenchers were determined, Table 2.3. After choosing an appropriate concentration of the polybromobenzene, these molar extinction coefficients were used to calculate the maximum allowable quencher concentration that would fit the requirement. The quencher must also meet energetic criteria in order for the

Table 2.3. Molar extinction coefficients of the polybromobenzenes and triplet quenchers in acetonitrile (ACN) and ethanol.[A]

Compound	ϵ_{300nm} (ACN) ($M^{-1}cm^{-1}$)	ϵ_{254nm} (ACN) ($M^{-1}cm^{-1}$)	ϵ_{254nm} (Ethanol) ($M^{-1}cm^{-1}$)
BB	---	123	136
124TrBB	10	616	1080
1235TBB	70	1433	1450
Fumaronitrile	---	0.414	---
Isoprene	---	40[B]	---

[A)] Unless otherwise stated, all values determined from absorbance calibration curves generated with standard solutions of known concentrations.

[B)] Murov, S. L. *Handbook of Photochemistry*, **1973**, Marcel Dekker, Inc., New York, pp. 4.

polybromobenzene triplet excited state, **ArBr**^{*3}, to successfully transfer its energy. The transfer demotes **ArBr**^{*3} to **ArBr** while promoting Q to its triplet excited state, Q^{*3}. This triplet excited state of the quencher must therefore, have an energy less than that of the polybromobenzene triplet.

Fumaronitrile, a commonly used triplet quencher,[26] was found to have a triplet energy of 79.9 kcal/mol[27] which is in slight excess of the triplet energies for the polybromobenzene compounds. However, it has been used successfully in triplet quenching studies for compounds with triplet excited state energies as low as 74 kcal/mol.[28] For this reason, triplet quenching studies utilizing fumaronitrile were conducted on **124TrBB** and **1235TBB**.

Adhering to the necessary conditions, solutions were prepared in duplicate with a constant polybromobenzene concentration, an internal standard, and various fumaronitrile concentrations. Samples were then degassed and photolyzed, using an actinometer to determine the intensity of the incident radiation. The appearance of products and disappearance of the initial polybromobenzenes were analyzed by gas chromatography. Product quantum yields with and without fumaronitrile were calculated, ratioed, and plotted against its concentration. Graphs of both **124TrBB** and **1235TBB**, Figures 2.11 and 2.12, respectively, revealed no dependence on the concentration of fumaronitrile, leading to the conclusion that products form through a singlet excimer mechanism or that triplet energy is not transferred.

Isoprene, another common triplet quencher, has a triplet energy of 60.1 kcal/mol.[29] This lies well below the triplet energies of the polybromobenzenes and is therefore better

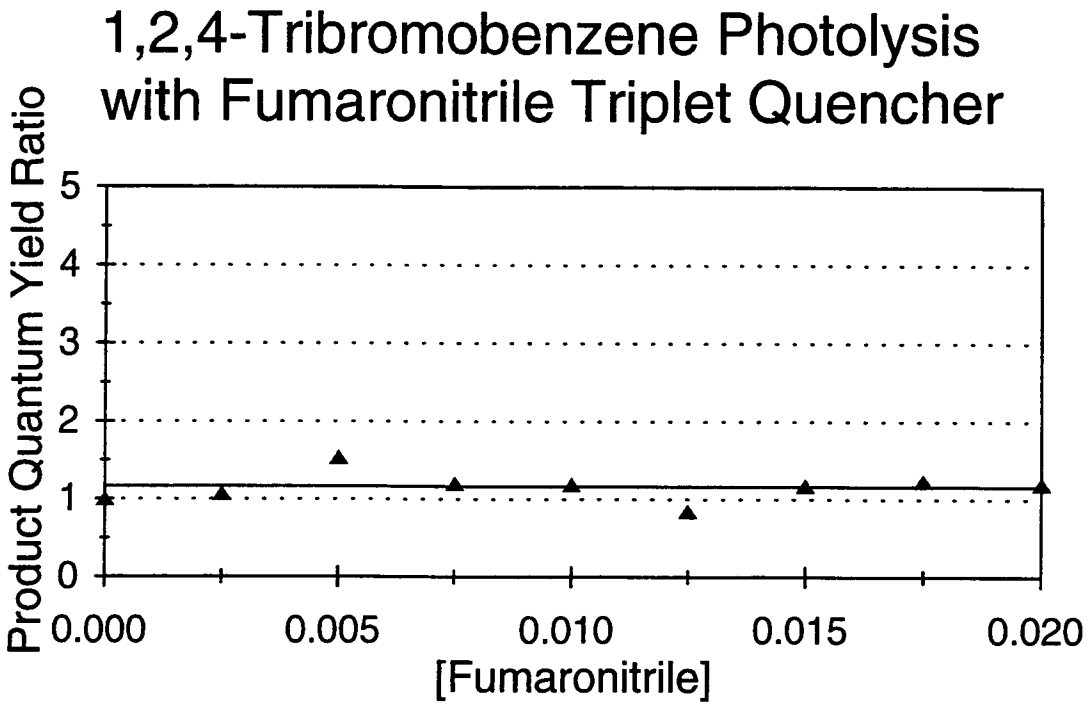

Figure 2.11. Photolysis of 1,2,4-tribromobenzene with fumaronitrile triplet quencher at 254 nm in acetonitrile. Product quantum yield ratio, $\Phi^0/\Phi = 1.2 \pm 0.2$.

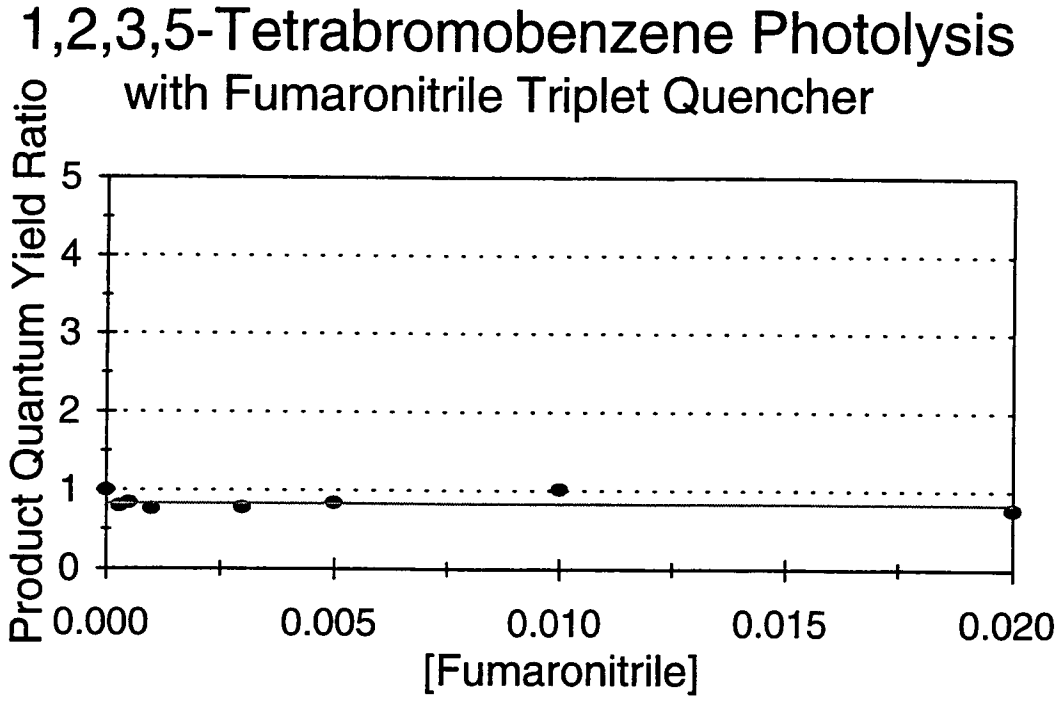

Figure 2.12. Photolysis of 1,2,3,5-tetrabromobenzene with fumaronitrile triplet quencher at 254 nm in acetonitrile. Product quantum yield ratio, $\Phi^0/\Phi = 0.83 \pm 0.09$.

suited for triplet quenching studies. Isoprene quenching experiments were performed on **BB**, **124TrBB**, and **1235TBB**.

Appropriate solutions were prepared in duplicate with constant polybromobenzene concentrations, an internal standard, and various amounts of isoprene. All samples were then degassed, photolyzed, and analyzed as described above. Product quantum yields with and without isoprene were calculated, ratioed, and plotted against the concentration of isoprene. Figures 2.13, 2.14, and 2.15, demonstrate that again the quantum yield of product formation from all three arenes, **BB**, **124TrBB**, and **1235TBB**, respectively, is independent of triplet quencher concentration. A singlet excimer intermediate mechanism is, thus, the best rationale. The isoprene triplet quenching graph of **BB**, Figure 2.16, also predicts what would have resulted if a triplet excimer intermediate were responsible for the debromination products. The prediction assumes a diffusion controlled quenching rate[30,31] at various hypothesized triplet excimer formation rate constants, k_{tex}, given in the legend of the graph.

Direct measurement of triplet reactivity can be accomplished using the method of Lamola and Hammond.[32,33,34] In this technique, the extent of triplet participation is monitored by the clean triplet[35] isomerization of *trans*-piperylene. The final stoichiometry is used to calculate ϕ_{isc}. The method has been used successfully for pentachlorobenzene,[36] 4-bromobiphenyl,[37] and 4-bromo[2.2]paracyclophane.[38] However, attempts by Takemura and coworkers[39] to determine the value of ϕ_{isc} for **BB** were unsuccessful and they eventually assumed that the value would be close to unity siting "difficulty" in the ϕ_{isc} measurement. Numerous attempts to directly measure ϕ_{isc} of

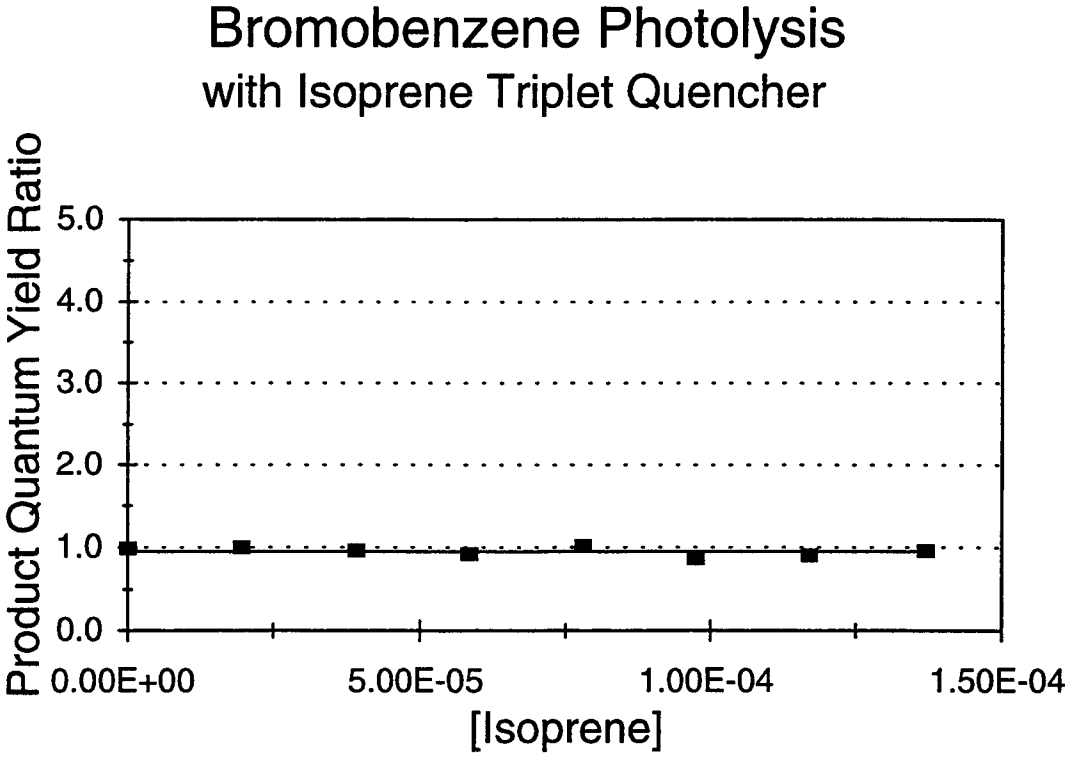

Figure 2.13. Photolysis of bromobenzene with isoprene triplet quencher at 254 nm in acetonitrile. Product quantum yield ratio, $\Phi^0/\Phi = 0.96 \pm 0.05$.

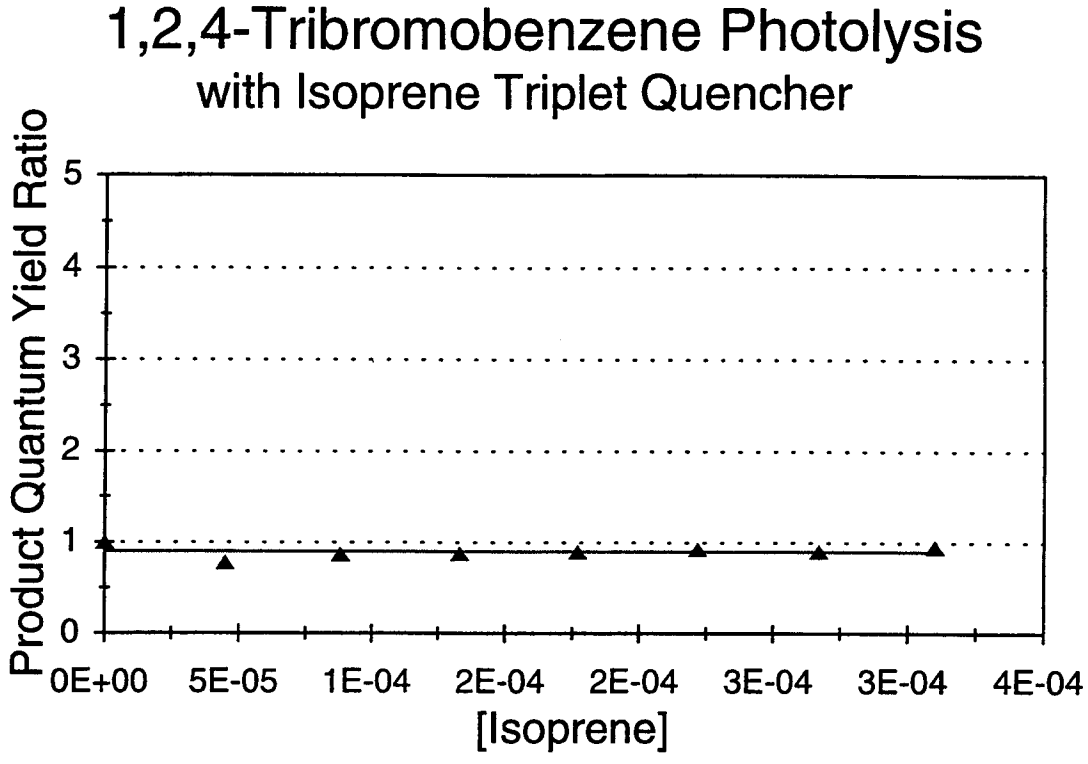

Figure 2.14. Photolysis of 1,2,4-tribromobenzene with isoprene triplet quencher at 254 nm in acetonitrile. Product quantum yield ratio, $\Phi^0/\Phi = 0.90 \pm 0.06$.

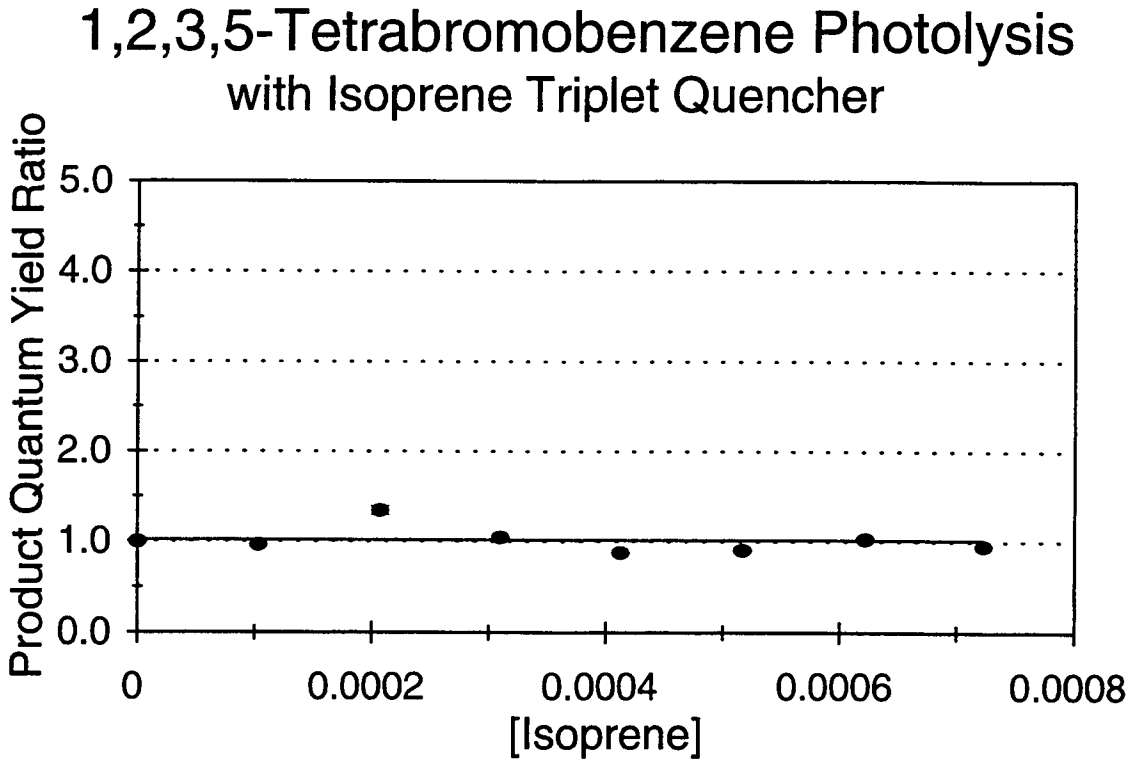

Figure 2.15. Photolysis of 1,2,3,5-tetrabromobenzene with isoprene triplet quencher at 254 nm in acetonitrile. Product quantum yield ratio, $\Phi^0/\Phi = 1.0 \pm 0.1$.

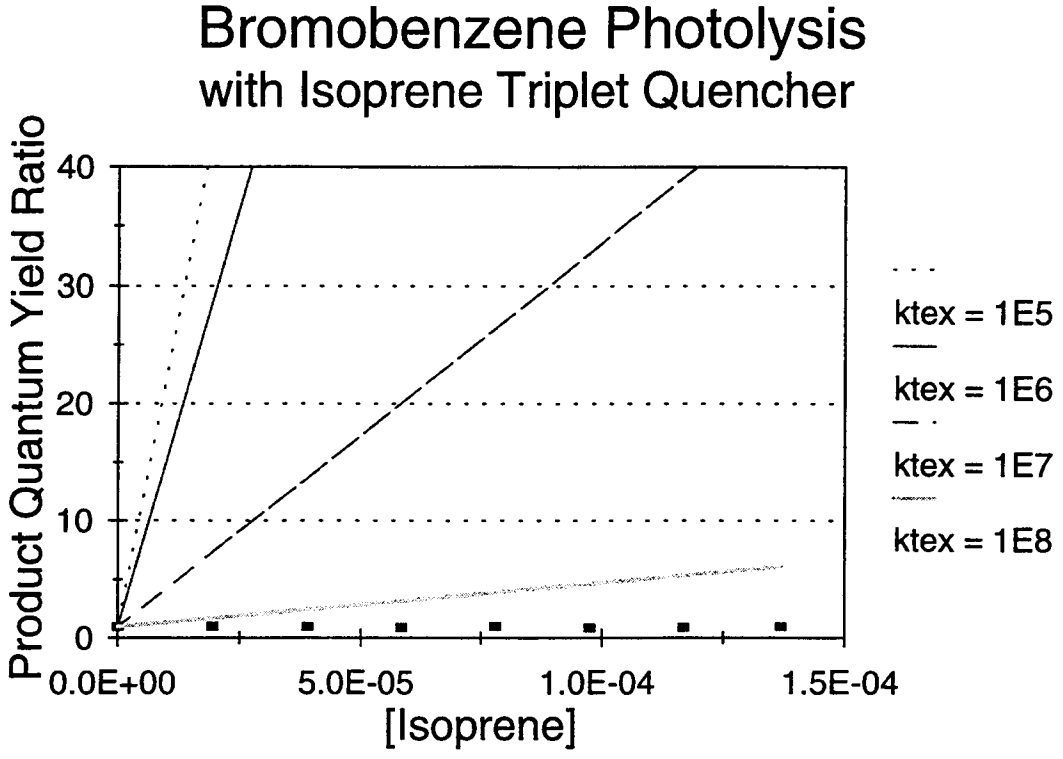

Figure 2.16. Photolysis of bromobenzene with isoprene triplet quencher. Squares represent actual data points where the product quantum yield ratio, $\Phi^0/\Phi = 0.96$. Various lines are hypothetical results of quenching at different triplet excimer formation rates.

1235TBB in this study were also unsuccessful. The reactions produced a large array of products which clouded the analysis of any isomerization. This was also accompanied by a rapid decrease in total piperylene content.

Radiative Quantum Yields:

Fluorescence quantum yield, Φ_f, and phosphorescence quantum yield, Φ_p, determinations were carried out on each polybromobenzene. 9,10-Diphenylanthracene[40] was used as a fluorescence standard[41] directly for the calculation of Φ_f, and in conjunction with a phosphorimeter factor[42] to predict Φ_p. Ethanol was selected as a solvent, for its ability to form a rigid glass at 77°K, availability of fluorescence actinometry data, similarity to the acetonitrile photolysis solvent (polarity, refractive index, viscosity, absorbance, and density), and ease of use. Very low concentrations of the polybromobenzenes and diphenylanthracene were used to avoid self quenching. Fluorescence and phosphorescence emission spectra of the sample compounds were obtained under identical instrumental and experimental conditions as that of the reference standard. Equations 2.5 and 2.6 were used to calculate the quantum yields. The indices

$$\Phi_f(s) = \frac{\Phi_f(r) \cdot \int I_s(\lambda)d\lambda \cdot D_r \cdot n_s^2}{\int I_r(\lambda)d\lambda \cdot D_s \cdot n_r^2} \qquad \textbf{(2.5)}$$

$$\Phi_p(s) = \frac{\Phi_f(r)}{P} \cdot \frac{\int I_s(\lambda)d\lambda \cdot D_r \cdot n_s^2}{\int I_r(\lambda)d\lambda \cdot D_s \cdot n_r^2} \qquad \textbf{(2.6)}$$

s and r represent sample and reference, respectively, the integrals denote the areas underneath the emission spectra where I is intensity and λ is wavelength, D is the optical density or absorbance at the wavelength of excitation, and n is the refractive index of the solvent.

The phosphorimeter factor, P in equation 2.6, accounts for the delay time, t_d, that is experienced prior to measuring the phosphorescence signal and the actual time in which the emission spectra is measured, referred to as the gate time, t_g. Because of the necessary delay, to avoid fluorescence, only a fraction of the total signal is observed. The delay will affect each substrate differently depending on its triplet lifetime, τ_p, and instrumental conditions under which the measurements are taken. Assuming a first order rate law, the phosphorimeter factor is therefore, given by equation 2.7.[43]

$$P = [\exp(-t_d/\tau)][1 - \exp(-t_g/\tau)] \qquad (2.7)$$

The resulting fluorescence and phosphorescence quantum yields for **BB**, **124TrBB**, and **1235TBB** are shown in Table 2.1. The fluorescence quantum yields are suprisingly high for compounds consisting of one, three, and particularly four large bromine substituents. Enhanced spin-orbit coupling should promote S $\rightarrow$ T transitions, and favor phosphorescence as the radiative decay pathway. However, as evidenced in the photodebromination of these polybromobenzenes, singlet reactivity is unexpectedly dominant.

Fluorescence Quenching:

Fluorescence quenching studies further verify the existence of the singlet excimers. A partial kinetic mechanism that details the singlet decay pathways is illustrated in Scheme 2.3. The bromoarene is excited to the singlet state, $\mathbf{ArBr}^{*1}$, by the source of the luminescence spectrometer. From here it may undergo non-radiative decay, k_{nr}, or radiative decay, fluorescence, k_f, back to the ground state, form a singlet excimer which produces debromination products, or intersystem cross to the excited triplet state. The quantum yield of fluorescence is given by equation 2.8.

$$\Phi_f = \frac{k_f}{k_f + k_{nr} + k_{isc} + k_{ex}[ArBr]} \qquad \textbf{(2.8)}$$

At extremely low concentrations of the polybromobenzene the last term in the denominator will become minimal and may be excluded. This conditional fluorescence quantum yield, Φ_f^0, is related back to the original yield in the same manner as that taken for the triplet quenching experiments, resulting in a relationship Φ_f^0 / Φ_f, termed the fluorescence quantum yield ratio, expressed in equation 2.9.

$$\frac{\Phi_f^0}{\Phi_f} = 1 + \frac{k_{ex}[ArBr]}{k_f + k_{nr} + k_{isc}} = 1 + k_{ex}\tau_f\,[ArBr] \qquad \textbf{(2.9)}$$

Self quenching will be evident if a plot of the fluorescence quantum yield ratio against the aryl bromide concentration is linear. The slope of the predicted line is $k_{ex}\tau_f$, where τ_f is the singlet lifetime of the particular polybromobenzene.

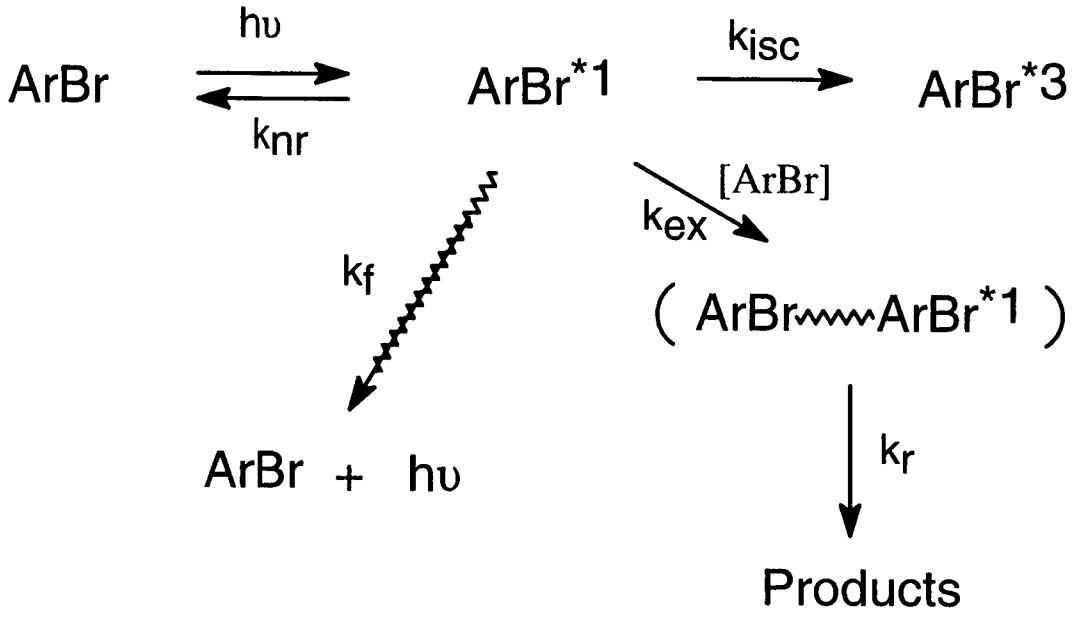

Scheme 2.3. Kinetic mechanism of polybromobenzene fluorescence quenching.

Fluorescence quenching experiments were conducted on **BB**, **124TrBB**, and **1235TBB**. Sample solutions of various concentrations were prepared in absolute ethanol and nitrogen purged. Fluorescence emission spectra were obtained for the polybromobenzene samples and the 9,10-diphenylanthracene fluorescence actinometer under identical instrumental parameters, except the wavelength of excitation and emission filters. Equation 2.5 was then used to determine the fluorescence quantum yield of each sample solution. The sample of lowest concentration was designated as Φ_f^0 and related to itself and all other samples in the ratio form, Φ_f^0 / Φ_f. Stern-Volmer plots of the fluorescence quantum yield ratio against the polybromobenzene concentration were generated and found to be linear for all three compounds. Figures 2.17, 2.18, and 2.19, illustrate the excellent correlation coefficients resulting from the linear regressions, 0.990, 1.000, and 1.000, respectively. Using the slopes and singlet lifetimes 4.8 ns, 2.6 ns, and 4.7 ns, corresponding rates of singlet excimer formation, k_{ex}, for **BB**, **124TrBB**, and **1235TBB** were calculated to be 9.04×10^{12} s^{-1}, 1.90×10^{14} s^{-1}, and 1.06×10^{14} s^{-1}, respectively. These experimental observations validate the self quenching mechanism and confirm the existence of singlet excimer intermediates. The k_{ex} values indicate a diffusion controlled process of singlet excimer formation. The same conclusion was drawn from both degassed and aerated direct photolysis experiments.

Conclusions

Direct photodebromination of bromobenzene, 1,2,4-tribromobenzene, and 1,2,3,5-tetrabromobenzene lead to debrominated products with regiochemistry determined by

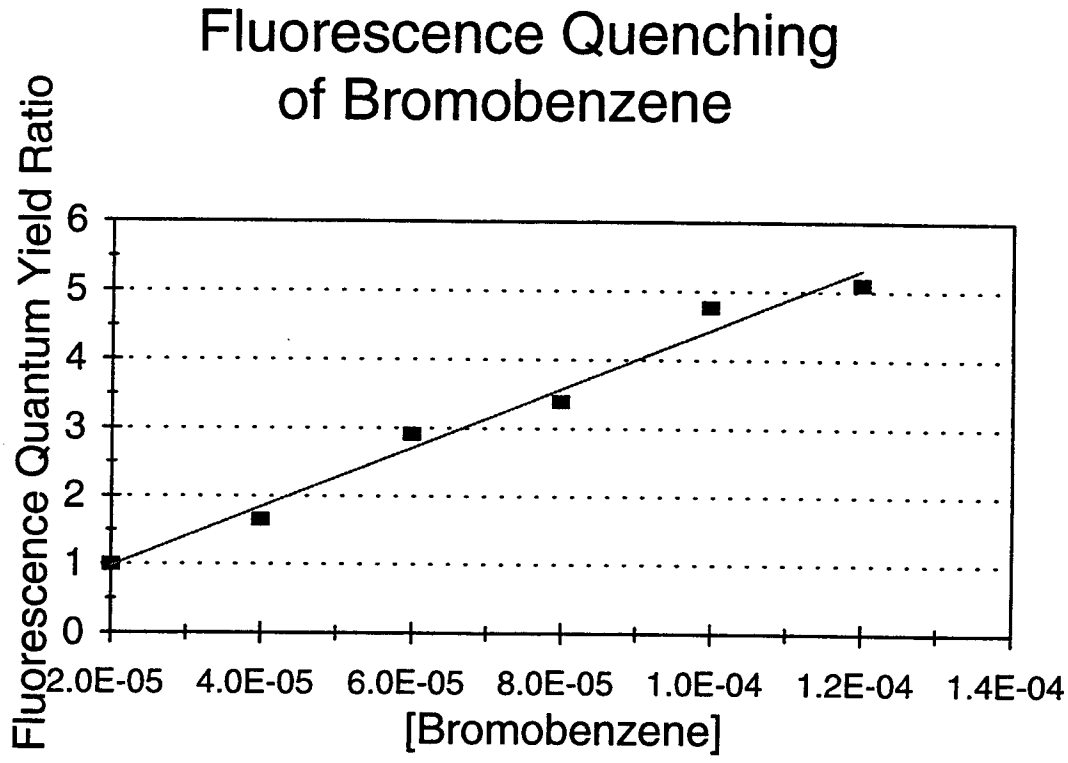

Figure 2.17. Bromobenzene fluorescence quenching in ethanol at room temperature.

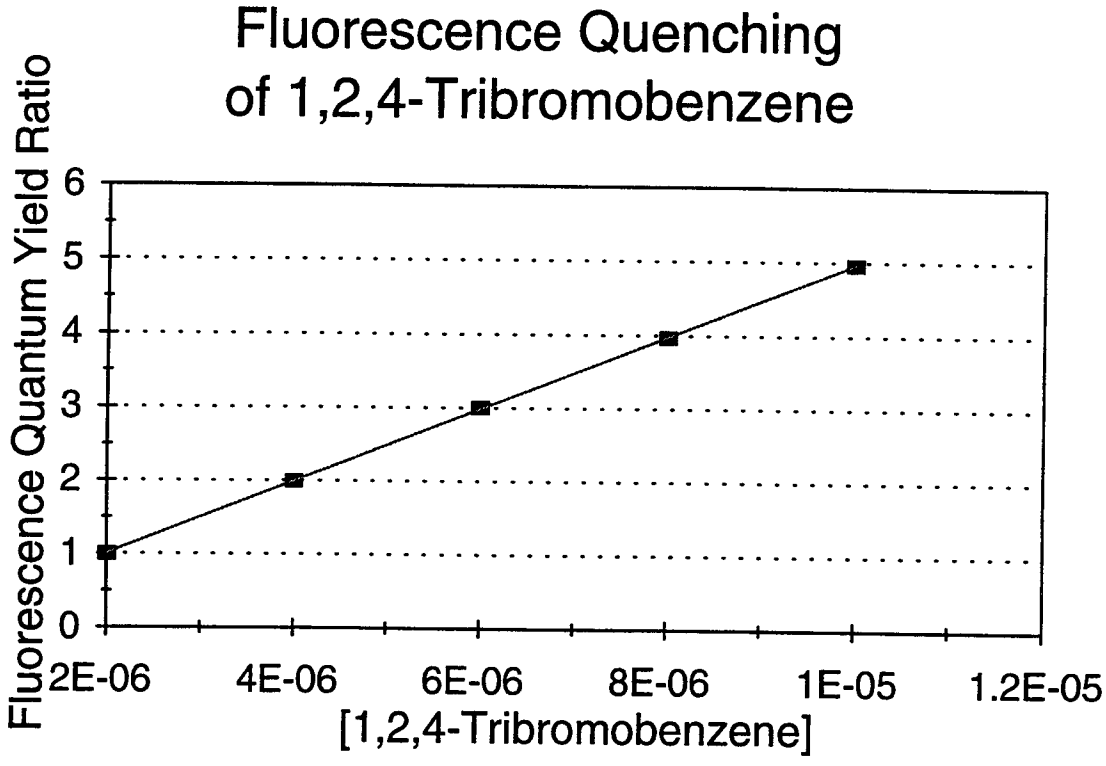

Figure 2.18. 1,2,4-Tribromobenzene fluorescence quenching in ethanol at room temperature.

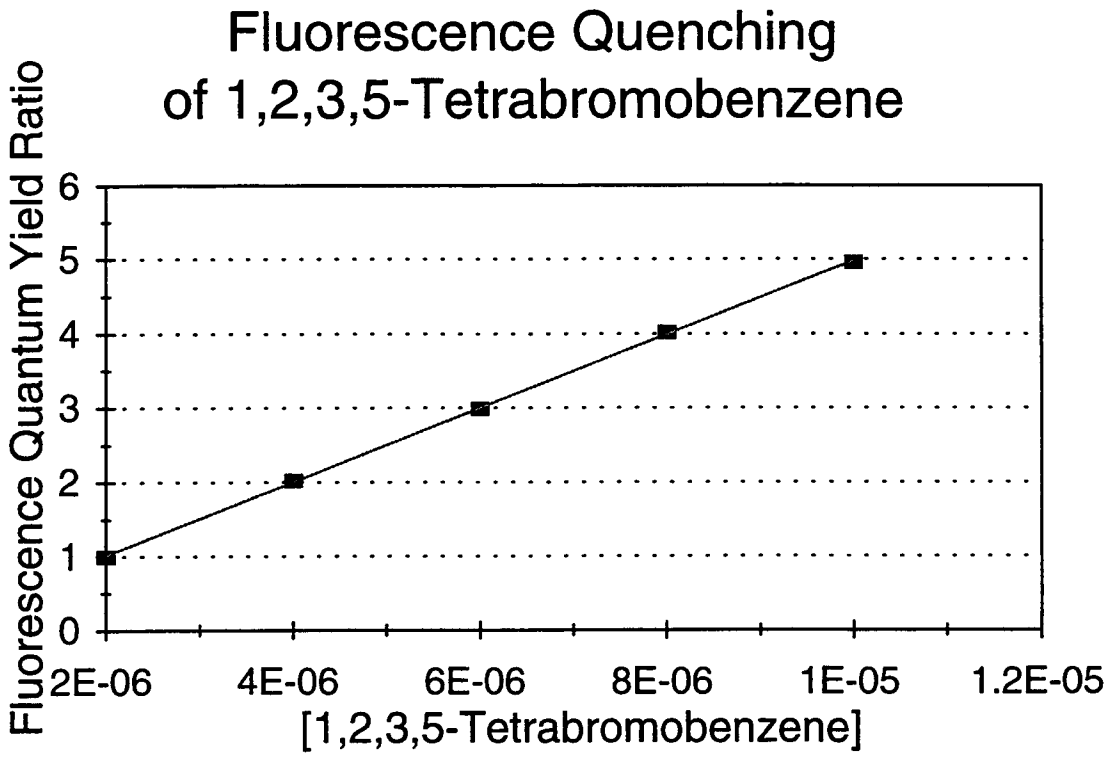

Figure 2.19. 1,2,3,5-Tetrabromobenzene fluorescence quenching in ethanol at room temperature.

removal of *ortho* bromine interactions. The linearity of Stern-Volmer plots, inverse product quantum yield versus inverse polybromobenzene concentration, under both degassed and aerated experimental conditions, is consistent with a product determining excimer intermediate with no evidence of direct homolytic C-Br bond cleavage. The photodebrominations were not affected by fumaronitrile or isoprene triplet quenchers, suggesting that the excimer is of singlet state origin. Radiative quantum yields also demonstrate the dominant singlet reactivity with high fluorescence quantum yields and low phosphorescence quantum yields. Singlet excimer intermediates were verified by fluorescence quenching experiments on all three polybromobenzenes which showed remarkably linear quenching plots. Using singlet lifetimes and values obtained from the various plots, the singlet excimer intermediate formation was determined to be diffusion controlled. It is this authors opinion that direct measuring attempts of ϕ_{isc} were unsuccessful due its low value. All evidence indicates that the photodebromination is dominated by singlet reactivity. With this the case, ϕ_{isc} must be low.

Experimental

Materials:

Bromobenzene (Aldrich Gold Label, 99+%), 1,2-dibromobenzene (Aldrich, 98%), 1,3-dibromobenzene (Aldrich, 97%), 1,4-dibromobenzene (Aldrich, 98%), and 1,3,5-tribromobenzene (Fluka Chemika, 98%) were used as received. 1,2,4-Tribromobenzene was recrystallized from absolute ethanol. 1,2,3-Tribromobenzene and 1,2,3,5-tetrabromobenzene were synthesized and purified according to the procedures decribed

below. The acetonitrile solvent, fresh ChromAR HPLC grade, was used as purchased from Mallinckrodt Chemical as it was found to be pure by GC analysis. Fumaronitrile (Aldrich, 98%) and isoprene (Aldrich, 99%) were used as received for quenching studies. Spectroscopy performed in ethanol was conducted with dehydrated absolute 200 proof alcohol from McCormick Distilling Co., Inc. Aldrichs' 99% pure 9,10-diphenylanthracene was used for the fluorescence quantum yield standard in all luminescence studies.

General Procedure for Photolysis:

Samples for photolysis were transferred in duplicate 1.000 mL aliquots to quartz phototubes. The phototubes containing samples to be degassed were then fitted with sliding glass stoppers via a screw in nylon adapter. Stoppers were lightly greased with Dow Corning high vacuum grease and two o-rings were used to ensure a good seal. The vacuum line system consists of two rotary pumps and a mercury diffusion pump. Degassing was accomplished by four freeze-pump-thaw cycles to a pressure of at least 5×10^{-5} torr. Samples which were not degassed were simply corked prior to photolysis. All samples were irradiated in a Rayonet merry-go-round reactor (The Southern New England Co.) equipped with up to eight preconditioned (warmed up for at least an hour) 254 nm mercury low pressure arc lamps, and overhead fan to maintain a constant temperature of 25-26 °C. Upon removal from the reactor, all phototubes were placed in the dark for a minimum of two hours to assure cessation of reaction.

Azoxybenzene Actinometry:[44]

Actinometry is used to determine the incident radiation intensity of the lamps that the sample solutions are exposed to. For this reason, sample solutions and actinometry solutions were irradiated simultaneously within the reactor. Actinometry solutions were prepared by dissolving 8-10 mg of azoxybenzene (Janssen Chimica, 97%, stored in the dark) in 5 mL of 95% ethanol and then transferring 1.000 mL aliquots in triplicate to the phototubes. After photolysis, 0.500 mL was removed from each solution and diluted to 5.00 mL with 5% KOH in 95% ethanol. This same procedure was also carried out on the original non-irradiated solution to serve as a blank. All solutions were placed in the dark for at least two hours and until spectrophotometric analysis could be performed. The alcohol product, 2-hydroxyazobenzene, of the intramolecular photorearrangement[45] has a known molar extinction coefficient at 458 nm, ϵ_{458}. The absorbance of the irradiated actinometry solutions against the blank were measured on an HP 8452A Diode Array Spectrophotometer with HP 89531A MS-DOS UV/VIS operating software, or an older model HP 8451A Diode Array Spectrophotometer. The Beer-Lambert law was then used to determine the concentration. Using this, the quantum yield for the reaction (0.017 at 254 nm),[44] and taking the dilution factor into account results in the following incident radiation intensity in moles/minute.

$$I_0^i = \frac{A_{458} V_1 V_3}{V_2 l \varepsilon_{458} \phi_\lambda t}$$

where A is absorbance, V_1 is the volume irradiated, V_2 is the volume of irradiated

solution withdrawn, V_3 is the volume of the flask in which the dilution is performed, l is the pathlength of the cell used to measure the absorbance, ϕ_λ is the quantum yield at the specific wavelength, and t is the time of irradiation. A condition for the validity of an actinometer is that it and the samples must absorb all of the incident radiation[46] by maintaining an absorbance at the wavelength of radiation greater than 2. The concentrations of azoxybenzene used above ensure this, and using measured molar extinction coefficients of **BB**, **124TrBB**, and **1235TBB**, determined using the newer HP diode array spectrophotometer and given in Table 2.3, minimum concentrations of the polybromobenzene compounds were calculated and employed.

Product Analyses:

Photolysis mixtures were analyzed using a Varian 3300 Gas Chromatograph with flame ionization detector (FID) and splitless injection, which was computer interfaced to an HP 35900D A/D Interface Board running real time analysis with the HP 3365 Series II ChemStation software. An Econo-Cap Carbowax (polyethylene glycol) capillary column from Alltech of 30 m × 0.25 mm ID × 0.25 μm film was used in all cases. The injector and detector were maintained at 250 °C and 300 °C, respectively, while the temperature program was varied depending on the photolysis mixture in order to obtain separation of isomers and sufficient elucidation conditions. Standard grade helium in series with Alltechs' Hydro Purge II moisture trap, Oxy-Purge N non-indicating high capacity (500 cc) oxygen trap, and AT-Super Indicating Oxy-Trap (20 cc capacity) was used as the carrier gas. Identification and quantification of photoproducts were determined by

retention times and response factors of standards using octadecane (Aldrich, 97%) as an internal standard. Response factor calibration curves were constructed by injecting several samples of known concentrations and plotting the area response ratio of the compound (X) to internal standard (IS) against the concentration ratio of compound to internal standard.

$$\frac{Area_X}{Area_{IS}} = \frac{[X]m_X}{[IS]}$$

Once the response, m_X, had been determined, the photolysis mixtures with unknown concentrations of X, [X], were easily calculated. All concentrations reported are given in moles per liter (M).

Synthesis of 1,2,3,5-Tetrabromobenzene:

1,2,3,5-Tetrabromobenzene was synthesized by the deamination of 2,4,6-tribromoaniline utilizing *tert*-butyl nitrite and bromination via cupric bromide, similar to the procedure of chlorination to form 1,2,3,5-tetrachlorobenzene.[47] In a 100 mL, three-necked, round-bottom flask equipped with reflux condenser connected to a drying tube, 2.682 g (12.01 mmol) of oven-dried, anhydrous cupric bromide (Allied Chemical) and 1.547 g (15.00 mmol) of *tert*-butyl nitrite (Aldrich, 90%) were vigorously stirred in freshly distilled acetonitrile and heated to an oil bath temperature of 65-68 °C. Then 3.298 g (10.00 mmol) of 2,4,6-tribromoaniline (Aldrich, 98%) was added through a funnel. The temperature was maintained for an hour. After which, the reaction mixture

was allowed to slowly cool to room temperature while stirring. The crude product was worked up with 20% hydrochloric acid, extracted with diethyl ether, and dried over anhydrous magnesium sulfate. Purification of the product was accomplished by column chromatography using a 5½ × 18 cm silica gel column with a hexane solvent system, the latter chosen based on thin layer chromatography results.[48] GC/MS analysis was completed on an HP Series II 5890 Gas Chromatograph with HP 5971 Series Mass Selective Detector equipped with an HP-5 (5% diphenyl, 95% dimethyl polysiloxane) capillary column. The pure product had a fragmentation pattern and mass to charge ratio (m/z = 393) consistent with that of tetrabromobenzene. Identification of the 1,2,3,5-tetrabromobenzene isomer was verified by ^{1}H NMR (δ = 7.73 ppm singlet) and decoupled ^{13}C NMR (δ = 135, 127, 126.5, and 122 ppm).

Synthesis of 1,2,3-Tribromobenzene:

1,2,3-Tribromobenzene was synthesized by the deamination of 2,6-dibromoaniline (Janssen Chimica, 97%) utilizing *tert*-butyl nitrite and bromination via cupric bromide. The same reactant ratios and procedure described for the synthesis of 1,2,3,5-tetrabromobenzene were followed except the reaction was allowed to proceed for 75 min before allowing it to come to room temperature. Purification of the crude product was not possible by simple column chromatography because 1,2,3,5-tetrabromobenzene was formed as a side product. Their separation was achieved by isothermal (300 °C) preparative gas chromatography on an HP F&M Scientific 700 Chromatograph equipped with a ⅜ inch × 10 ft SE-30 (polydimethyl siloxane 100% gum) packed column and

thermoconductivity detector (TCD). Standard grade helium was used as the carrier gas with a flow rate of approximately 50 mL/min in the sample column and approximately 30 mL/min in the smaller reference column. Analysis of the product was done using GC/NCIMS equipped with an SE-54 (5% phenyl, 95% methylpolysiloxane) Alltech Econo-Cap capillary column using a 90 - 275 °C, 20 °C per minute temperature program. GC/NCIMS equipment consists of a Varian 3400 Gas Chromatograph with splitless injection interfaced to a Finnigan 4023 Mass Spectrometer with ionization module set to negative ion chemical ionization mode using methane (Matheson, ultra high purity, 99.97%) as the buffer gas. The mass to charge ratio (m/z = 314) and fragmentation pattern observed was indicative of tribromobenzene. Comparison of retention times under GC/ FID conditions (above) on the Carbowax capillary column revealed that the product was neither 1,2,4- or 1,3,5-tribromobenzene. Verification of 1,2,3-tribromobenzene was completed by ^{1}H NMR (δ_1 = 7.02 ppm triplet and δ_2 = 7.58 ppm doublet, with areas of 0.9360 and 2.0000, respectively).

Luminescence Studies:

Fluorescence quantum yields, phosphorescence quantum yields, fluorescence quenching, and phosphorescent lifetime determinations were carried out on a Perkin-Elmer LS50B Luminescence Spectrometer equipped with the FL Data Manager software package. Solutions for room temperature analysis were transferred to a fluorescence quartz cuvette, nitrogen purged within the cell compartment, and quickly septa sealed. All emission spectra obtained were an average of three scans at a scan speed of 500

nm/min and manually set PMT voltage of 780 V. The polybromobenzenes were excited at 254 nm with a 290 nm emission filter in place while the 9,10-diphenylanthracene standard was excited at 332 nm with a 350 nm emission filter. Slit widths, excitation and emission, were varied depending on the experiment but the standards'setting was always consistent with that of the polybromobenzene sample. Under phosphorescence mode the delay, delay range (for lifetimes), gate, cycle times, and the number of flashes were adjusted according to the sample. Low temperature analyses were conducted with the accompanying Perkin-Elmer low temperature housing which was filled with liquid nitrogen for collection of spectra. Solutions were nitrogen purged prior to introduction into the 1 mm cylindrical quartz cell and immediately frozen.

Acknowledgements

This work has been supported by the National Institute of Environmental Health Sciences and the N. L. Tartar Research Foundation.

References

1. Buser, H. R. *Anal. Chem.*, **1986**, *58*, 2913-2919.

2. Bieniek, B.; Bahadir, M.; Korte, F. *Heterocycles*, **1989**, *28*, 719-722.

3. Klusmeier, W.; Vogler, P.; Ohrbach, K. H.; Weber, H.; Kettrup, A. *J. Anal. App. Pyrolysis*, **1988**, *13*, 277-285.

4. Freeman, P. K.; Clapp, G. E.; Stevenson, B. K. *Tetrahedron Letters*, **1991**, *32*, 5705-5708.

5. Freeman, P. K.; Ramnath, N.; Richardson, A. D. *J. Org. Chem.*, **1991**, *56*, 3643-3646.

6. Freeman, P. K.; Hatlevig, S. A. *Topics in Current Chemistry*, **1993**, *168*, 48-91.

7. Bunce, N. J.; Hayes, P. J.; Lemke, M. E. *Can. J. Chem.*, **1983**, *61*, 1103-1104.

8. Barltrop, J. A.; Coyle, J. D. *Excited States in Organic Chemistry*, **1975**, John Wiley & Sons, New York, NY, pp. 21-24.

9. Freeman, P. K.; Jang, J-S.; Ramnath, N. *J. Org. Chem.*, **1991**, *56*, 6072-6079.

10. Kavarnos, G. J. *Fundamentals of Photoinduced Electron Transfer*, **1993**, VCH Publishers, Inc., New York, NY, pp. 53-61.

11. Freeman, P. K.; Jang, J-S.; Ramnath, N. *J. Org. Chem.*, **1991**, *56*, 6072-6079.

12. Carey, F. A.; Sundberg, R. J. *Advanced Organic Chemistry. Part A: Structure and Mechanisms*, 3rd Ed., **1990**, Plenum Press, New York, NY, pp. 288-289.

13. McMillen, D. F.; Golden, D. M. *Ann. Rev. Phys. Chem.*, **1982**, *33*, 493.

14. Benson, S. W. *Thermochemical Kinetics*, **1968**, Wiley, New York, NY, pp. 215.

15. Marchetti, A. P.; Kearns, D. R. *J. Am. Chem. Soc.*, **1967**, *89*, 768-777.

16. Carey, F. A.; Sundberg, R. J. *Advanced Organic Chemistry. Part A: Structure and Mechanisms*, 3rd Ed., **1990**, Plenum Press, New York, NY, pp. 186.

17. Bunce, N. J.; LaMarre, J.; Vaish, S. P. *Photochemistry and Photobiology*, **1984**, *39*, 531-533.

18. Barltrop, J. A.; Coyle, J. D. *Excited States in Organic Chemistry*, **1975**, John Wiley & Sons, New York, NY, pp. 101.

19. Wilkinson, F.; Dubois, J. T. *J. Chem. Phys.*, **1963**, *39*, 377-383.

20. Ware, W. R. *J. Phys. Chem.*, **1962**, *66*, 455-458.

21. Birks, J. B. *Photophysics of Aromatic Molecules*, **1970**, Wiley-Interscience, London, pp. 496.

22. Clark, W. D. K.; Steel, C. *J. Am. Chem. Soc.*, **1971**, *93*, 6347.

23. Murov, S. L.; Carmichael, I.; Hug, G. L. *Handbook of Photochemistry*, 2nd Ed., **1993**, Marcel Dekker, Inc., New York, NY, pp. 208.

24. Kavarnos, G. J. *Fundamentals of Photoinduced Electron Transfer*, **1993**, VCH Publishers, Inc., New York, NY, pp. 291.

25. Performed in the laboratory of Dr. Joseph W. Nibler with Steve Mayer.

26. Dalton, J. C.; Wriede, P. A.; Turro, N. J. *J. Am. Chem. Soc.*, **1970**, *92*, 1318-1326.

27. Determined from 0-0 band of phosphorescence emission spectra obtained in absolute ethanol at 77°K.

28. Freeman, P. K.; Ramnath, N.; Richardson, A. D. *J. Org. Chem.*, **1991**, *56*, 3643-3646.

29. Hammond, G. S.; Liu, R. S. H. *J. Chem. Soc.,Chem. Commun.*, **1963**, *85*, 477-478.

30. Murov, S. L. *Handbook of Photochemistry*, **1973**, Marcel Dekker, Inc., New York, NY, pp. 59.

31. Fry, A. J.; Liu, R. S. H.; Hammond, G. S. *J. Am. Chem. Soc.*, **1966**, *88*, 4781-4782.

32. Lamola, A. A.; Hammond, G. S. *J. Chem. Phys.*, **1965**, *43*, 2129-2135.

33. Hammond, G. S.; Turro, N. J.; Leermakers, P. A. *J. Phys. Chem.*, **1962**, *66*, 1144-1147.

34. Hammond, G. S.; Saltiel, J.; Lamola, A. A.; Turro, N. J.; Bradshaw, J. S.; Cowan, D. O.; Counsell, R. C.; Vogt, V.; Dalton, C. *J. Am. Chem. Soc.*, **1964**, *86*, 3197-3217.

35. Coxon, J. M.; Halton, B. *Organic Photochemistry*, 2nd Ed., **1987**, Cambridge University Press, New York, NY, pp. 23-26.

36. Freeman, P. K.; Ramnath, N.; Richardson, A. D. *J. Org. Chem.*, **1991**, *56*, 3643-3646.

37. Freeman, P. K.; Jang, J.-S.; Ramnath, N. *J. Org. Chem.*, **1991**, *56*, 6072-6079.

38. Jang, J.-S. *Thesis*, **1990**, Oregon State University.

39. Takemura, T.; Yamada, Y.; Bada, H. *Chem. Phys.*, **1982**, *68*, 171-177.

40. Morris, J. V.; Mahaney, M. A.; Huber, J. R. *J. Phys. Chem.*, **1976**, *80*, 969-974.

41. Demas, J. N.; Crosby, G. A. *J. Phys. Chem.*, **1971**, *75*, 991-1024.

42. Parker, C. A. *Photoluminescence of Solutions*, **1968**, Elsevier Publishing Co., New York, NY, pp. 275.

43. Originated from conversations with Dr. Christine Pastorek and Dr. T. Darrah Thomas.

44. Bunce, N. J.; LaMarre, J.; Vaish, S. P. *Photochemistry and Photobiology*, **1984**, *39*, 531-533.

45. Bunce, N. J.; Schoch, J-P.; Zerner, M. C. *J. Am. Chem. Soc.*, **1977**, *99*, 7986-7991.

46. Calvert, J. G.; Pitts, J. N. *Photochemistry*, **1966**, John Wiley & Sons, New York, NY, pp. 781.

47. Doyle, M. P.; Seigfried, B.; Dellaria, J. F. *J. Org. Chem.*, **1977**, *42*, 2426-2431.

48. Casey, M.; Leonard, J.; Lygo, B.; Proctor, G. *Advanced Practical Organic Chemistry*, **1990**, Chapman and Hall, pp. 166-176.

Chapter 3

Photodebromination of Polybromobenzenes in the Presence of Electron Donors

Tara Lin Couch and Peter K. Freeman*

Department of Chemistry
Oregon State University
Corvallis, OR 97331

Introduction

The chemistry, and particularly the photochemistry, of halogenated aromatic compounds is currently a topic of great interest. These compounds are widely used for a variety of industrial purposes and are environmentally significant due to their toxicity and persistence.[1,2,3] Photodehalogenation has been shown to be a plausible method of halogen removal,[4,5,6] which then allows microorganisms to partake in their biodegradation process.[7] It has also been shown that photodehalogenation of some polyhaloarenes may be enhanced in the presence of electron donors.[8,9,10,11,12] In this study, the effect of two of these electron donors, triethylamine and sodium borohydride, on the photodebromination of polybromobenzenes has been determined.

Results and Discussion

The direct photodebromination of bromobenzene (**BB**), 1,2,4-tribromobenzene (**124TrBB**), and 1,2,3,5-tetrabromobenzene (**1235TBB**) cleanly results in the removal of bromine substituents via singlet state excimer intermediates.[13] The nature of the excimer intermediate, a complexed dimer originating from the ground state and singlet excited state, is believed to be partially charge separated, but not necessarily highly polar.[14] Exciplexes, formed by a complex of unlike compounds, are much more understood, and exhibit a complete charge separation.[15] The characteristic charge distributions can be exploited to increase product yields by using polar solvents. When an electron donor is added to the polybromobenzene photodebromination process, formation of exciplex intermediates, both singlet and triplet state, are encouraged through an electron transfer

reaction mechanism which provides additional product forming pathways that compete with singlet excimer initiated products.[16,17] Using triethylamine, TEA, as the electron donor creates an exciplex between a polybromobenzene radical anion and a TEA radical cation.[18] With sodium borohydride, $NaBH_4$, as the electron donor the exciplex is composed of a polybromobenzene radical anion and a borohydride radical.[19,20,21] Both exciplexes are depicted in Figure 3.1.

A mechanistic description of the donor assisted photodebromination of **BB**, **124TrBB**, and **1235TBB**, collectively abbreviated **ArBr**, with contributions from the singlet excimer, a triplet quencher, a singlet state exciplex, and a triplet state exciplex is given in Scheme 3.1. Absorption of 254 nm radiation promotes **ArBr** to the first excited singlet state, $\mathbf{ArBr}^{*1}$, which can then form a singlet excimer, k_{ex}, produce a singlet exciplex, k_{plex}, deactivate by fluorescence or non-radiative decay, k_d, or intersystem cross, k_{isc}, to a triplet excited state, $\mathbf{ArBr}^{*3}$. From the latter, a triplet exciplex may be formed, k_{tplex}, quenching can occur, k_q, or phosphorescence or non-radiative triplet decay, k_{td}, will demote the excited state. All the excited state complexes (singlet exciplex, singlet excimer, and triplet exciplex) are capable of producing debromination products (k_{pr}, k_r, and k_{tpr}, respectively), as mentioned, but may also undergo back electron or charge transfer (k_{pe}, k_e, and k_{tpe}, respectively).

Degassed versus Aerated Photolysis:

When oxygen, a well established triplet quencher, is completely removed from the photolysis, by sufficient degassing, a competition is set up for product formation

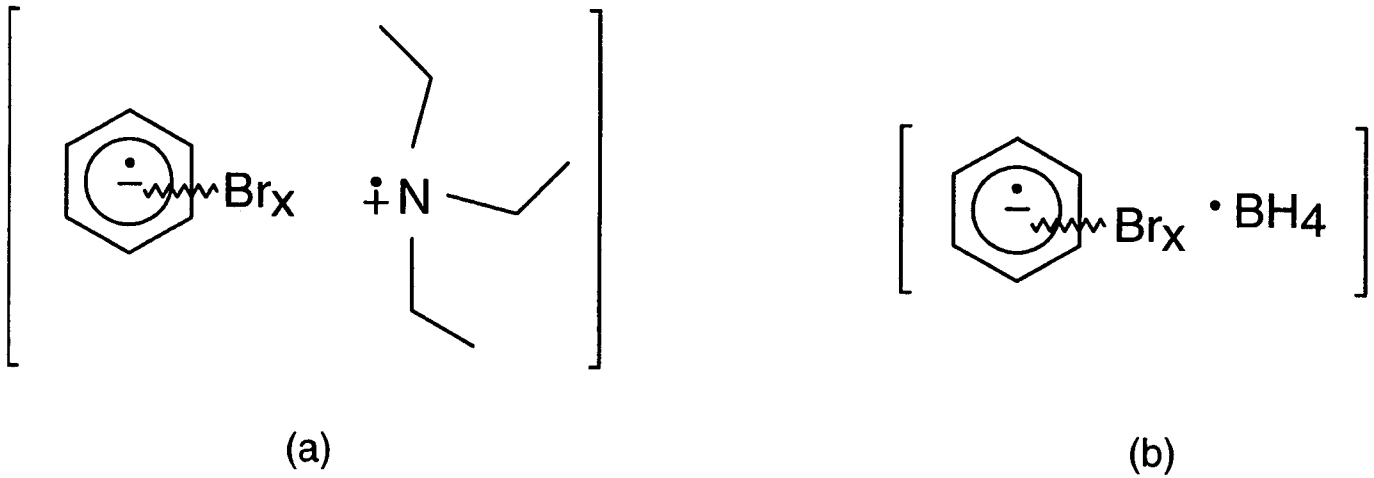

Figure 3.1. Proposed polybromobenzene singlet exciplexes with (a) triethylamine and (b) sodium borohydride.

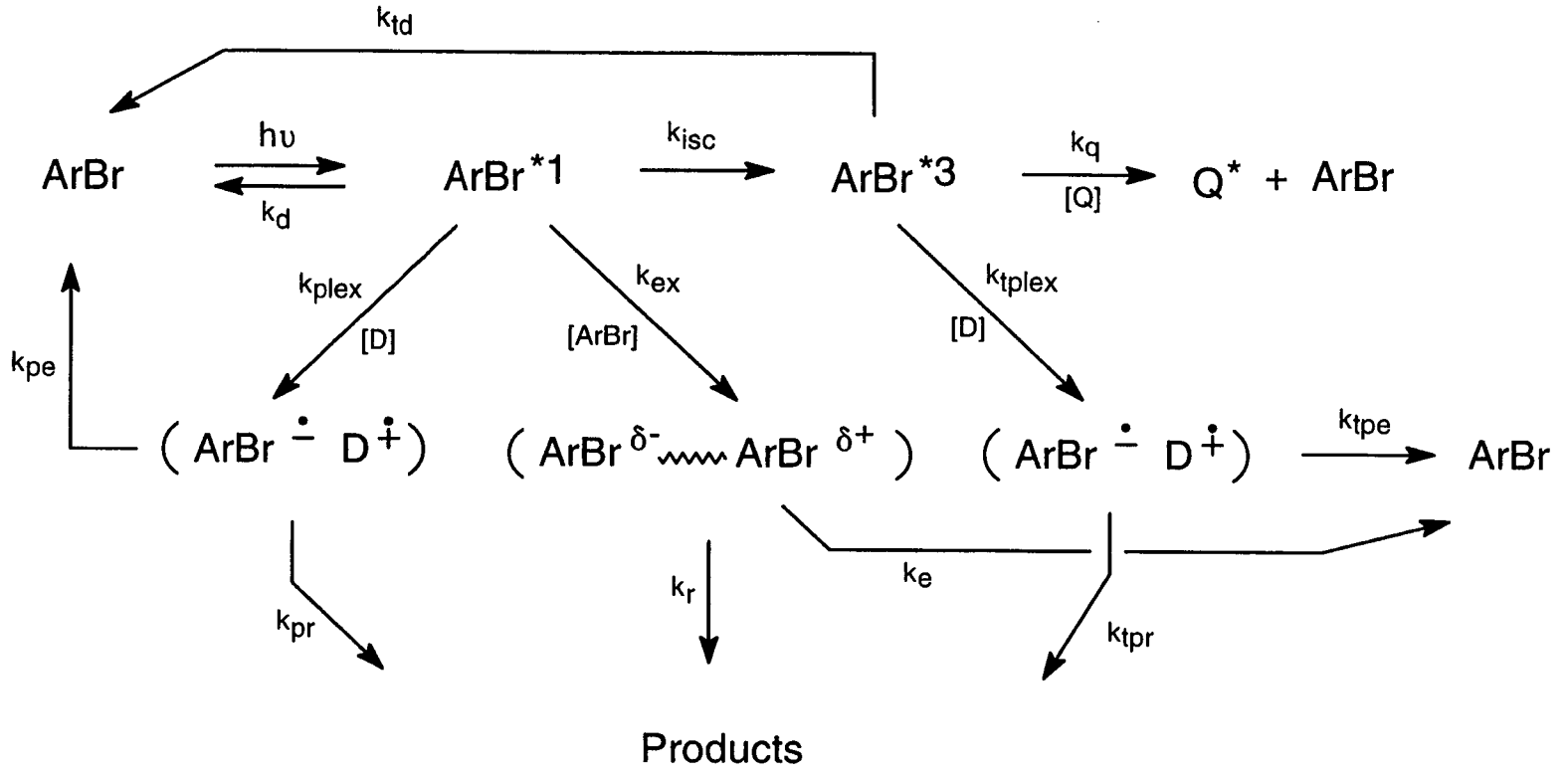

Scheme 3.1. Polybromobenzene photodebromination mechanism involving triplet quencher, singlet excimer, and possible triplet and singlet exciplexes.

between the three complexes. Using the steady state assumption,[22] a kinetic analysis of this competition may be formulated, Appendix D. A Stern-Volmer plot of the inverse product quantum yield, $1/\Phi_{products}$, against the inverse concentration of the electron donor, 1/[D], will be non-linear if this competition exists, equation 3.1.

$$\frac{1}{\Phi_{products}} = \frac{(k_d + k_{isc} + k_{ex}[ArBr] + k_{plex}[D])(k_{td} + k_{tplex}[D])}{(F_p k_{plex}[D] + F k_{ex}[ArBr])(k_{td} + k_{tplex}[D]) + F_{tp} k_{isc} k_{tplex}[D]} \qquad \textbf{(3.1)}$$

The singlet excimer will generate a flat horizontal region of the plot due to this pathways independence from the donor concentration, even though competition from the singlet and triplet exciplexes will cause the plot to be quadratic overall. However, if only one state of an exciplex is produced a linear relationship between $1/\Phi_{products}$ and 1/[D] will result, corresponding to either the singlet or triplet exciplex formation, equations 3.2 and 3.3, respectively. Here F_p is the efficiency of product formation from singlet exciplex, F_{tp} is the efficiency of product formation from the triplet exciplex, and ϕ_{isc} represents the efficiency of intersystem crossing.

$$\frac{1}{\Phi_{products}} = \frac{k_d + k_{isc}}{F_p k_{plex}[D]} + \frac{1}{F_p} \qquad \textbf{(3.2)}$$

$$\frac{1}{\Phi_{product}} = \frac{k_{td}}{F_{tp} \phi_{isc} k_{tplex}[D]} + \frac{1}{F_{tp} \phi_{isc}} \qquad \textbf{(3.3)}$$

Performing a linear regression on this region will provide an intercept and a slope, which

can be mathematically related as a ratio, intercept/slope, of $k_{plex} / (k_d + k_{isc})$ for a singlet exciplex and k_{tplex} / k_{td} for a triplet exciplex.

When oxygen is present, Q = O_2, its extremely effective triplet quenching ability quickly irradicates any triplet moiety that is formed[23] and eliminates the possibility of a triplet exciplex in Scheme 3.1. Taking this condition into account, the previous kinetic analysis is still non-linear, but markedly simplifies to equation 3.4.

$$\frac{1}{\Phi_{products}} = \frac{k_{isc} + k_d + k_{plex}[D] + k_{ex}[ArBr]}{F_p k_{plex}[D] + F k_{ex}[ArBr]} \qquad \textbf{(3.4)}$$

Now even with competition between singlet complexes, two distinct portions of the Stern-Volmer plot will be evident. One independent of the inverse donor concentration from the singlet excimer, and another linearly dependent region due to the singlet exciplex, respresented above as equation 3.2. Relating the intercept to the slope, in ratio format, again gives $k_{plex} / (k_{isc} + k_d)$ which may be rewritten as $k_{plex}\tau_f$, where τ_f is the polybromobenzene singlet lifetime. The rate of singlet exciplex formation may be calculated from this expression.

Photolysis experiments under both degassed and aerated conditions were conducted on **124TrBB** in the presence of TEA in acetonitrile. The concentration of **124TrBB**, one which is known to produce a singlet excimer, was held constant while TEA concentrations were varied in a range that ensured that the polybromobenzene absorbed the majority of the incident radiation, calculated from measured molar extinction coefficients, ϵ_{254} (616 $M^{-1}cm^{-1}$ for **124TrBB** and 45.5 $M^{-1}cm^{-1}$ for TEA).

Product quantum yields were calculated from the appearance of the dibromobenzene products, 18 ± 2% conversion (degassed) and 7 ± 1% conversion (aerated), and plotted against the corresponding inverse TEA concentrations. Both conditions, degassed and aerated, produced linear plots, Figures 3.2 and 3.3, with good correlation coefficients, 0.985 and 0.997, respectively. The observed linearity suggests that for the photodebromination of **124TrBB**, the presence of TEA results in an exciplex rather than an excimer. Furthermore, oxygen does not significantly quench the reaction. In fact, the intercept to slope ratios for degassed and aerated solutions are similar, 1778 ± 162 and 952 ± 61, respectively, indicating that both proceed through the same reaction pathway, a singlet exciplex. This result is also consistent with the previous excimer study, which showed that singlet reactivity for **BB**, **124TrBB**, and **1235TBB** is dominant. For this reason, the remaining studies were conducted in aerated solutions.

Photolysis experiments on **BB** and **1235TBB** in the presence of TEA were also performed in acetonitrile. The polybromobenzene concentrations were held constant as the concentration of TEA was varied, making sure that **BB** and **1235TBB** absorbed the majority of the incident radiation, as determined by molar extinction coefficients, ϵ_{254} (123.3 $M^{-1}cm^{-1}$, 1433 $M^{-1}cm^{-1}$, and 45.5 $M^{-1}cm^{-1}$, for **BB**, **1235TBB**, and TEA, respectively). For **BB**, the extent of reaction, 10 ± 4%, and the quantum yield were calculated by the loss of **BB** starting material. A graph of the inverse quantum yield against the inverse TEA concentration was then constructed, Figure 3.4, and observed to be linear, with a reasonable correlation coefficient, 0.973. The result suggests that the mechanism of **BB** photodebromination is also driven by exciplex formation in the

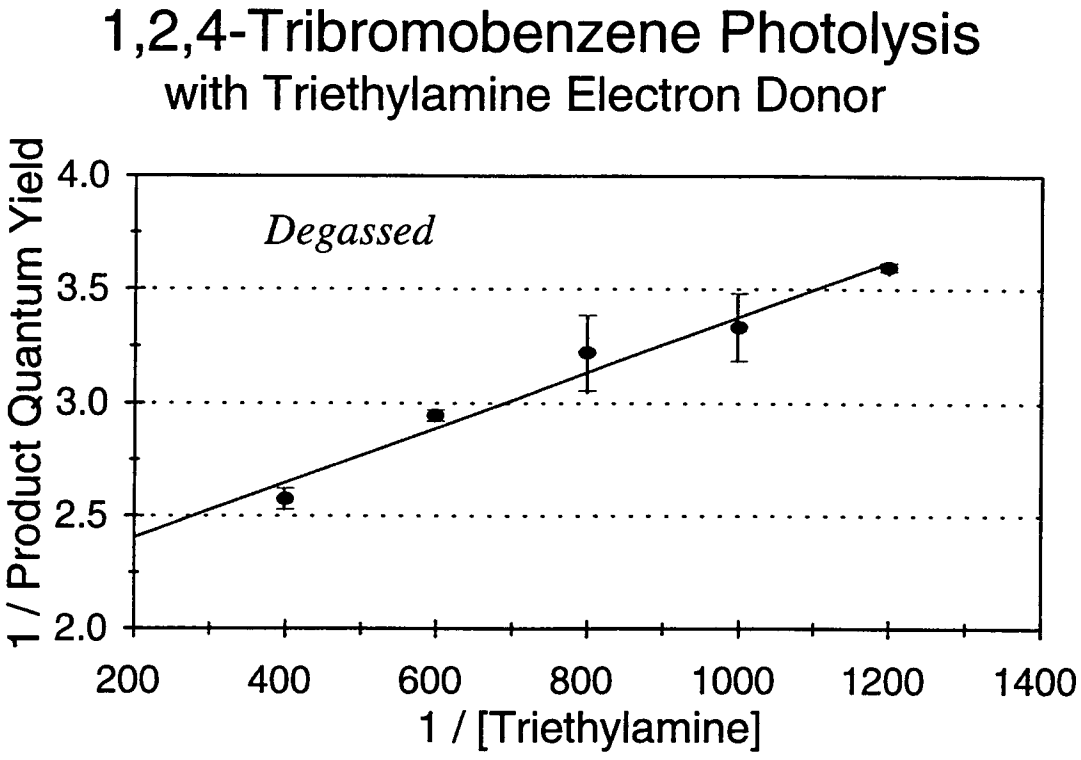

Figure 3.2. Degassed photodebromination of 1,2,4-tribromobenzene with triethylamine at 254 nm in acetonitrile.

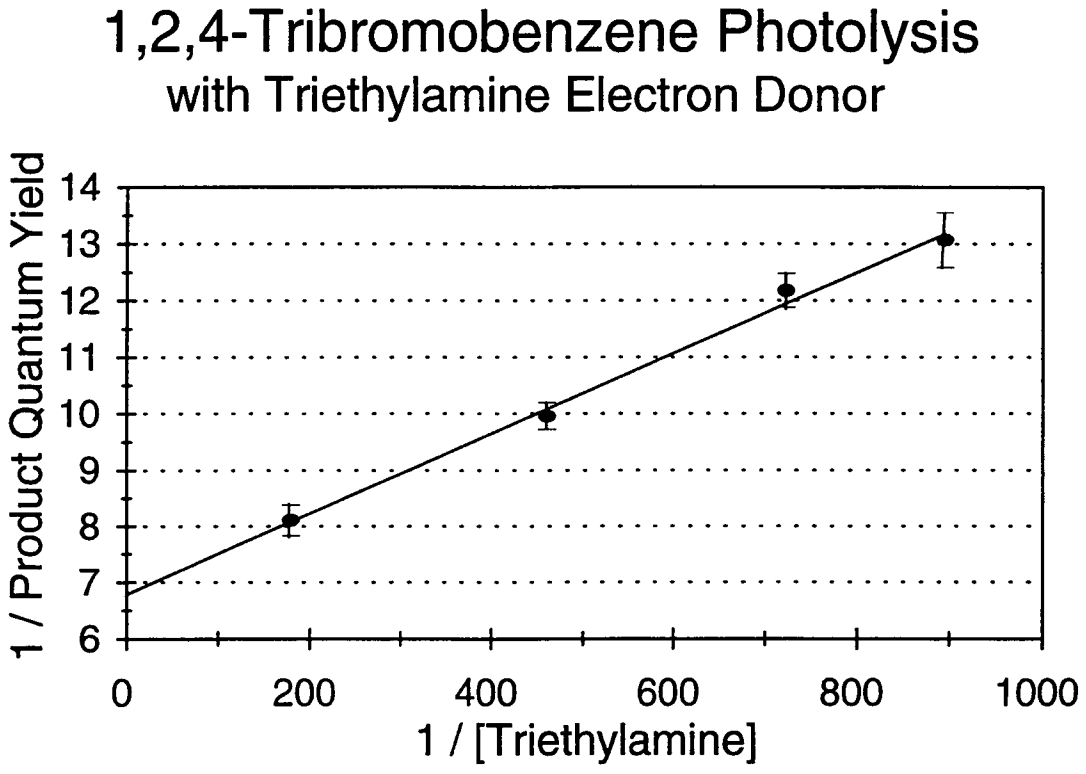

Figure 3.3. Photodebromination of 1,2,4-tribromobenzene with triethylamine at 254 nm in acetonitrile.

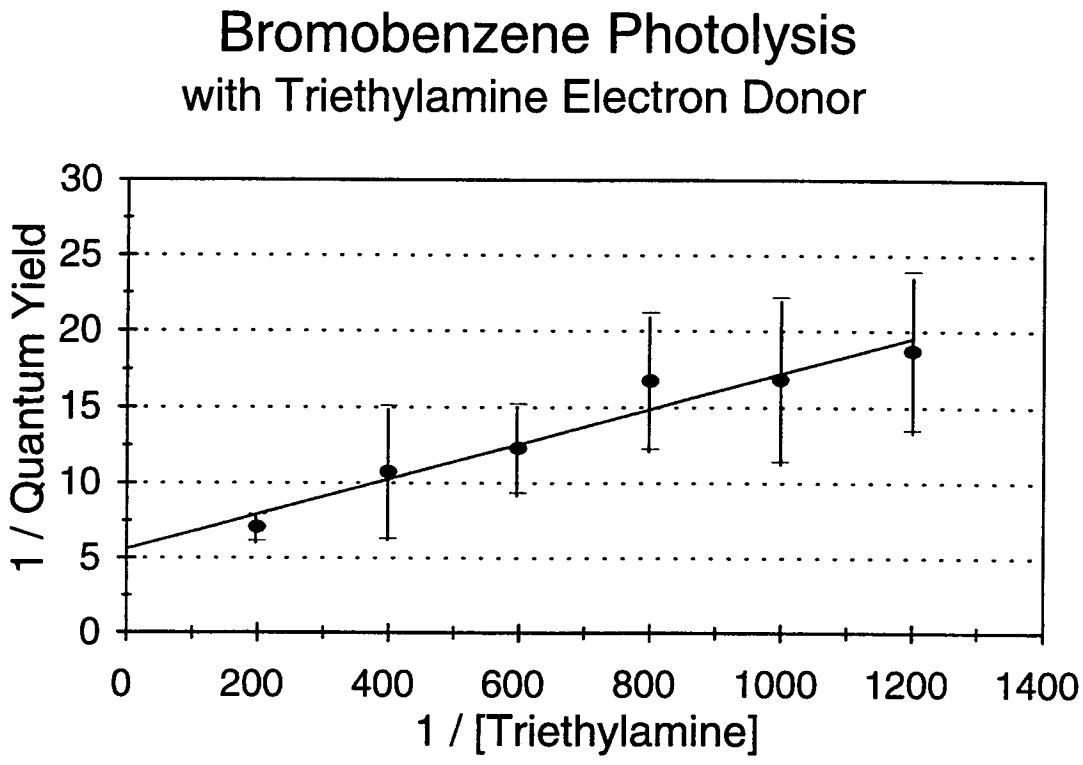

Figure 3.4. Photodebromination of bromobenzene with triethylamine at 254 nm in acetonitrile.

presence of TEA. The results of the photolysis of **1235TBB** differ. Using the product quantum yield of an 11 ± 2% conversion reaction, the Stern-Volmer plot is non-linear, Figure 3.5. This result, pertaining to equation 3.4, indicates that for **1235TBB**, singlet exciplex and singlet excimer complexes compete in the photodebromination. The linear portion of the graph displays a good correlation coefficient, 0.978, as does the flat independent region which exhibits a $1/\Phi_{products}$ value of 8.6 ± 0.2.

$NaBH_4$ was also used as an electron transfer reagent. Photolysis experiments were conducted on **BB**, **124TrBB**, and **1235TBB** in acetonitrile with a 4% deionized water content. The latter does not have a chromophore which absorbs around the wavelength of excitation so its concentration range was kept to that of the TEA electron donor for consistency. **BB**, **124TrBB**, and **1235TBB** concentrations were maintained at values similar to those of the TEA experiments, and reactions were kept to conversions of 18 ± 13%, 8 ± 3%, and 22 ± 5%, respectively. Product quantum yields were determined, disappearance quantum yield for **BB**, and their inverse was plotted against the inverse $NaBH_4$ concentration. From the resulting graphs, Figures 3.6, 3.7, and 3.8, it is clear that the plots for **BB** and **124TrBB** are linear, while that for **1235TBB** is not, respectively. Correlation coefficients for **BB**, 0.990, and **124TrBB**, 0.981, are good. The graph of **1235TBB** again has two regions, each with good precision, a 0.997 correlation coefficient for the exciplex portion and an average $1/\Phi_{products}$ value of 11.6 ± 0.3 for the excimer range. This reflects the rationale that in the presence of $NaBH_4$, **BB** and **124TrBB** proceed solely through singlet exciplexes, but **1235TBB** reacts through both a singlet exciplex and a singlet excimer.

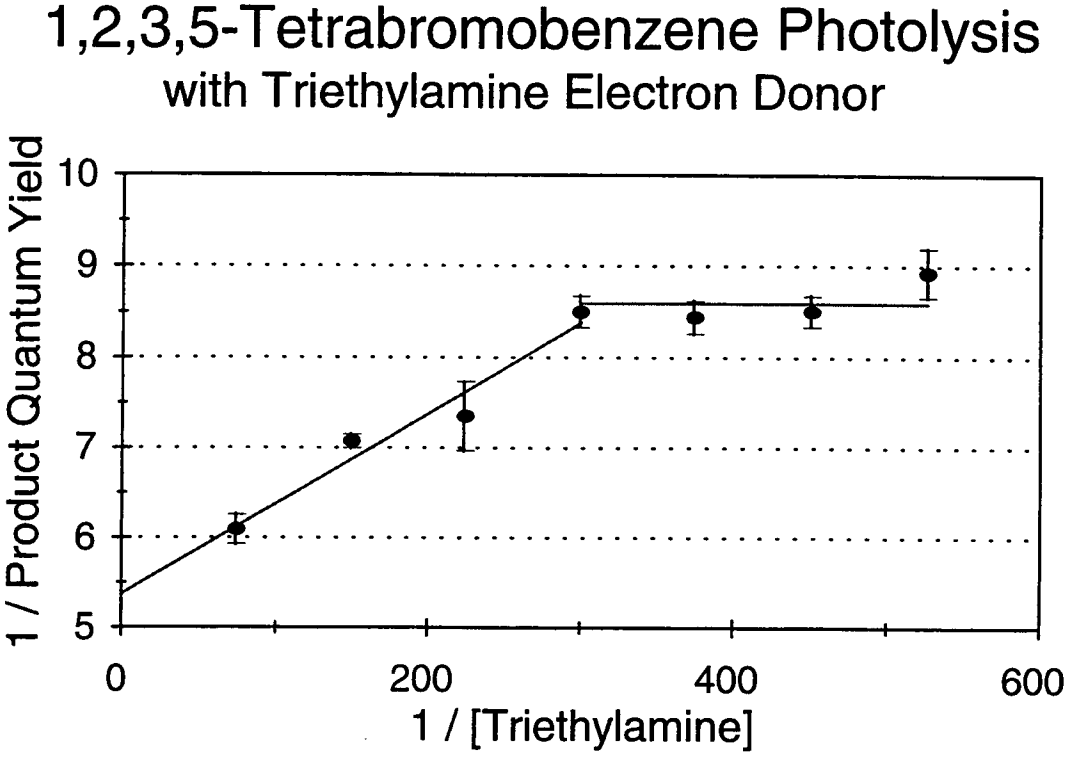

Figure 3.5. Photodebromination of 1,2,3,5-tetrabromobenzene with triethylamine at 254 nm in acetonitrile.

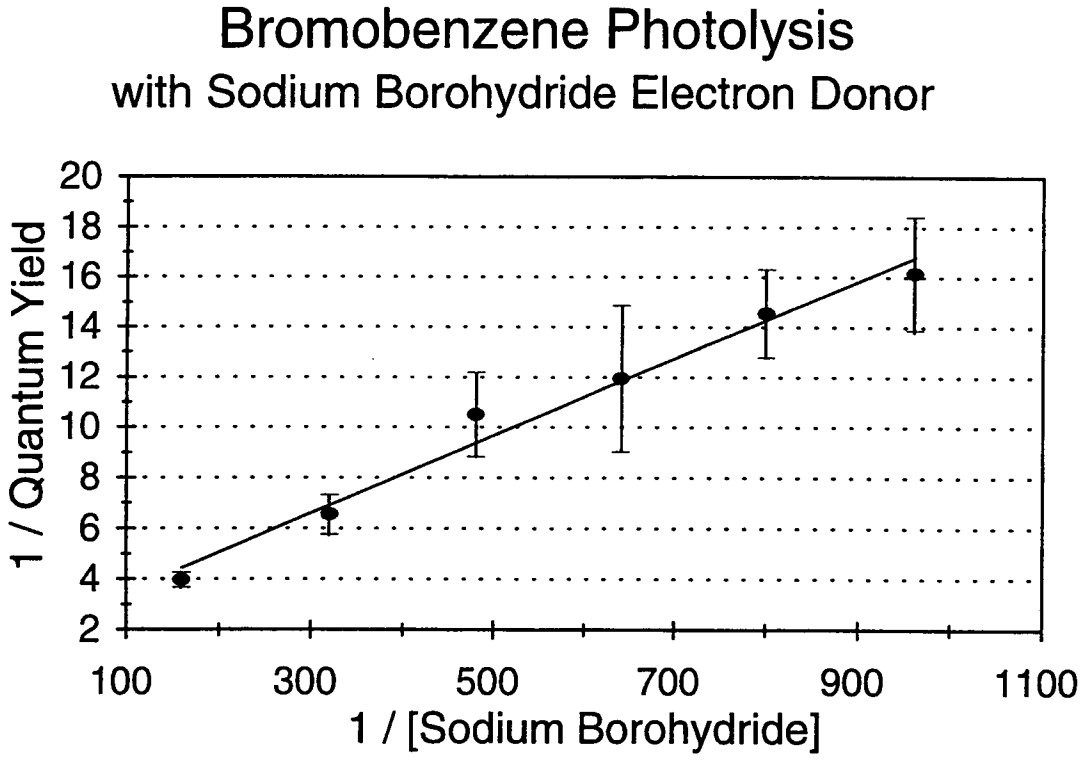

Figure 3.6. Photodebromination of bromobenzene with sodium borohydride at 254 nm in acetonitrile.

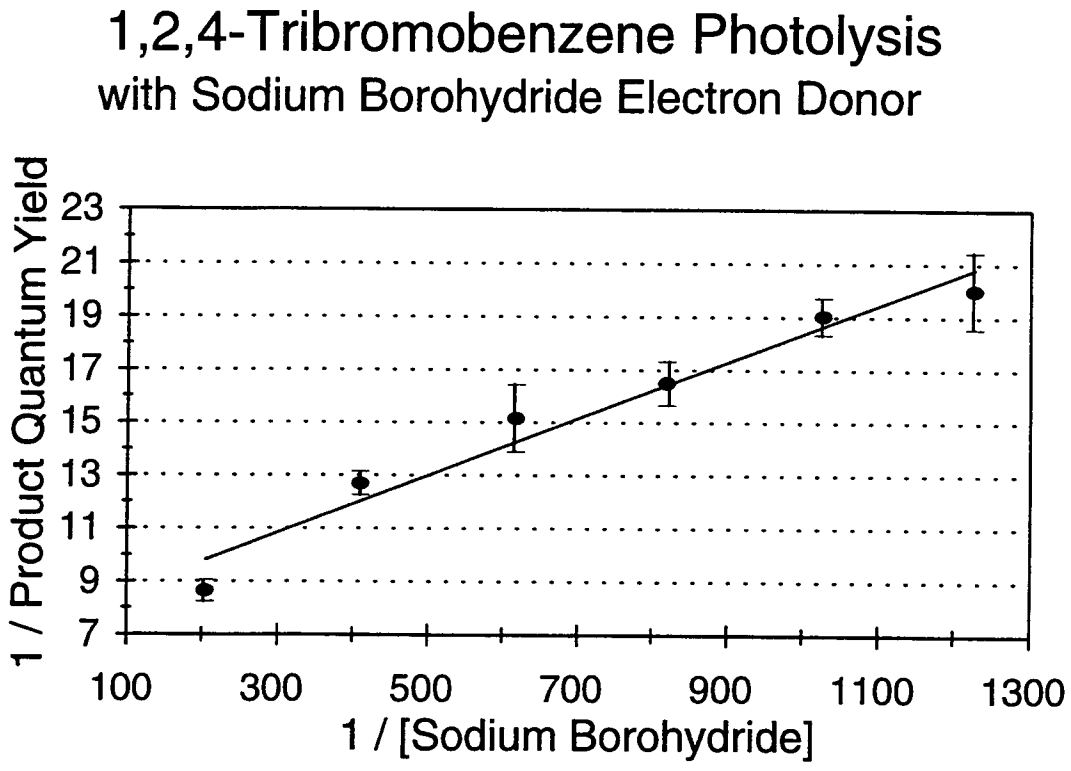

Figure 3.7 Photodebromination of 1,2,4-tribromobenzene with sodium borohydride at 254 nm in acetonitrile.

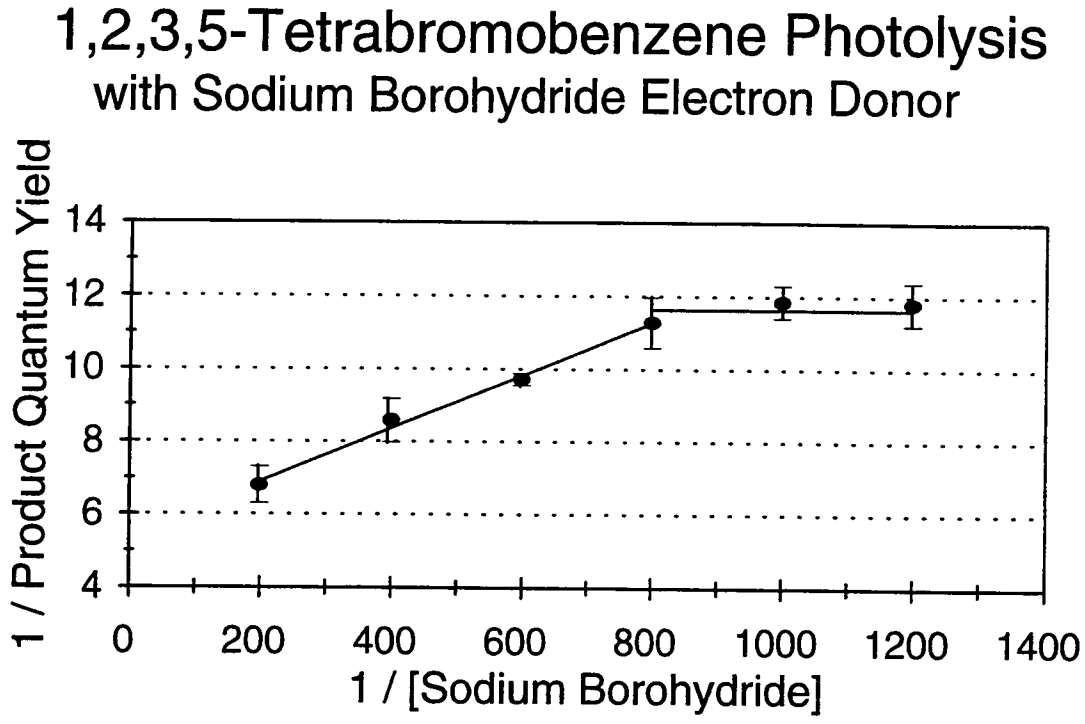

Figure 3.8. Photodebromination of 1,2,3,5-tetrabromobenzene with sodium borohydride at 254 nm in acetonitrile.

As mentioned previously, the rate of formation of the singlet exciplexes, k_{plex}, may be determined from the intercept to slope ratio of the linear plots, given singlet polybromobenzene lifetimes; these are listed in Table 3.1. From the table it is apparent that formation of the exciplex is diffusion controlled, as it must be to compete with singlet excimer formation. Caldwell et al, have also reported diffusion contolled exciplex formation rates for a variety of electron donors, including TEA.[24] It is also interesting to note that the TEA exciplex appears to have a slightly faster formation rate than that of the $NaBH_4$ exciplex for **BB**, however exciplex formation rate constants for **124TrBB** and **1235TBB**, are quite close for the two reagents. The presence of the electron donors also increases the photolability of the photodebrominations, as illustrated in Table 3.2. When TEA is used as the donor, it increases the efficiency of the reaction by at least 24% and when $NaBH_4$ is the donor it increases by at least 39%.

Fluorescence quenching experiments can be used to identify a singlet exciplex. As the concentration of the electron donating species is gradually increased the likelihood of exciplex formation will increase proportionally. Since exciplex formation is in direct competition with fluorescence, a decrease in the luminescence signal will be observed. Several attempts at fluorescence quenching of **1235TBB** with TEA were unsuccessful, in that the fluorescence quantum yield of the polybromoarene did not change with quencher concentration. From the previous experiments with **1235TBB**, it was demonstrated that a competition between exciplex and excimer intermediates arise as the electron donor concentration approaches 3.3×10^{-3} M. Fluorometric measurements cannot be made at this concentration, because of excessive absorption of the excitation radiation at 254 nm

Table 3.1. Singlet exciplex formation rates for the polybromobenzenes in acetonitrile.

Photolysis Reaction	Intercept / Slope [A]	k_{plex} [B] (s^{-1})
BB with TEA	486 ± 112	1.0×10^{11}
BB with $NaBH_4$	128 ± 46	2.7×10^{10}
124TrBB with TEA	952 ± 61	3.7×10^{11}
124TrBB with $NaBH_4$	707 ± 105	2.7×10^{11}
1235TBB with TEA	537 ± 111	1.1×10^{11}
1235TBB with $NaBH_4$	747 ± 49	1.6×10^{11}

[A] Errors calculated by propagation.

[B] Determined with singlet lifetimes, τ_f, of 4.8 ns, 2.6 ns, and 4.7 ns for **BB**, **124TrBB**, and **1235TBB**, respectively, which were calculated from $\tau^0_f\Phi_f$ where τ^0_f is a maximum of 5 ns for each polybromobenzene.

Table 3.2. Affect of triethylamine and sodium borohydride electron donors on the quantum yield of bromobenzene, 1,2,4-tribromobenzene, and 1,2,3,5-tetrabromobenzene aerated photodebromination reactions.

Compound	$\Phi_{products}$ Excimer	$\Phi_{products}$ [A] TEA Exciplex	$\Phi_{products}$ [B] BH_4^- Exciplex	Increase in Reaction
BB				
2.00×10^{-2} M	0.075	0.1	---	36%
2.00×10^{-2} M	0.075	---	0.17	56%
124TrBB				
5.00×10^{-3} M	0.049	0.12	---	58%
3.98×10^{-3} M	0.046	---	0.097	53%
1235TBB				
2.97×10^{-3} M	0.0964	0.13	---	24%
2.04×10^{-3} M	0.0839	---	0.14	39%

[A] TEA concentration of 4.00×10^{-3} M.
[B] $NaBH_4$ concentration of 4.00×10^{-3} M.

and the corresponding loss of the fluorescence signal. Therefore, it was necessary to scale down the concentrations of both **1235TBB** and TEA by factors of 100, utilizing a constant 3.56×10^{-5} M **1235TBB** solution and varying TEA concentrations of 0 to 1.25×10^{-4} M. At these lower concentrations, the effective exciplex concentration is too low to significantly affect the polybromobenzene fluorescence. Assuming that k_f is 2.1×10^8 s^{-1}, k_{ex} is 1.5×10^{11}, k_{plex} is 1.1×10^{11}, and Φ_f is one,[25] the definition of the fluorescence quantum yield shows that only approximately a 9% change would be expected at the highest TEA concentration employed.

Nature of Product Determining Intermediate:

All three polybromobenzenes have been shown to form singlet excimer intermediates[26] and singlet exciplex intermediates at diffusion controlled rates. The preference for one intermediate over the other can be examined mathematically by recalling that equation 3.4 kinetically governs the photodebromination process. For only a singlet exciplex to develop, equation 3.5 must be true.

$$F_p k_{plex}[D] \; > \; F k_{ex}[ArBr] \qquad \textbf{(3.5)}$$

The efficiencies of product formation from the singlet intermediates, F and F_p for the excimers and exciplexes, respectively, of **BB**, **124TrBB**, and **1235TBB** were retrieved as the inverse intercept from the linear portions of the appropriate Stern-Volmer plots. These values are 0.11, 0.072, and 0.14 for F; 0.18, 0.15, and 0.19 for F_p with TEA; and 0.051, 0.13, and 0.18 for F_p with $NaBH_4$, corresponding to **BB**, **124TrBB**, and **1235TBB**,

respectively. Since all the F variables and the intermediate formation rates are almost identical for each individual polybromobenzene, the relative concentrations of **ArBr** to the participating electron donor must be the overriding factor. In accordance with equation 3.5, this translates into an [**ArBr**]/[D] ratio less than 1 for exciplex formation. Table 3.3 illustrates the conditions under which the donor assisted photodebrominations of **BB**, **124TrBB**, and **1235TBB** were conducted. From the table, it is clear that the ratio values of **1235TBB** with both TEA and $NaBH_4$ as the donor are in complete agreement with this mathematical procedure. However, **BB** and **124TrBB** display the exact opposite of what would be predicted, by exhibiting [**ArBr**]/[D] values greater than 1 for the region that corresponds to the exciplex intermediate. In other words, even though **BB** and **124TrBB** should kinetically be forming singlet excimers, they are instead forming singlet exciplexes. The only explanation would seem to be that in these cases the reaction is not a function of a pure kinetic argument.

Regiochemistry:

To investigate the nature of the exciplex intermediate further, the regiochemical outcomes from the photodebromination of **124TrBB** and **1235TBB** were compared. It was previously shown, Chapter 2, that when going through a singlet excimer, the regiochemical outcome of the photodebromination was determined by the removal of *ortho*-bromine strain.[27,28,29] However, the excimer intermediate is not a charge separated species, and is therefore likely to give differing regiochemistry.

Table 3.3. Polybromobenzene exciplex conditions.

Polybromobenzene	[TEA]	[$NaBH_4$]	[**ArBr**]/[TEA]	[**ArBr**]/[$NaBH_4$]
BB [A]	8.33×10^{-4}	1.04×10^{-3}	24.0	19.2
	1.00×10^{-3}	1.25×10^{-3}	20.0	16.0
	1.25×10^{-3}	1.56×10^{-3}	16.0	12.8
	1.67×10^{-3}	2.08×10^{-3}	12.0	9.62
	2.50×10^{-3}	3.12×10^{-3}	8.00	6.41
	5.00×10^{-3}	6.24×10^{-3}	4.00	3.21
124TrBB [B]	1.12×10^{-3}	8.15×10^{-4}	4.46	4.88
	1.38×10^{-3}	9.73×10^{-4}	3.62	4.09
	2.17×10^{-3}	1.22×10^{-3}	2.30	3.26
	5.55×10^{-3}	1.62×10^{-3}	0.901	2.46
	---	2.44×10^{-3}	---	1.63
	---	4.88×10^{-3}	---	0.816
1235TBB [C]	1.90×10^{-3}	8.34×10^{-4}	*1.56*	*2.45*
	2.22×10^{-3}	1.00×10^{-3}	*1.34*	*2.04*
	2.66×10^{-3}	1.25×10^{-3}	*1.12*	1.63*
	3.33×10^{-3}	1.67×10^{-3}	0.892*	1.22
	4.45×10^{-3}	2.50×10^{-3}	0.667	0.816
	6.66×10^{-3}	5.00×10^{-3}	0.446	0.408
	1.33×10^{-2}	---	0.223	---

[A] Bromobenzene concentration held at 2.00×10^{-2} M for both exciplex reactions.
[B] 1,2,4-Tribromobenzene concentration held at 5.00×10^{-3} M and 3.98×10^{-3} M, for triethylamine and sodium borohydride exciplex reactions, respectively.
[C] 1,2,3,5-Tetrabromobenzene concentration held at 2.97×10^{-3} M and 2.04×10^{-3} M, for triethylamine and sodium borohydride exciplex reactions, respectively.
Values in *italic* correspond to the excimer region of the **1235TBB** Stern-Volmer plot.
* "Rollover point" observed in the Stern-Volmer plot.

The non-photochemical reduction of **124TrBB** with 4-4'-di-*tert*-butylbiphenyl radical anion in tetrahydrofuran, THF, is an example of a well established electron transfer reaction.[30,31] The lithium 4-4'-di-*tert*-butylbiphenylide reagent, LiDBB, serves as an electron transfer agent and leads to the debromination of **124TrBB**, Figure 3.9. If the exciplex mechanisms, TEA and $NaBH_4$, are also electron transfer mechanisms, as proposed, their regiochemical outcome should be similar to that of the LiDBB reaction. To rule out the possibility of a solvent effect, the photolysis of **124TrBB** with TEA was also carried out in THF, but resulted in the same regiochemistry as that found in acetonitrile.

The regiochemistry of all debromination reactions carried out on **124TrBB** are given in Table 3.4. Unexpectedly, the regiochemistry from the singlet excimer reaction is not much different from that of the electron transfer mechanisms. It also appears that both the TEA exciplex and the BH_4^- exciplex produce regiochemistry which is very similar to the LiDBB electron transfer reaction. The regiochemistry of all debromination reactions of **1235TBB** are given in Table 3.5. As with **124TrBB**, the regiochemistry of the excimer is suprisingly similar to that of the exciplexes.

Assuming that the donor assisted photodebrominations of **124TrBB** and **1235TBB** proceed through aryl radical anions which preferentially cleave a bromide ion,[32] computational predictions of the corresponding regiochemical outcomes were prepared. Gaussian 94,[33] *ab initio* ROHF/6-31G* geometry optimizations were performed for each competing pathway for **124TrBB** and **1235TBB** as shown in Figures 3.10 and 3.11, respectively. In the case of **124TrBB**, the calculations illustrate that

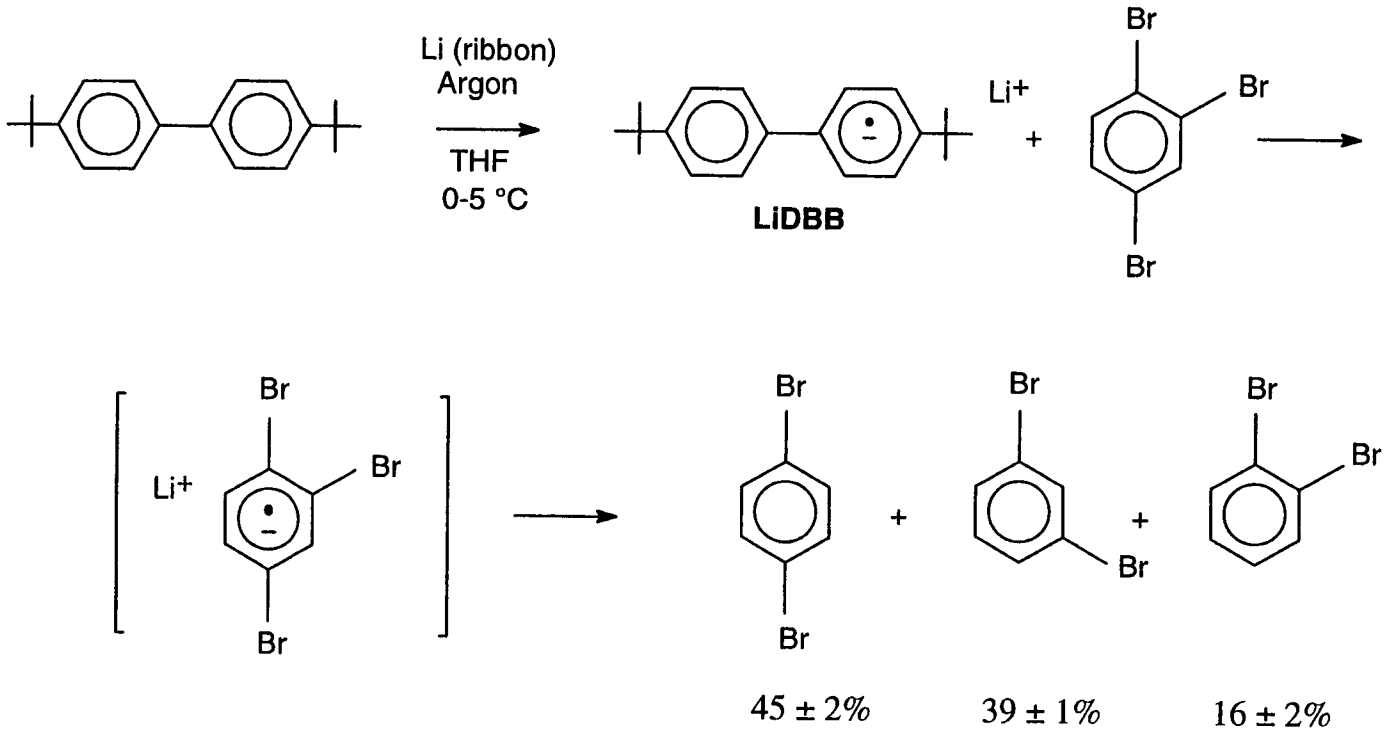

Figure 3.9. Reduction of 1,2,4-tribromobenzene by LiDBB radical anion.

Table 3.4 Regiochemical outcome of various photodebromination reactions of 1,2,4-tribromobenzene.

Reaction	*para*-Dibromobenzene (%)	*meta*-Dibromobenzene (%)	*ortho*-Dibromobenzene (%)
Excimer[A]	44.1 ± 0.2	48.7 ± 0.2	7.3 ± 0.1
LiDBB reduction[B]	45 ± 2	39 ± 1	16 ± 2
Exciplex: TEA[C]	53.0 ± 0.6	39.2 ± 0.4	7.8 ± 0.2
Exciplex: TEA[A]	56.2 ± 0.1	38.4 ± 0.2	5.4 ± 0.2
Exciplex: $NaBH_4$[A]	42.7 ± 0.4	46.4 ± 0.3	11.0 ± 0.5
Computational Prediction[D]	72	25	3

[A] Aerated photolysis in acetonitrile at 254 nm.
[B] Chemical reduction in dry tetrahydrofuran under inert atmosphere.
[C] Degassed photolysis in acetonitrile at 254 nm.
[D] Determined from the Arrhenius equation using *ab initio* ROHF/6-31G* energies.

Table 3.5. Regiochemical outcome of various photodebromination reactions of 1,2,3,5-tetrabromobenzene.

Reaction[A]	1,3,5-Tribromobenzene (%)	1,2,4-Tribromobenzene (%)	1,2,3-Tribromobenzene (%)
Excimer	62.9 ± 0.6	31.5 ± 0.4	5.6 ± 0.6
Exciplex: TEA	54.1 ± 0.6	40.7 ± 0.3	5.2 ± 0.2
Exciplex: $NaBH_4$	63 ± 1	35.8 ± 0.5	1.6 ± 0.7
Computational Prediction[B]	58	42	< 1

A) Aerated photolysis in acetonitrile at 254 nm.
B) Determined from the Arrhenius equation using *ab initio* ROHF/6-31G* energies.

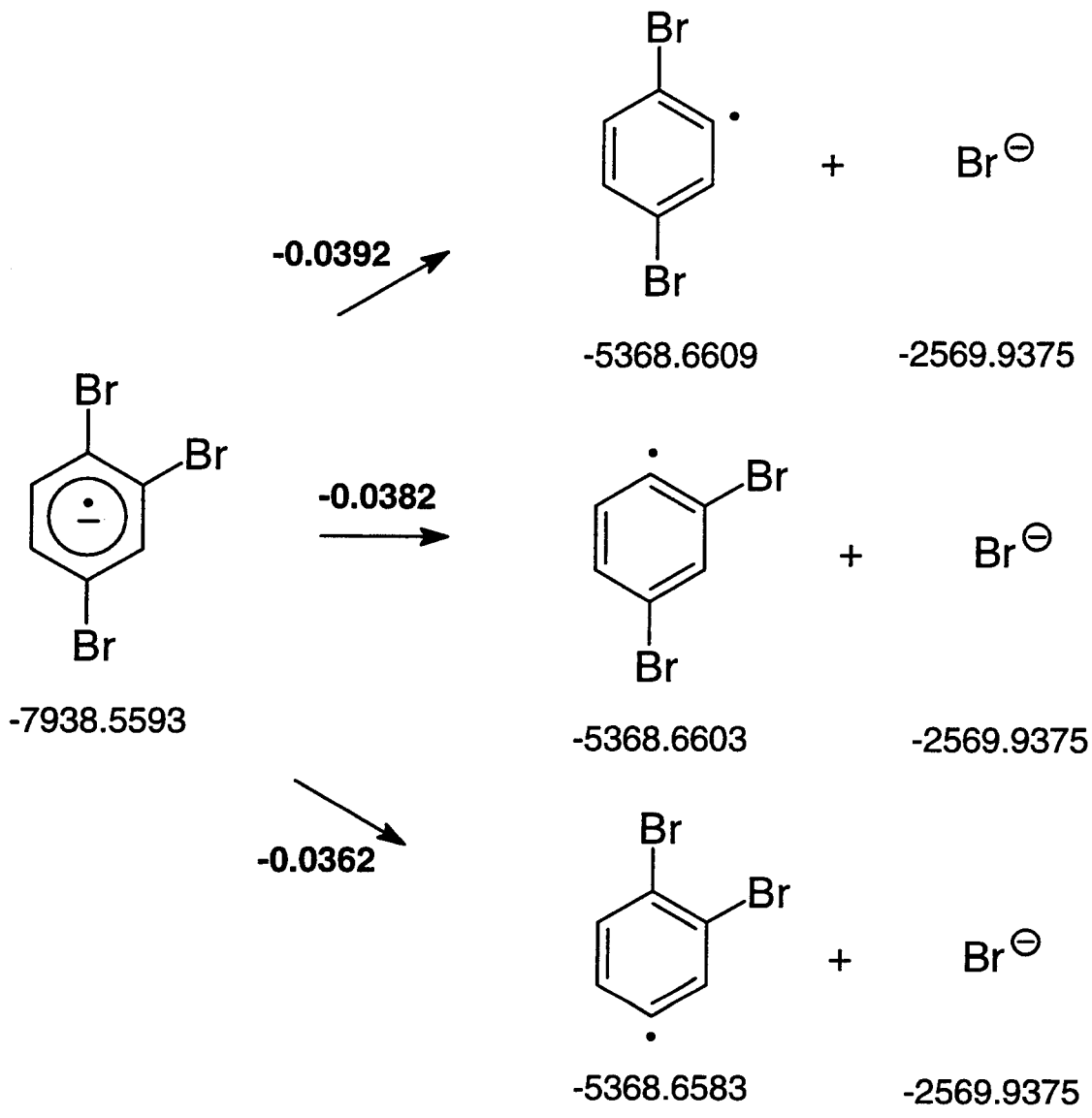

Figure 3.10. Computational ROHF/6-31G* regiochemical prediction of 1,2,4-tribromobenzene donor assisted photodebromination. Energies given in Hartrees.

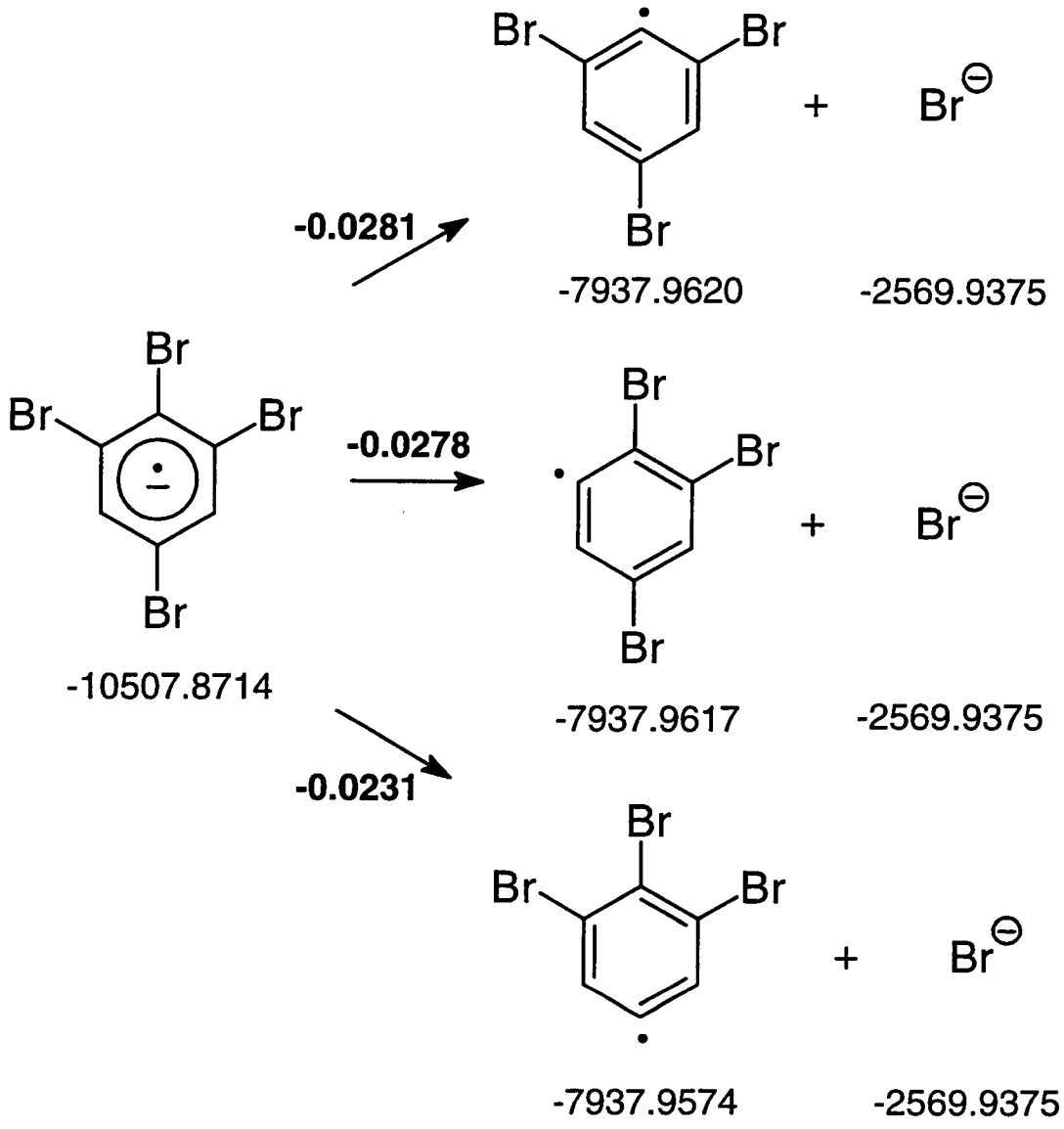

Figure 3.11. Computational ROHF/6-31G* regiochemical prediction of 1,2,3,5-tetrabromobenzene donor assisted photodebromination. Energies given in Hartrees.

formation of the *para*-dibromobenzene isomer provides the most exothermic pathway. For **1235TBB**, the 1,3,5-aryl radical is preferred. The activation energies of the competing processes were used to make quantitative kinetic predictions based on the Arrhenius equation, equation 3.6, where k_r is the rate of the reaction, E_a is the activation energy, R is the gas constant, and T is the temperature in Kelvin.

$$k_r = A \exp\left(\frac{-E_a}{RT}\right) \qquad \textbf{(3.6)}$$

The constant A is an entropy term which is assumed to be the same for the competing pathways since they all correspond to cleavage of an aromatic C-Br bond from either the tri- or tetra- substituted polybromobenzene. By dividing the rates of both *para*- and *meta*-dibromobenzene formation by the rate of *ortho*-dibromobenzene formation a regiochemical prediction was determined for **124TrBB**. In a similar manner a **1235TBB** Arrhenius prediction was determined using the formation of 1,2,3-tribromobenzene as the divisor. These computational predictions are included in the regiochemical comparisons for both **124TrBB** and **1235TBB**, Tables 3.4 and 3.5, respectively. This computational prediction of **124TrBB** is qualitatively correct, but the amount of *para*-dibromobenzene appears to be overestimated. In the case of **1235TBB**, the computational prediction agrees remarkably well with the experimentally observed results of donor assisted photodebromination.

Conclusions

In conclusion, the photodebrominations of **BB**, **124TrBB**, and **1235TBB** are modestly enhanced in the presence of electron donors, TEA and $NaBH_4$, by the diffusion controlled formation of singlet exciplex intermediates. Formation of the **1235TBB** exciplexes have been kinetically explained, but formation of the **BB** and **124TrBB** exciplexes cannot be described in the same manner. Exciplex intermediates of **124TrBB** and **1235TBB** with TEA and $NaBH_4$ appear to be charge separated species, according to regiochemical observations and comparisons. Moreover, their regiochemistries are suprisingly similar to those of excimer complexes suggesting a similar type of charge distribution in the different intermediates. Computational regiochemical predictions have also been used to confirm the charge separated species of the donor assisted photodebromination of **1235TBB**.

Experimental

Materials:

Bromobenzene (Aldrich Gold Label, 99+%), 1,2-dibromobenzene (Aldrich, 98%), 1,3-dibromobenzene (Aldrich, 97%), 1,4-dibromobenzene (Aldrich, 98%), and 1,3,5-tribromobenzene (Fluka Chemika, 98%) were used as received. 1,2,4-Tribromobenzene was recrystallized from absolute ethanol. 1,2,3-Tribromobenzene and 1,2,3,5-tetrabromobenzene were synthesized and purified according to the procedures decribed previously, Chapter 2. The acetonitrile solvent, fresh ChromAR HPLC grade, was used as purchased from Mallinckrodt Chemical as it was found to be pure by GC analysis.

Triethylamine was distilled prior to use. Drying reagent, anhydrous magnesium sulfate powder (Mallinckrodt Analytical reagent AR) was used without further purification. $NaBH_4$, obtained from Aldrich, was kept well sealed at all times, and fresh solutions were prepared just prior to use.

General Procedure for Photolysis:

Samples for photolysis were transferred in duplicate 1.000 mL aliquots to quartz phototubes. The phototubes containing samples to be degassed were then fitted with sliding glass stoppers via a screw-in-nylon adapter. Stoppers were lightly greased with Dow Corning high vacuum grease and two o-rings were used to ensure a good seal. The vacuum line system consists of two rotary pumps and a mercury diffusion pump. Degassing was accomplished by four freeze-pump-thaw cycles to a pressure of at least 5×10^{-5} torr. Samples which were not degassed were simply corked prior to photolysis. All samples were irradiated in a Rayonet merry-go-round reactor (The Southern New England Co.) equipped with up to eight preconditioned (warmed up for at least an hour) 254 nm mercury low pressure arc lamps, and an overhead fan to maintain a constant temperature of 25-26 °C. The phototubes are confined within the rotating merry-go-round surrounded by the lamps. All the tubes are, therefore, equidistant from every lamp reducing errors caused by uneven radial distribution. Upon removal from the reactor, all phototubes were placed in the dark for a minimum of two hours to assure cessation of reaction.

Azoxybenzene Actinometry:[34]

Actinometry is used to determine the incident radiation intensity of the lamps that the sample solutions are exposed to. For this reason, sample solutions and actinometry solutions were irradiated simultaneously within the reactor. Actinometry solutions were prepared by dissolving 8-10 mg of azoxybenzene (Janssen Chimica, 97%, stored in the dark) in 5 mL of 95% ethanol and then transferring 1.000 mL aliquots in triplicate to the phototubes. After photolysis, 0.500 mL was removed from each solution and diluted to 5.00 mL with 5% KOH in 95% ethanol. This same procedure was also carried out on the original non-irradiated solution to serve as a blank. All solutions were placed in the dark for at least two hours and until spectrophotometric analysis could be performed. The product of the intramolecular photorearrangement, 2-hydroxyazobenzene,[35] has a known molar extinction coefficient at 458 nm, ϵ_{458}. The absorbance of the irradiated actinometry solutions against the blank were measured on an HP 8452A Diode Array Spectrophotometer with HP 89531A MS-DOS UV/VIS operating software, or an older model HP 8451A Diode Array Spectrophotometer. The Beer-Lambert law was then used to determine the concentration. Using this, the quantum yield for the reaction (0.017 at 254 nm),[34] and taking the dilution factor into account results in the following incident radiation intensity in moles/minute.

$$I_0^i = \frac{A_{458} V_1 V_3}{V_2 l \varepsilon_{458} \phi_\lambda t}$$

where A is absorbance, V_1 is the volume irradiated, V_2 is the volume of irradiated

solution withdrawn, V_3 is the volume of the flask in which the dilution is performed, l is the pathlength of the cell used to measure the absorbance, ϕ_λ is the quantum yield at the specific wavelength, and t is the time of irradiation. A condition for the validity of an actinometer is that it and the samples must absorb all of the incident radiation[36] by maintaining an absorbance at the wavelength of radiation greater than 2. The concentrations of azoxybenzene used above ensure this, and using measured molar extinction coefficients of **BB**, **124TrBB**, and **1235TBB**, determined using the newer HP diode array spectrophotometer, minimum concentrations of the polybromobenzene compounds were calculated and employed.

Product Analyses:

Photolysis mixtures were analyzed using a Varian 3300 Gas Chromatograph with flame ionization detector (FID) and splitless injection, which was computer interfaced to an HP 35900D A/D Interface Board running real time analysis with the HP 3365 Series II ChemStation software. An Econo-Cap Carbowax (polyethylene glycol) capillary column from Alltech of 30 m × 0.25 mm ID × 0.25 μm film was used in all cases. The injector and detector were maintained at 250 °C and 300 °C, respectively, while the temperature program was varied depending on the photolysis mixture in order to obtain separation of isomers and sufficient elucidation conditions. Standard grade helium in series with Alltechs' Hydro Purge II moisture trap, Oxy-Purge N non-indicating high capacity (500 cc) oxygen trap, and AT-Super Indicating Oxy-Trap (20 cc capacity) was used as the carrier gas. Identification and quantification of photoproducts were determined by

retention times and response factors of standards using octadecane (Aldrich, 97%) as an internal standard. Response factor calibration curves were constructed by injecting several samples of known concentrations and plotting the area response ratio of the compound (X) to internal standard (IS) against the concentration ratio of compound to internal standard.

$$\frac{Area_X}{Area_{IS}} = \frac{[X]m_X}{[IS]}$$

Once the response, m_X, had been determined, the compositions of the photolysis mixtures with unknown concentrations of X, [X], were easily calculated. All concentrations reported are given in moles per liter (M).

Radical Anion Reduction of 1,2,4-Tribromobenzene with Lithium 4-4'-di-*tert*-butylbiphenyl:

A 100 mL, oven dried, three-necked Morton flask was set up and very brisk argon flow (floating stoppers) initiated immediately to provide an inert atmosphere. A heat gun was also used to drive off any remaining moisture in the flask. 1.3334 g of 4-4'-di-*tert*-butylbiphenyl (Aldrich, 99%), dried in a vacuum desiccator over phosphorous pentoxide, was weighed out and transferred into the reaction flask via funnel. Approximately 25 mL of dry tetrahydrofuran solvent was collected from a potassium metal/benzophenone continuous distillation apparatus and then poured into the reaction flask. The flask was then lowered into a room temperature water bath located inside a sonicator and

sonication[37,38,39,40] begun. Two freshly cut pieces, 29.5 mg total, of lithium metal were then added after being previously dipped into toluene to clean off any residual oil. Upon its addition the metal immediately began releasing a dark green color; within 4 min the entire solution turned a deep forest green indicating the formation of the biphenyl radical anion. The bath temperature was then dropped to 0-5 °C by adding ice and NaCl. To maintain this temperature within the sonicator the ice had to be replenished every 10-15 min. After 4½ hrs, 1.2641g of 1,2,4-tribromobenzene and 8.97×10^{-4} mmol of octadecane (internal standard) were added with an isopropyl alcohol/dry ice bath in place. Additional dry ice was added as needed to maintain the low temperature. After 20 min the reaction was quenched with distilled water. Immediately a light colored precipitate/slurry formed along with a separate golden brown organic layer. The organic layer was extracted with pentane and dried over anhydrous magnesium sulfate. Pentane was distilled off using a rotary evaporator and the remaining light yellow solid allowed to air dry. A small amout of the product was dissolved in acetonitrile and analyzed using the same procedure as with the photolysis mixtures. The entire reaction, on the same scale, was conducted again, but this time two reaction flasks were utilized. The receiving flask was a 100 mL, oven-dried, three-necked, round-bottom flask containing a glass-covered magnetic stir bar, also under an inert argon atmosphere, resting in a 24 °C water bath. The biphenyl radical anion solution was prepared as above and then cannulated into the receiving flask of 1,2,4-tribromobenzene, octadecane, and tetrahydrofuran solvent. As the reaction proceeded the solution turned a burnt orange color. Transfer of the entire radical anion solution took approximately 30 min but aliquots were taken at 15, 20, and

25 min intervals as well. As before, the reactions were quenched with distilled water, extracted with pentane, dried, dissolved in acetonitrile, and analyzed.

Acknowledgements

This work has been supported by the National Institute of Environmental Health Sciences and the N. L. Tartar Research Foundation.

References

1. Watanabe, I.; Kashimoto, T.; Tatsukawa, R. *Bull. Environ. Contam. Toxicol.*, **1986**, *36*, 778-784.

2. Bieniek, D.; Bahadir, M.; Korte, F. *Heterocycles*, **1989**, *28*, 719-722.

3. Klusmeier, W.; Vogler, P.; Ohrbach, K.-H.; Weber, H.; Kettrup, A. *J. Anal. App. Pyrolysis*, **1988**, *13*, 277-285.

4. Freeman, P. K.; Jang, J.-S.; Ramnath, N. *J. Org. Chem.*, **1991**, *56*, 6072-6079.

5. Freeman, P. K.; Clapp, G. E.; Stevenson, B. K. *Tetrahedron Letters*, **1991**, *32*, 5705-5708.

6. Freeman, P. K.; Ramnath, N.; Richardson, A. D. *J. Org. Chem.*, **1991**, *56*, 3643-3646.

7. Freedman, B. *Environmental Ecology: The Impacts of Pollution and Other Stresses on Ecosystem Structure and Function*, **1989**, Academic Press, Inc., New York, NY, pp. 147-158.

8. Epling, G. A.; Florio, E. *Tetrahedron Letters*, **1986**, *27*, 675-678.

9. Bunce, N. J.; Gallacher, J. C. *J. Org. Chem.*, **1982**, *47*, 1955-1958.

10. Bunce, N. J. *J. Org. Chem.*, **1982**, *47*, 1948-1955.

11. Davidson, R. S.; Goodin, J. W.; *Tetrahedron Letters*, **1981**, *22*, 163-166.

12. Párkányi, C.; Lee, Y. J. *Tetrahedron Letters*, **1974**, *13*, 1115-1118.

13. Couch, T. L. *Thesis*, **1996**, Oregon State University, Chapter 2.

14. Kavarnos, G. J. *Fundamentals of Photoinduced Electron Transfer*, **1993**, VCH Publishers, Inc., New York, NY, pp. 53-61.

15. Gordon, M.; Ware, W. R. *The Exciplex*, **1975**, Academic Press, Inc., New York, NY, pp. 7.

16. Bunce, N. J.; Ravanal, L. *J. Am. Chem. Soc.*, **1977**, *99*, 4150-4152.

17. Bunce, N. J.; Pilon, P.; Ruzo, L. O.; Sturch, D. J. *J. Org. Chem.*, **1976**, *41*, 3023-3025.

18. Ohashi, M.; Tsujimoto, K.; Seki, K. *J. Chem. Soc. Chem. Commun.*, **1973**, 384.

19. Barltrop, J. A.; Bradbury, D. *J. Am. Chem. Soc.*, **1973**, *95*, 5085-5086.

20. Epling, G. A.; Florio, E. *J. Chem. Soc. Chem. Commun.*, **1986**, *3*, 185-186.

21. Tsujimoto, K.; Tasaka, S.; Ohashi, M. *J. Chem. Soc. Chem. Commun.*, **1975**, 758-759.

22. Carey, F. A.; Sundberg, R. J. *Advanced Organic Chemistry. Part A: Structure and Mechanisms*, 3rd Ed., **1990**, Plenum Press, New York, NY, pp. 186.

23. Barltrop, J. A.; Coyle, J. D. *Excited States in Organic Chemistry*, **1975**, John Wiley & Sons, New York, NY, pp. 101.

24. Caldwell, R. A.; Creed, D.; Ohta, H. *J. Am. Chem. Soc.*, **1975**, *97*, 3246-3247.

25. The fluorescence quantum yield of a 9.75×10^{-7} M 1,2,3,5-tetrabromobenzene solution in ethanol was measured to be 0.94 in Chapter 2 of this thesis.

26. Couch, T. L. *Thesis*, **1996**, Oregon State University, Chapter 2.

27. Bunce, N. J.; Safe, S.; Ruzo, L. O. *J. Chem. Soc. Perkin I*, **1975**, 1607-1610.

28. Safe, S.; Hutzinger, O. *J. Chem. Soc. Chem. Commun.*, **1971**, 446.

29. Safe, S.; Hutzinger, O. *J. Chem. Soc. Perkin I*, **1972**, 686.

30. Freeman, P. K; Hutchinson, L. L. *J. Org. Chem.*, **1980**, *45*, 1924-1930.

31. Freeman, P. K.; Ramnath, N. *J. Org. Chem.*, **1991**, *56*, 3646-3651.

32. Experimentally determined in Chapter 5 of this thesis.

33. Frisch, M. J.; Trucks, G. W.; Schlegel, H. B.; Gill, P. M. W.; Johnson, B. G.; Robb, M. A.; Cheeseman, J. R.; Keith, T. A.; Petersson, G. A.; Montgomery, J. A.; Raghavachari, K.; Al-Laham, M. A.; Zakrzewski, V. G.; Ortiz, J. V.; Foresman, J. B.; Cioslowski, J.; Stefanov, B. B.; Nanayakkara, A.; Challacombe, M.; Peng, C. Y.; Ayala, P. Y.; Chen, W.; Wong, M. W.; Andres, J. L.; Replogle, E. S.; Gomperts, R.; Martin, R. L.; Fox, D. J.; Binkley, J. S.; Defrees, D. J.; Baker, J.; Stewart, J. P.; Head-Gordon, M.; Gonzalez, C.; Pople, J. A. *Gaussian, Inc.*, **1995**, Pittsburgh, PA.

34. Bunce, N. J.; LaMarre, J.; Vaish, S. P. *Photochemistry and Photobiology*, **1984**, *39*, 531-533.

35. Bunce, N. J.; Schoch, J-P.; Zerner, M. C. *J. Am. Chem. Soc.*, **1977**, *99*, 7986-7991.

36. Calvert, J. G.; Pitts, J. N. *Photochemistry*, **1966**, John Wiley & Sons, New York, NY, pp. 781.

37. Karaman, R.; He, G.; Blasko, A.; Bruice, T. *J. Org. Chem.*, **1993**, *58*, 438.

38. Rawson, D.; Meyers, A. I. *Tetrahedron Letters*, **1991**, *32*, 2095.

39. Karaman, R.; Kohlman, D.; Fry, J. *Tetrahedron Letters*, **1990**, *31*, 6155-6158.

40. Karaman R.; Fry, J. *Tetrahedron Letters*, **1989**, *30*, 4935.

Chapter 4

Computational Determination of Intersystem Crossing for Halogenated Aromatic Compounds with Heavy Atoms

Tara Lin Couch and Peter K. Freeman*

Department of Chemistry
Oregon State University
Corvallis, OR 97331

Introduction

When a ground state molecule absorbs a photon it is promoted into a singlet excited state. From this point it may undergo radiative deactivation, non-radiative deactivation, dynamic quenching, or photochemistry. There are two forms of non-radiative decay, internal conversion and intersystem crossing. The former is a vibrational relaxation process which brings the singlet state to another singlet of lower energy. Intersystem crossing is an isoenergetic transition that involves a singlet state crossing over to an upper vibrational level of a triplet state. This process requires a change in multiplicity due to a reorientation of electron spin. The rate of intersystem crossing is determined by a variety of factors including the presence of heavy atoms (heavy atom effect), symmetry requirements, the energy gap between the states involved, and the electronic configurations of those states.[1] The phenomenon of the strongly forbidden singlet to triplet intersystem crossing transition occurs by spin-orbit coupling, SOC. SOC is the coupling of the magnetic moment of the spinning electron with the orbital magnetic field arising from the orbital motion of the charged electron.[2] Heavy atoms affect SOC exponentially due to the Hamiltonian operator, H_{SO}, which itself is proportional to Z^4 where Z is the atomic number.[2] Therefore, when heavy atoms are added to a compound, either internally or externally, H_{SO} and SOC increase and enhanced intersystem crossing should be observed.

Experimental observations attributed to the heavy atom effect are:[3] (i) increased singlet-triplet absorption, (ii) increased non-radiative decay rates from T_1, (iii) decreased phosphorescence lifetimes, (iv) increased phosphorescence quantum yields, and (v)

decreased fluorescence quantum yields. Halogenated naphthalenes are prime examples of these characteristics.[4] Polychlorobenzenes also seem to follow the heavy atom effect by reacting through predominantly triplet intermediates in photochemical reactions.[5] However, the photodebrominations of bromobenzene, 1,2,4-tribromobenzene, and 1,2,3,5-tetrabromobenzene have been shown to proceed through solely singlet excimer intermediates[6] or when an electron donor is present singlet exciplex intermediates.[7] In this study, the absence of a heavy atom effect that these and several other compounds exhibit was investigated utilizing Gaussian *ab initio* computational methods.

Historical Background

Other examples of compounds that contain heavy atoms but which do not exhibit the heavy atom effect have appeared for decades. However, limited attention has been given to these or to their cause. In 1949, McClure[8] observed that triplet lifetimes of halogenated naphthalenes decrease with increasing atomic number, but halogenated benzenes did not follow this trend "quite as well". Triplet lifetimes were reported for *para*-dibromobenzene (0.30 ms), 1,3,5-tribromobenzene (0.74 ms), and 1,2,4,5-tetrabromobenzene (0.55 ms) in EPA at 77°K.

In 1968, Kearvell and Wilkinson determined fluorescence quantum yields for anthracene, 9-bromoanthracene, and 9,10-dibromoanthracene, $\Phi_f = 0.26$, 0.05, and 0.22, respectively. The values do not steadily decrease with bromination as would be expected and instead suggest enhanced SOC in 9-bromoanthracene but not 9,10-dibromoanthracene.[9] Recently Hamanoue et. al. and Soloveichik et. al. have shown that

the photodebromination of 9-bromoanthracene and 9,10-dibromoanthracene by amine proceeds through a diffusion controlled singlet exciplex[10] with no evidence of triplet exciplex formation, indicating limited SOC for both substituted anthracenes.[11]

In the early seventies, Dreeskamp and Zander proposed that the fluorescence of perylene and 3-bromoperylene, among others, are not significantly quenched by alkyl iodides because intersystem crossing is prevented by a wide energy gap between S_1 and the lowest triplet state of the hydrocarbons.[12,13,14] Also notable from this study was the unchanged fluorescence quantum yield of perylene upon bromine substitution, where Φ_f = 0.98 for both perylene and 3-bromoperylene. In 1992, the first *ab initio* computational method was applied to this phenomenon by Caldwell and coworkers. Based on a series of vinyl chlorides, they reported significantly increased SOC for substrates able to access non-planar conformations.[15] Since then Zimmerman has also investigated SOC using computational methods, but not pertaining to heavy atoms.[16] Normal and inverse heavy atom effects have been discussed in terms of SOC by Michl, however, the 2-in-2 model which was used is not applicable to the large aromatic ring systems that will be discussed here.[17]

Results and Discussion

None of the polybromobenzenes that have been studied exhibit the heavy atom effect. Bromobenzene, 1,2,4-tribromobenzene, and 1,2,3,5-tetrabromobenzene undergo photodebromination via singlet intermediates (excimer or exciplex), show no decrease in phosphorescent lifetimes with increasing bromine substitution, have low

phosphorescence quantum yields, and high fluorescence quantum yields.[18] Even in the presence of numerous internal heavy atoms the intersystem crossing transition is not enhanced and in fact shows evidence of being a rather noncompetitive pathway. To investigate why, Gaussian 94[19] *ab initio* configuration interaction singles,[20] CIS, calculations have been conducted on a series of compounds which have known heavy atom effect tendencies. The ground state geometries of all compounds were first optimized at the AM1 semi-empirical level, then expanded to HF/STO-3G theory, and finally to HF/6-31G*. The final geometries were then used to perform the CIS calculations to predict excited singlet and triplet states at the same level of theory.[21]

A triplet state wavefunction produced through the SOC interaction, Ψ_T, is governed by equation 4.1, which illustrates the importance of the Hamiltonian operator, the energy gap between the singlet, E_{Sk}, and triplet states, E_T, involved in the transition, and the wavefunctions of pure singlet and triplet states, Ψ^0_{Sk} and Ψ^0_T, respectively.[22,23]

$$\Psi_T = \psi^0_T + \sum_k \frac{\langle \psi^0_{Sk} | H_{SO} | \psi^0_T \rangle}{E_T - E_{Sk}} \cdot \psi^0_{Sk} \qquad \textbf{(4.1)}$$

Quantum mechanics postulates that the probability density is given by $|\Psi|^2$, therefore the probability of the ISC transition is also dependent on these factors.[24] Normally, when a heavy atom is added to a compound the equation becomes dominated by the Hamiltonian operator, which results in the enhanced SOC triplet state,[25] referred to as the heavy atom effect. However, it is apparent that even when certain compounds possess one or more heavy atoms, SOC is not enhanced and may even be diminished or eliminated. For these

compounds, some other factor must be playing a vital role in the determination of spin-orbit coupling.

From equation 4.1 it is clear that if the energy gap, $\Delta E = E_T - E_{sk}$, becomes too large ($\Delta E > 30$ kcal/mol according to Turro),[26] the second term will approach zero, and no state mixing will occur. Energy levels of the triplets and singlets obtained in this study were, therefore, carefully scrutinized. Intersystem crossing, ISC, generally occurs from the lowest lying excited singlet state, S_1, to the nearest lower lying excited triplet state, T_n. This transition, $S_1 \rightarrow T_n$, will have the smallest available energy gap. In the case of the polybromobenzenes, the energy gaps corresponding to this transition are quite low, as depicted in Table 4.1. Accordingly, ΔE cannot be responsible for the diminished SOC and consequent lack of a heavy atom effect that is experimentally observed.

Another factor contributing to SOC is symmetry. Equation 4.1 describes how the triplet state under SOC is dependent on the wavefunctions of the pure singlet and triplet states which are to mix. If the Hamiltonian operator is symmetric (even) and the wavefunctions of the excited states are orthogonal, their product will be zero.[27] Under these conditions, no mixing takes place and ISC is strictly forbidden. When the wavefunctions are thought of in symmetric terms, orthogonality will result from singlet and triplet wavefunctions of different symmetry. The spatial intergral would be non-zero only if Ψ^0_{Sk} and Ψ^0_T belong to the same irreducible representation of the molecular point group.[28]

Bromobenzene, 1,2,4-tribromobenzene, and 1,2,3,5-tetrabromobenzene CIS calculations result in $S_1 \rightarrow T_n$ transitions that would require a symmetry forbidden

Table 4.1. Intersystem crossing computational study.

Compound	Heavy Atom Effect?	ϕ_{isc}	Transition (state symmetry)	$\Delta E [T_n - S_1]$ (kcal/mol)[A]
Bromobenzene	no	NA	S_1 (B2) → T_5 (B1)	-6.42
			T_4 (B2)	-10.88
			T_3 (A1)	-28.07
			T_2 (B2)	-28.24
			T_1 (A1)	-65.86
1,2,4-Tribromobenzene	no	NA	S_1 (A′) → T_6 (A″)	-2.10
			T_5 (A′)	-9.56
			T_4 (A″)	-11.65
			T_3 (A′)	-26.66
			T_2 (A′)	-26.90
			T_1 (A′)	-63.73
1,2,3,5-Tetrabromobenzene	no	NA**	S_1 (B2) → T_6 (A2)	-7.76
			T_5 (B2)	-9.37
			T_4 (B1)	-13.64
			T_3 (B2)	-26.04
			T_2 (A1)	-26.23
			T_1 (A1)	-62.68
Naphthalene	no	*0.45*[B]	S_1 (B1U) → T_5 (B2U)	-5.79
			T_4 (B1U)	-13.39
			T_3 (B2U)	-23.31
			T_2 (A1)	-29.39
			T_1 (B1U)	-61.27
α-Chloronaphthalene	yes	*0.94*[B]	S_1 (A′) → T_5 (A′)	-4.89
			T_4 (A′)	-12.18
			T_3 (A′)	-22.14
			T_2 (A′)	-28.79
			T_1 (A′)	-60.50
α-Bromonaphthalene	yes	*0.998*[B]	S_1 (A′) → T_5 (A′)	-4.70
			T_4 (A′)	-11.97
			T_3 (A′)	-21.91
			T_2 (A′)	-28.60
			T_1 (A′)	-60.17
Benzene	no*	*0.96*[C]	S_1 (B2U) → T_3 (B2U)	-11.34
			T_2 (B2U)	-28.89
			T_1 (B2U)	-67.29
Chlorobenzene	yes	0.6[D]	S_1 (B2) → T_4 (B2)	-10.81
			T_3 (A1)	-28.21
			T_2 (B2)	-28.51
			T_1 (A1)	-66.11

Table 4.1. Continued.

ortho-Dichlorobenzene	yes	0.4[D]	S_1 (A1) → T_4 (A1) T_3 (B2) T_2 (A1) T_1 (B2)	-10.58 -27.95 -27.97 -65.51
1,2,4-Trichlorobenzene	yes	0.8[D]	S_1 (A′) → T_4 (A′) T_3 (A′) T_2 (A′) T_1 (A′)	-9.34 -27.08 -27.70 -64.52
1,2,4,5-Tetrachlorobenzene	yes	1.0[D]	S_1 (B2U) → T_4 (B2U) T_3 (B1U) T_2 (B2U) T_1 (B1U)	-8.84 -26.43 -27.24 -63.65
Pentachlorobenzene	yes	0.9[D]	S_1 (B2) → T_4 (B2) T_3 (A1) T_2 (B2) T_1 (A1)	-9.18 -26.25 -26.56 -63.13
Biphenyl	no	0.81[E]	S_1 (B3) → T_6 (A) T_5 (B1) T_4 (B2) T_3 (B3) T_2 (A) T_1 (B3)	-18.84 -21.71 -21.94 -23.46 -54.40 -62.53
4-Bromobiphenyl	yes	0.98[F]	S_1 (A) → T_6 (A) T_5 (B) T_4 (B) T_3 (A) T_2 (A) T_1 (A)	-17.36 -19.77 -21.13 -21.87 -52.74 -61.01
Anthracene	no*	*0.74*	S_1 (B1U) → T_4 (B1U) T_3 (B2U) T_2 (B3G) T_1 (B1U)	-6.15 -11.24 -27.00 -55.78
9-Bromoanthracene	yes	*0.95*	S_1 (A1) → T_4 (A1) T_3 (B2) T_2 (B2) T_1 (A1)	-5.32 -9.81 -25.26 -54.57
9,10-Dibromoanthracene	no*	*0.78*	S_1 (B1U) → T_4 (B1U) T_3 (B2U) T_2 (B3G) T_1 (B1U)	-4.49 -8.29 -23.27 -53.45

Table 4.1. Continued.

para-Dibromobenzene	no	NA	S_1 (B2U) → T_6 (B3U)	-1.64
			T_5 (B2G)	-6.32
			T_4 (B2U)	-9.66
			T_3 (B1U)	-27.04
			T_2 (B2U)	-27.55
			T_1 (B1U)	-64.66
1,2,4,5-Tetrabromobenzene	no	NA	S_1 (B2U) → T_7 (B2G)	-0.11
			T_6 (B3U)	-3.91
			T_5 (B2U)	-9.12
			T_4 (B1G)	-11.77
			T_3 (B1U)	-25.88
			T_2 (B2U)	-26.15
			T_1 (B1U)	-62.46

Numbers in italic respresent maximum values obtained from known fluorescence quantum yields, which therefore disregards nonradiative decay at the maximum. Fluorescence quantum yield references are sited.

[A] RCIS 6-31G* theory.

[B] Turro, N. J. *Modern Molecular Photochemistry*, **1978**, The Benjamin / Cummings Publishing Co., Inc., Menlo Park, CA, pp. 192.

[C] Parker, C. A.; Hatchard, C. G. *Chemical Physics*, **1962**, *87*, 664-676.

[D] Bunce, N. J.; Hayes, P. J.; Lemke, M. E. *Can. J. Chem.*, **1983**, *61*, 1103-1104.

[E] Sandros, K. *Acta Chemi Scand.*, **1969**, *23*, 2815.

[F] Freeman, P. K.; Jang, J.-S.; Ramnath, N. *J. Org. Chem.*, **1991**, *56*, 6072-6079.

* Highly triplet reactive.

** Measurement attempted, but unsuccessful (Chapter 2).

conversion from the wavefunction of the singlet state to the wavefunction of the triplet state, Table 4.1. For example, the S_1 state of bromobenzene has B2 symmetry whereas the T_5 state has B1 symmetry. Therefore S_1 cannot directly intersystem cross to the closest lower lying triplet state, T_n, and maintain symmetry. However, there are two still lower lying triplet states of bromobenzene that do have B2 symmetry, the same as that of S_1. The transition from $S_1 \rightarrow T_4$ has a ΔE of 10.88 kcal/mol, and the transition from $S_1 \rightarrow T_2$ has a demanding ΔE of 28.24 kcal/mol. The large energy gap of the latter would make this transition unlikely, but for $S_1 \rightarrow T_4$ the energy gap should not be limiting. Ultimately the triplet state, once attained, must relax down to T_1. This may be accomplished by direct SOC from $S_1 \rightarrow T_1$, or by an $S_1 \rightarrow T_n$ ISC transition followed by internal conversion from $T_n \rightarrow T_1$.[29] If the $S_1 \rightarrow T_4$ bromobenzene transition were to occur, it would necessarily be succeeded by three consecutive internal conversions. Due to the initial non-minimal energy gap and consequent internal conversion process, this transition is less likely. Therefore, it appears that conservation of symmetry must be maintained in the $S_1 \rightarrow T_n$ transition in order for the ISC mechanism to take place.

Halogenation of naphthalene is often given as a prime example of the heavy atom effect. CIS calculations on naphthalene, α-chloronaphthalene, and α-bromonaphthalene show that without substitution ISC is forbidden due to symmetry, but when a halogen is placed on the compound ISC is allowed by conservation of symmetry, Table 4.1. As noted above, the polychlorobenzenes also show evidence of the heavy atom effect. Calculations conducted on this series demonstrate that chlorobenzene, *ortho*-dichlorobenzene, 1,2,4-trichlorobenzene, 1,2,4,5-tetrachlorobenzene, and

pentachlorobenzene can all undergo an $S_1 \rightarrow T_n$ transition while maintaining symmetry within reasonable energy gaps, Table 4.1. Biphenyl, which does not have any heavy atoms and is not triplet reactive, is forbidden from the ISC transition, $S_1 \rightarrow T_6$, because symmetry cannot be conserved. 4-Bromobiphenyl, which has been shown to exhibit the effect,[30] may cross directly to the nearest triplet, T_6, without symmetry differences and only a moderate energy gap of 17.36 kcal/mol.

Since bromine substitution of anthracene has been shown to produce unusual results, calculations on anthracene, 9-bromoanthracene, and 9,10-dibromoanthracene were also conducted. In these anthracene moeities, the non-substituted compound has a reactive triplet, and therefore experiences ISC, as do the substituted anthracenes, even though 9,10-dibromoanthracene does not exhibit heavy atom tendencies. Calculations on these compounds show that in fact, all may undergo ISC within symmetry constraints. Finally, as previously stated, *para*-dibromobenzene and 1,2,4,5-tetrabromobenzene also illustrate no heavy atom effect characteristics. This computational study predicts that these polybromobenzenes do not undergo ISC because the ISC transitions, $S_1 \rightarrow T_6$ and $S_1 \rightarrow T_7$, respectively, are not symmetry conserved.

Conclusions

Of the compounds studied, those that are known to exhibit the heavy atom effect demonstrate that each may undergo a symmetry conserved $S_1 \rightarrow T_n$ transition with a reasonable energy gap. Compounds which do not adhere to the heavy atom effect do not have this option. For these compounds, even though it may be energetically possible, the

$S_1 \rightarrow T_n$ transition is a symmetry forbidden process. It is therefore concluded that conservation of symmetry must be maintained in the $S_1 \rightarrow T_n$ transition in order to induce intersystem crossing, and that energy gap restraints and the presence of heavy atoms are only secondary to this requirement. Furthermore, *ab initio* CIS computational methods may be used to predict the likelihood of efficient intersystem crossing and consequent triplet reactivity.

Acknowledgements

This work has been supported by the National Institute of Environmental Health Sciences and the N. L. Tartar Research Foundation.

References

1. Turro, N. J. *Modern Molecular Photochemistry*, **1978**, The Benjamin / Cummings Publishing Company, Inc., Menlo Park, CA, pp. 185.

2. Barltrop, J. A.; Coyle, J. D. *Excited States in Organic Chemistry*, **1975**, John Wiley & Sons, Ltd., Great Britain, pp. 21.

3. Kearvell, A.; Wilkinson, F. *Molecular Crystals*, **1968**, *4*, 69-81.

4. Turro, N. J. *Modern Molecular Photochemistry*, **1978**, The Benjamin / Cummings Publishing Company, Inc., Menlo Park, CA, pp. 192.

5. Bunce, N. J.; Hayes, P. J.; Lemke, M. E. *Can. J. Chem.*, **1983**, *61*, 1103-1104.

6. Couch, T. L. *Thesis*, **1996**, Oregon State University, Chapter 2.

7. Couch, T. L. *Thesis*, **1996**, Oregon State University, Chapter 3.

8. McClure, D. S. *J. Chem. Phys.*, **1949**, *17*, 905-913.

9. Kearvell, A.; Wilkinson, F. *Molecular Crystals*, **1968**, *4*, 69-81.

10. Hamanoue, K.; Nakayama, T.; Ikenaga, K.; Ibuki, K.; Otani, A. *J. Photochem. Photobiol. A: Chem.*, **1993**, *69*, 305-311.

11. Soloveichik, O. M.; Ivanov, V. L.; Kuz'min, M. G. *High Energy Chem.*, **1989**, *23*, 281.

12. Dreeskamp, H.; Zander, M. *Z. Naturforsch.*, **1973**, *28a*, 1743-1744.

13. Zander, M. *Z. Anal. Chem.*, **1973**, *263*, 19-23.

14. Dreeskamp, H.; Koch, E.; Zander, M. *Chem. Phys. Letters*, **1975**, *31*, 251.

15. Caldwell, R. A.; Jacobs, L. D.; Furlani, T. R.; Nalley, E. A.; Laboy, J. *J. Am. Chem. Soc.*, **1992**, *114*, 1623-1625.

16. Zimmerman, H. E.; Kutateladze, A. G. *J. Am. Chem. Soc.*, **1996**, *118*, 249-250.

17. Michl, J. *J. Am. Chem. Soc.*, **1996**, *118*, 3568-3579.

18. Couch, T. L. *Thesis*, **1996**, Oregon State University, Chapter 2.

19. Frisch, M. J.; Trucks, G. W.; Schlegel, H. B.; Gill, P. M. W.; Johnson, B. G.; Robb, M. A.; Cheeseman, J. R.; Keith, T. A.; Petersson, G. A.; Montgomery, J. A.; Raghavachari, K.; Al-Laham, M. A.; Zakrzewski, V. G.; Ortiz, J. V.; Foresman, J. B.; Ciosłowski, J.; Stefanov, B. B.; Nanayakkara, A.; Challacombe, M.; Peng, C. Y.; Ayala, P. Y.; Chen, W.; Wong, M. W.; Andres, J. L.; Replogle, E. S.; Gomperts, R.; Martin, R. L.; Fox, D. J.; Binkley, J. S.; Defrees, D. J.; Baker, J.; Stewart, J. P.; Head-Gordon, M.; Gonzalez, C.; Pople, J. A. *Gaussian, Inc.*, **1995**, Pittsburgh, PA.

20. Foresman, J. B.; Head-Gordon, M.; Pople, J. A.; Frisch, M. J. *J. Phys. Chem.*, **1992**, *96*, 135-149.

21. Hadad, C. M.; Foresman, J. B., Wiberg, K. B. *J. Phys. Chem.*, **1993**, *97*, 4293-4312.

22. Barltrop, J. A.; Coyle, J. D. *Excited States in Organic Chemistry*, **1975**, John Wiley & Sons, Ltd., Great Britain, pp. 22.

23. Gilbert, A.; Baggott, J. *Essentials of Molecular Photochemistry*, **1991**, Blackwell Scientific Publications, Boston, MA, pp. 41-42.

24. Levine, I. N. *Quantum Chemistry*, 4th Ed., **1991**, Prentice-Hall, Inc., Englewood Cliffs, NJ, pp. 14-16.

25. Gilbert, A.; Baggott, J. *Essentials of Molecular Photochemistry*, **1991**, Blackwell Scientific Publications, Boston, MA, pp. 32.

26. Turro, N. J. *Modern Molecular Photochemistry*, **1978**, The Benjamin / Cummings Publishing Company, Inc., Menlo Park, CA, pp. 186-187.

27. For an opposing view, which presumes that the Hamiltonian operator is antisymmetric see the text of McGlynn et al. McGlynn, S. P.; Azumi, T.; Kinoshita, M. *Molecular Spectroscopy of the Triplet State*, **1969**, Prentice-Hall, Inc., Englewood Cliffs, NJ, pp. 201.

28. Cotton, F. A. *Chemical Applications of Group Theory*, 3rd Ed., **1990**, John Wiley & Sons, Inc., New York, NY, pp. 110.

29. Turro, N. J. *Modern Molecular Photochemistry*, **1978**, The Benjamin / Cummings Publishing Company, Inc., Menlo Park, CA, pp. 185.

30. Freeman, P. K.; Jang, J-S.; Ramnath, N. *J. Org Chem.*, **1991**, *56*, 6072-6079.

Chapter 5

Mass Spectroscopic Analyses of Polybromobenzene Fragmentations

Tara Lin Couch, Peter K. Freeman*, and Max L. Deinzer

Departments of Chemistry and Agricultural Chemistry
Oregon State University
Corvallis, OR 97331

Introduction

The photodebromination of polybromoarenes is currently an area of active research. Polybromoarenes are used in a variety of industrial processes, but, are quite toxic and persistent.[1,2,3] Their photodegradation, which involves consecutive photodebrominations, has been proposed as an alternative to high temperature incineration[4] and the mechanism of the photolytic removal of bromine substituents from polybromobenzenes has been studied.[5] In the latter, it was found that the addition of electron donors enhance photolability while inducing a singlet exciplex product determining intermediate, which creates a charge separated aryl radical anion and donor radical cation, with triethylamine, or donor radical, with sodium borohydride. In this study, negative chemical ionization mass spectrometry (NCIMS) is used to generate polybromobenzene radical anions and then determine their corresponding fragmentation pathways.[6]

Results and Discussion

NCIMS is a soft ionization technique that provides structural and fragmentation information due to the low energy of the electrons involved. This low energy causes the electron to be captured by a molecule, M, in a process known as associative resonance capture, equation 5.1, that then induces moderate fragmentation of the radical anion of the parent molecule.[7] This technique is very well suited for halogenated ring systems

$$M + e^- \rightarrow M^{-\cdot} \qquad \textbf{(5.1)}$$

because of their high electron affinity which enables them to stabilize the negative charge. A buffer gas, in this case methane, is used to aid in this stabilization. This method is also very sensitive because only negative ions are detected. For a molecule such as a polybromobenzene, this means that spectra should consist of only a parent radical anion, bromide ion, and aryl carbanion. The natural abundance of the bromine isotopes,[8] 50.69% ^{79}Br and 49.31% ^{81}Br, create a distinct isotopic pattern which easily identifies the number of bromine atoms present and when coupled with the mass to charge ratio, m/z, provides a simple identification of the polybromobenzene compounds.

Mode of Fragmentation:

When the electron is captured to create a parent ion, the following step involves either the loss of bromide ion, k_1, or bromine atom, k_2, as depicted in Scheme 5.1. The sum of the rate terms, Σk_{inst}, is the loss of bromide ion or carbanion due to instrumental parameters. Assuming steady state concentrations of the bromide ion and the carbanion, a kinetic relationship between the two can be formulated, equation 5.2.

$$\frac{[Br^-]}{[Carbanion]} = \frac{k_1}{k_2} \qquad \textbf{(5.2)}$$

The amount of each ion is proportional to the total isotopic pattern intensities, and thus, NCIMS can be used to determine the relative rate of bromide ion bond fission to bromine atom bond fission.

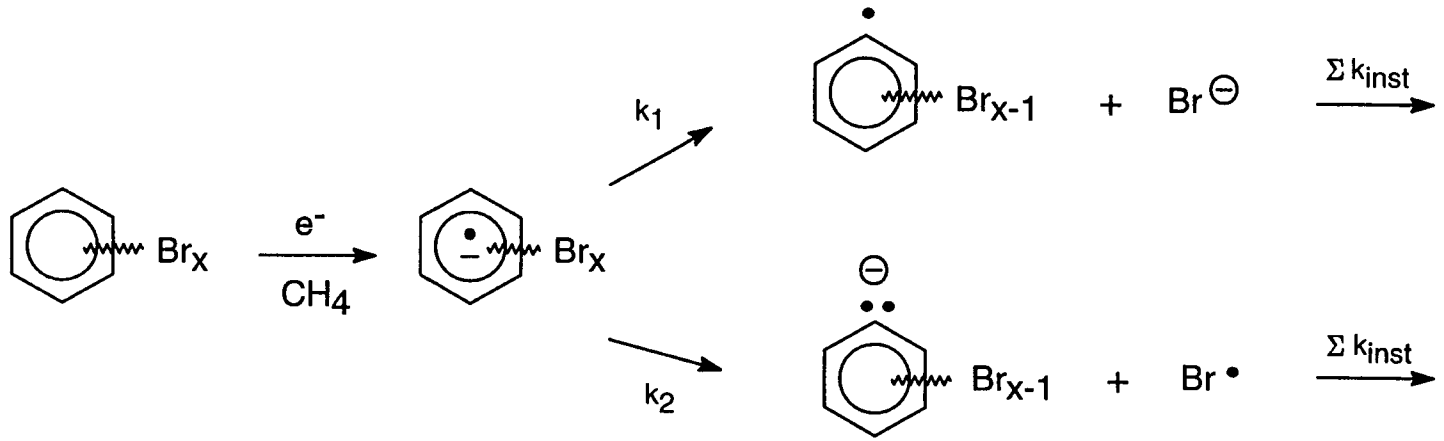

Scheme 5.1. Possible polybromobenzene fragmentations by NCIMS.

The Hammett equation is used to investigate how the particular bromine substituent pattern affects this ratio.[9] The loss of bromide ion from the polybromobenzene, k_1, is referenced to its loss from bromobenzene, k^0_1, in equation 5.3, and bromine atom fission from the polybromobenzene, k_2, is referenced to the same fission in bromobenzene, k^0_2, in equation 5.4.

$$\log(\frac{k_1}{k_1^0}) = \rho_1 \Sigma\sigma \qquad \textbf{(5.3)}$$

$$\log(\frac{k_2}{k_2^0}) = \rho_2 \Sigma\sigma \qquad \textbf{(5.4)}$$

The modes of fission are then related by subtracting equation 5.4 from equation 5.3. This results in equation 5.5 where $\Delta\rho = \rho_1 - \rho_2$, which reflects the sensitivity of the reactions to substituent effects.

$$\log(\frac{k_1}{k_2}) = \Delta\rho \Sigma\sigma + \log(\frac{k_1^0}{k_2^0}) \qquad \textbf{(5.5)}$$

This analysis implies that a single ground state radical anion is generated. However, due to the distribution of electron energies within the mass spectrometer, it is likely that different excited states may be responsible for the fragmentation process. Even though these may arise from separate intermediates, the fragmentation options are still the same: cleavage to produce an aryl radical and bromide ion or cleavage to produce an aryl carbanion and bromine atom. The substituent constant, $\Sigma\sigma$, of equation 5.5 is a

representation of the location of the bromine substituent relative to bromobenzene (*meta*, *para*, or *ortho*), and is a summation term due to the existence of more than one bromine substituent.[10] It was determined by using the removed bromine as the place of origin, and thus will vary for each isomer. The regiochemical selectivity of the electron transfer mechanism must also be taken into consideration for 1,2,3-tribromobenzene (**123TrBB**), 1,2,4-tribromobenzene (**124TrBB**), 1,2,3,5-tetrabromobenzene (**1235TBB**), and pentabromobenzene (**PBB**). The regiochemistry of the electron transfer mechanisms of **124TrBB** and **1235TBB** have been previously determined.[11] Donor assisted photodebromination and chemical reduction of **124TrBB** resulted in an average of 49.2 ± 0.8% *para*-dibromobenzene (***p*DBB**), 40.8 ± 0.5% *meta*-dibromobenzene (***m*DBB**), and 10.1 ± 0.7% *ortho*-dibromobenzene (***o*DBB**). The photodebromination of **1235TBB** with triethylamine and sodium borohydride produced 58.6 ± 0.8% 1,3,5-tribromobenzene (**135TrBB**), 38.3 ± 0.4% **124TrBB**, and 3.4 ± 0.5% **123TrBB**. The experimental outcome of an electron transfer debromination of **123TrBB** has not been performed. However, based on the results of **1235TBB**, the regiochemistry was predicted to be 60.5% ***m*DBB** to 39.5% ***o*DBB** in accordance with the **135TrBB** : **124TrBB** comparison. The regiochemical outcome of an electron transfer mechanism of **PBB** is also not known and there is no accurate comparison to be made. Therefore all possible bromine removal pathways were assumed to proceed competitively, resulting in 33.3% **1235TBB**, 33.4% 1,2,4,5-tetrabromobenzene (**1245TBB**), and 33.3% 1,2,3,4-tetrabromobenzene (**1234TBB**). With this procedure and substituent values of $\sigma_{meta} = 0.37$,[12] $\sigma_{para} = 0.26$,[12]

and $\sigma_{ortho} = 0.31$,[13] the summation of the substituent constants, $\Sigma\sigma$, for all the polybromobenzenes were determined, Table 5.1.

A Hammett plot is then constructed by plotting the log of the ratio of bromide ion to carbanion (k_1/k_2) against $\Sigma\sigma$. The resulting polybromobenzene graph, Figure 5.1, illustrates a large negative slope,[14] $\Delta\rho$, indicative of reactions which have a substantial difference in sensitivity to substituent effects. Furthermore, the negative sign suggests that electron withdrawing groups favor carbanion formation rather than aryl radical formation. This is consistent with the ability of the more substituted polybromobenzenes to accommodate the negative charge in carbanion formation. Overall the Hammett plot demonstrates that bromide ion fragmentation, k_1, is the dominant form of polybromobenzene radical anion fragmentation.

"Additional Bromine" Process:

As mentioned previously, the NCIMS fragmentation of **124TrBB** should result in spectra with isotopic patterns corresponding to a parent **124TrBB** radical anion, bromide ion, and dibromophenyl carbanion. However, much to our surprise, the fragmentation also produced a pattern consistent with a tetrabromobenzene radical anion. Upon further inspection it was found that ***o*DBB**, ***m*DBB**, ***p*DBB**, and **123TrBB** also exhibited this "additional bromine" process. The fact that the **135TrBB** isomer did not, led us to believe that a steric effect must be encountered in this case.[15] Figures 5.2 and 5.3 illustrate the observed "addition" relative to normal fragmentation for the dibromobenzenes and tribromobenzenes, respectively.

Table 5.1. Determination of summation of sigma values.

Compound	Removal Position	Statistical Workup	Σσ
***o*DBB**	---	100% ($1\sigma_{ortho}$)	0.31
***m*DBB**	---	100% ($1\sigma_{meta}$)	0.37
***p*DBB**	---	100% ($1\sigma_{para}$)	0.26
123TrBB	2	60.5% ($2\sigma_{ortho}$)	
	1 or 3	39.5% ($1\sigma_{ortho} + 1\sigma_{meta}$)	0.64
124TrBB	2	49.2% ($1\sigma_{ortho} + 1\sigma_{meta}$)	
	1	40.8% ($1\sigma_{ortho} + 1\sigma_{para}$)	
	4	10.1% ($1\sigma_{meta} + 1\sigma_{para}$)	0.63
135TrBB	---	100% ($2\sigma_{meta}$)	0.74
1235TBB	2	58.6% ($2\sigma_{ortho} + 1\sigma_{para}$)	
	1 or 3	38.3% ($1\sigma_{ortho} + 2\sigma_{meta}$)	
	5	3.4% ($2\sigma_{meta} + 1\sigma_{para}$)	0.95
1245TBB	---	100% ($1\sigma_{ortho} + 1\sigma_{meta} + 1\sigma_{para}$)	0.94
PBB	3	33.4% ($2\sigma_{ortho} + 2\sigma_{meta}$)	
	2 or 4	33.3% ($2\sigma_{ortho} + 1\sigma_{meta} + 1\sigma_{para}$)	
	1 or 5	33.3% ($1\sigma_{ortho} + 2\sigma_{meta} + 1\sigma_{para}$)	1.31
HBB	---	100% ($2\sigma_{ortho} + 2\sigma_{meta} + 1\sigma_{para}$)	1.62

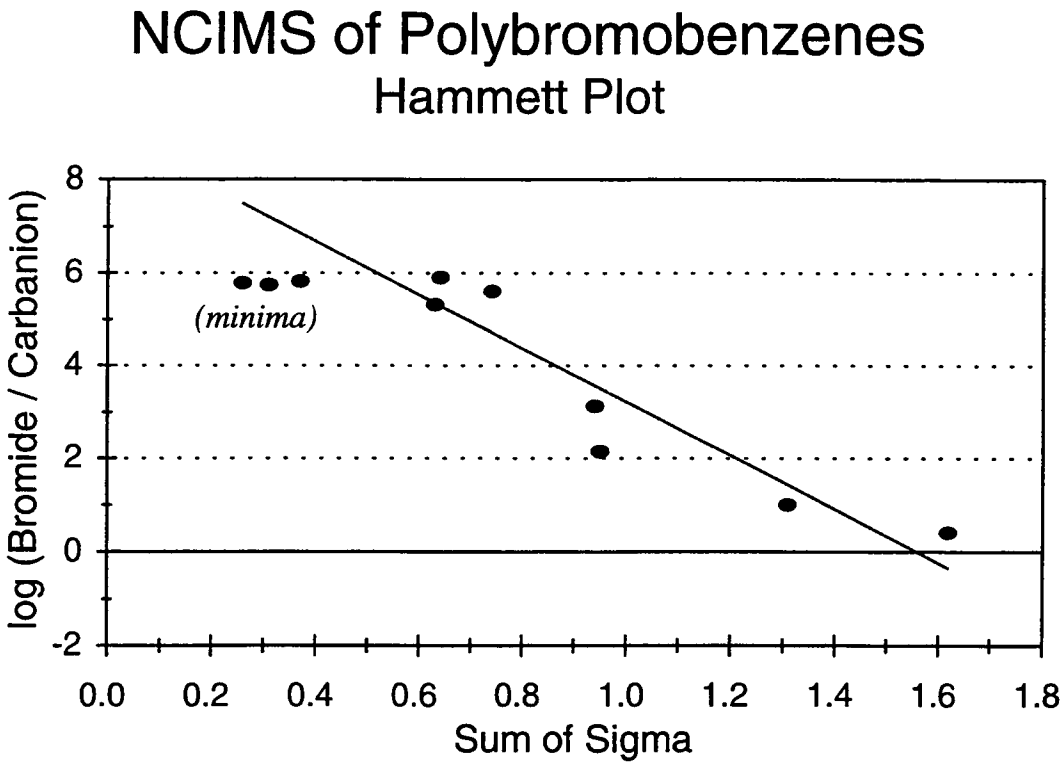

Figure 5.1. Polybromobenzene radical anion fragmentation mode.

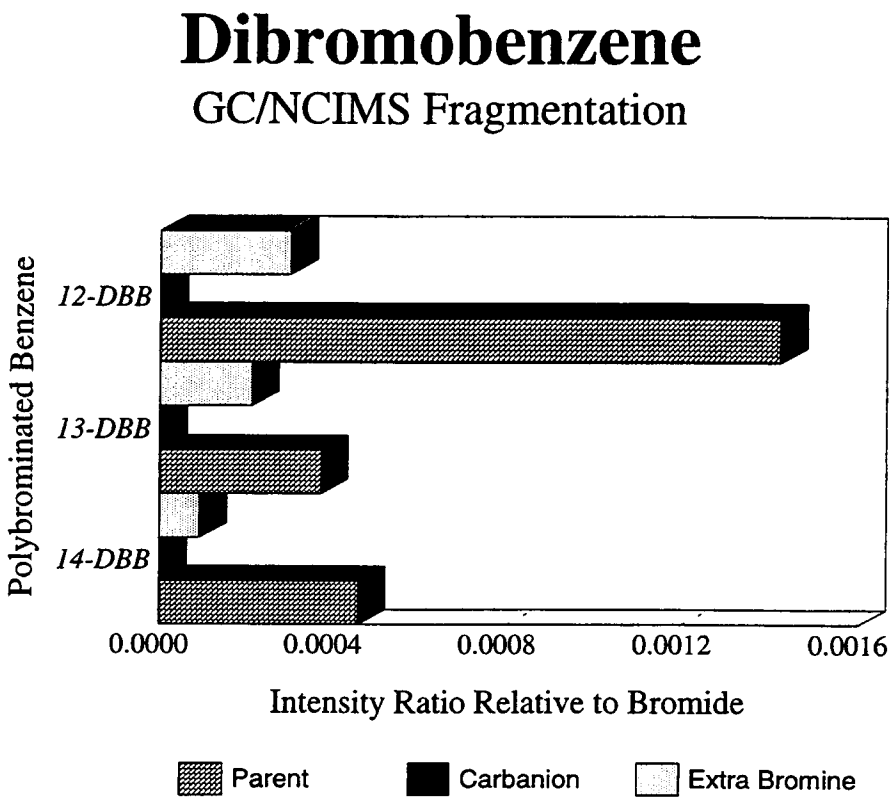

Figure 5.2. GC/NCIMS fragmentation of the dibromobenzene isomers.

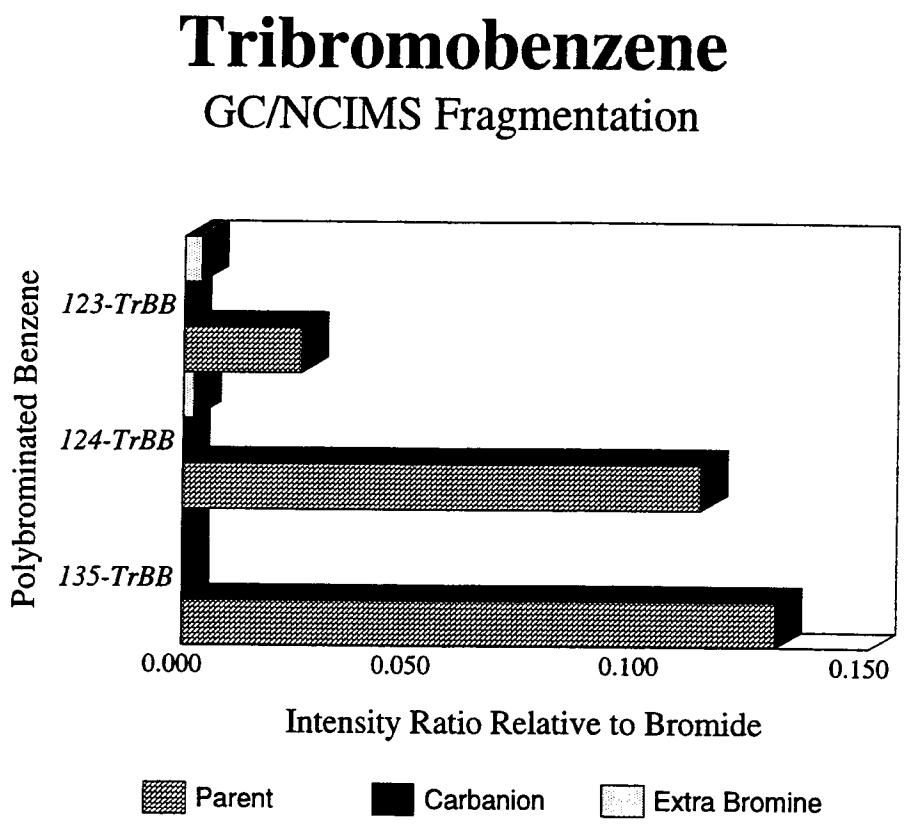

Figure 5.3. GC/NCIMS fragmentation of the tribromobenzene isomers.

Since the dibromobenzenes and the tribromobenzenes react through almost exclusively bromide ion fission, it is concluded that a large amount of bromide ion is present in the source of the spectrometer. If this ion has a sufficient lifetime it may then react with a non-ionized parent molecule according to Scheme 5.2. The formation of bromide ion is then given by equation 5.6.

$$\frac{d[Br^-]}{dt} = k_1[ArBr_x^{-\cdot}] + k_F[ArBr_{x+1}^{-\cdot}] - \Sigma k_{inst}[Br^-] - k_{add}[Br^-][ArBr_x] \quad \textbf{(5.6)}$$

Using the steady state assumption, the concentration of bromide ion may be rewritten as equation 5.7.

$$[Br^-] = \frac{k_1[ArBr_x^{-\cdot}] + k_F[ArBr_{x+1}^{-\cdot}]}{\Sigma k_{inst} + k_{add}[ArBr_x]} \quad \textbf{(5.7)}$$

If no secondary fragmentation occurs, k_F, the equation simplifies, and may be rearranged to produce equation 5.8 which suggests that a ratio of the parent ion, $ArBr_x^{-\cdot}$, to bromide ion should be linear with respect to the neutral parent molecule concentration, $[ArBr_x]$.

$$\frac{[ArBr_x^{-\cdot}]}{[Br^-]} = \frac{\Sigma k_{inst}}{k_1} + \frac{k_{add}[ArBr_x]}{k_1} \quad \textbf{(5.8)}$$

Experiments were conducted in which the concentrations of ***o*DBB**, ***m*DBB**, ***p*DBB**, **123TrBB**, and **124TrBB** were steadily varied over a large dynamic range. The total isotopic pattern intensity of the parent ion over the bromide ion was then plotted against

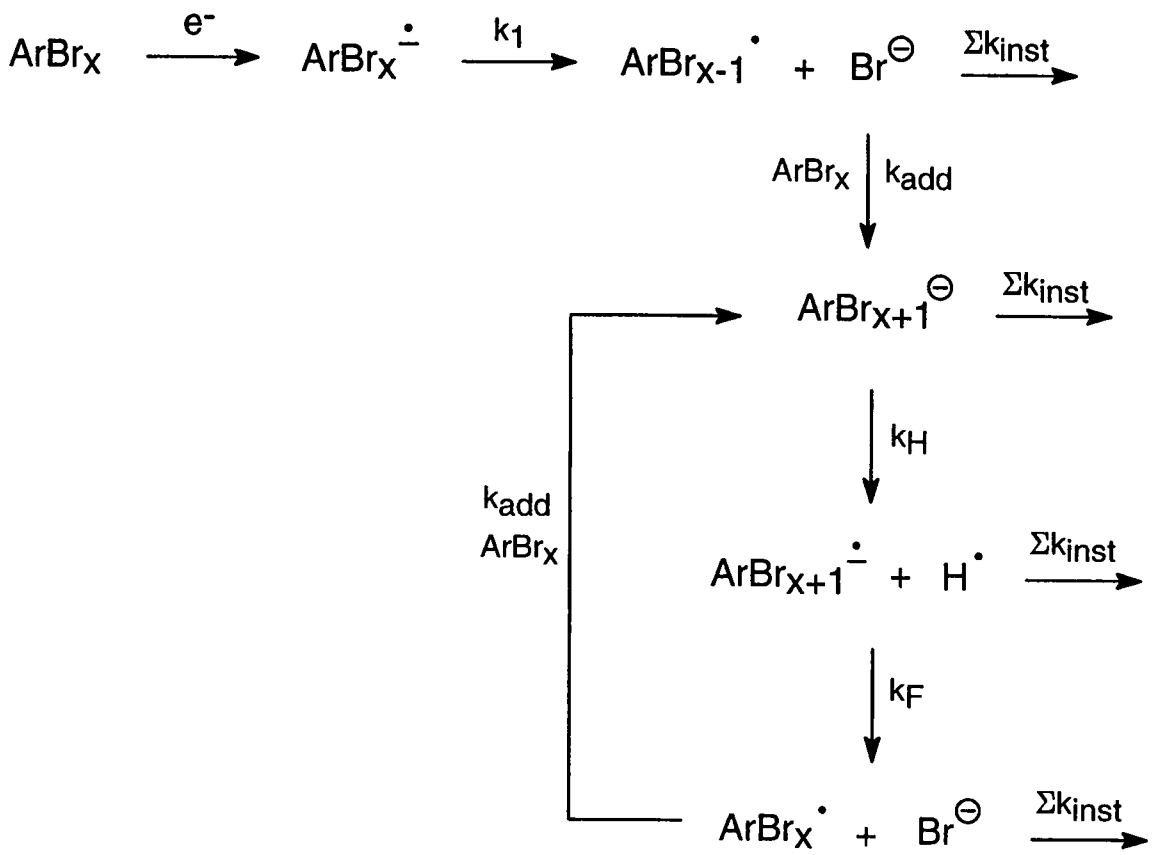

Scheme 5.2. Proposed mechanism for the "additional bromine" process observed for ***o*DBB**, ***m*DBB**, ***p*DBB**, **123TrBB**, and **124TrBB** under NCIMS conditions.

the concentration of the neutral polybromobenzene. Figures 5.4 and 5.5, corresponding to the di- and tribromobenzene series, respectively, depict only a segment of the total concentration range studied, but demonstrate the non-linearity observed over the entire range. These results illustrate that equation 5.8 does not accurately represent the reaction mechanism, and that a secondary fragmentation from the radical anion addition product, $ArBr_{x+1}^{-\cdot}$, probably does occur as in equation 5.7.

In order to supply a secondary bromide ion source, methylene bromide was added as a reagent gas. If equation 5.7 is correct, enhancing the concentration of bromide ion while maintaining a constant concentration of the polybromobenzene of interest, $ArBr_x$ and $ArBr_x^{-\cdot}$, should increase the addition product. Thus, methylene bromide was bled in both prior to and immediately following the introduction of the polybromobenzenes into the mass spectrometer source, with and without methane as a buffer gas. However, this procedure resulted in no addition product and little standard NCIMS structural information. Instead it appears that the presence of the methylene bromide may have increased the energy of the electrons which caused a more electron impact type fragmentation in the spectrometer.

In the specific case of **124TrBB** addition, bromide ion could attack the non-ionized ring at either position five or six, but not three, in accordance with the non-reactivity of **135TrBB**. Substitution at position five would result in a **1245TBB** radical anion while substitution at position six would result in a **1235TBB** radical anion as shown in Scheme 5.3. Of course, from mass spectra it is impossible to tell which tetrabromobenzene radical anion is generated (m/z is the same for isomers).

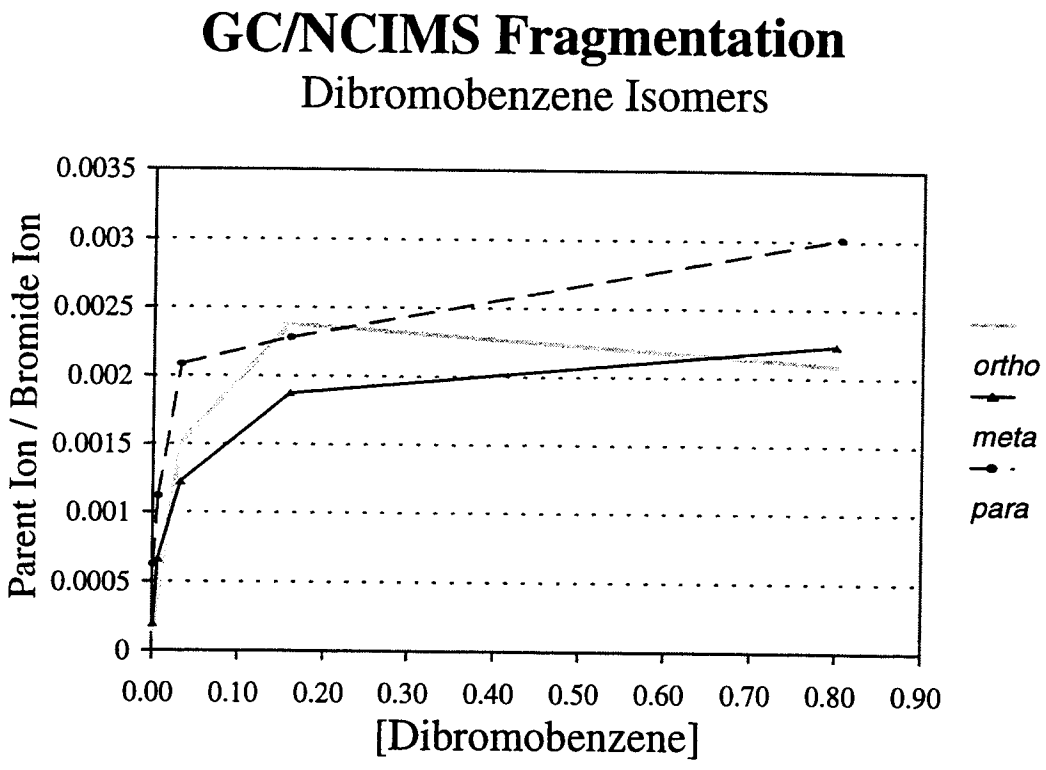

Figure 5.4. Concentration study of the dibromobenzene isomers under GC/NCIMS conditions.

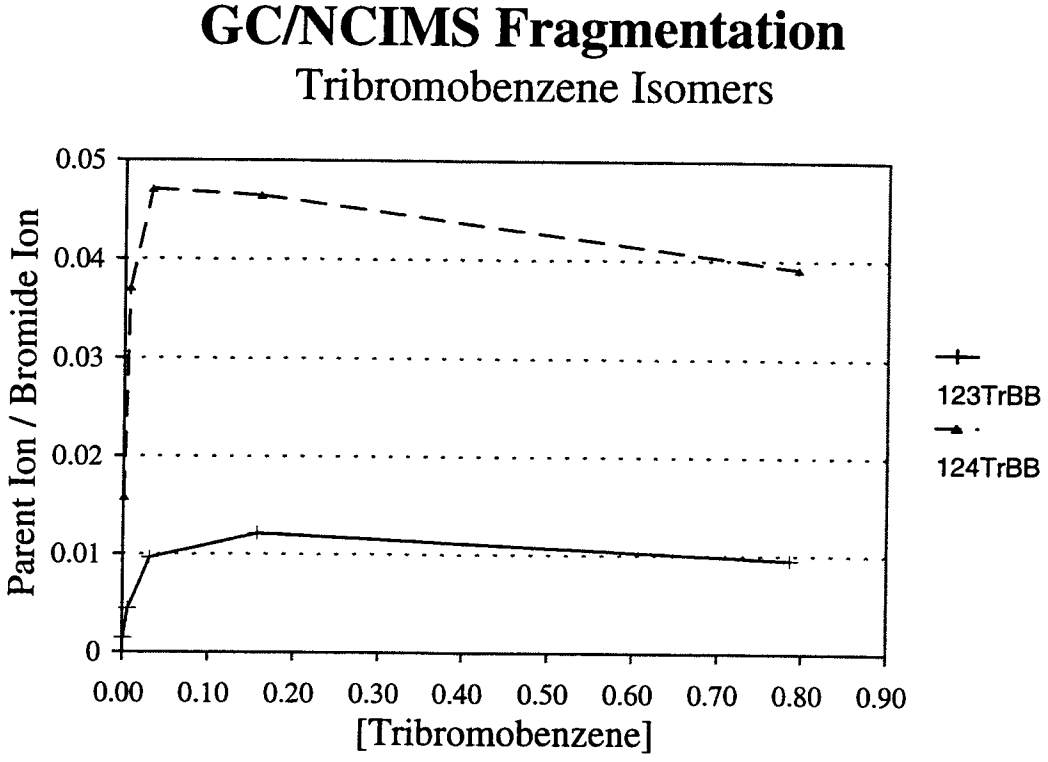

Figure 5.5. Concentration study of the tribromobenzene isomers under GC/NCIMS conditions.

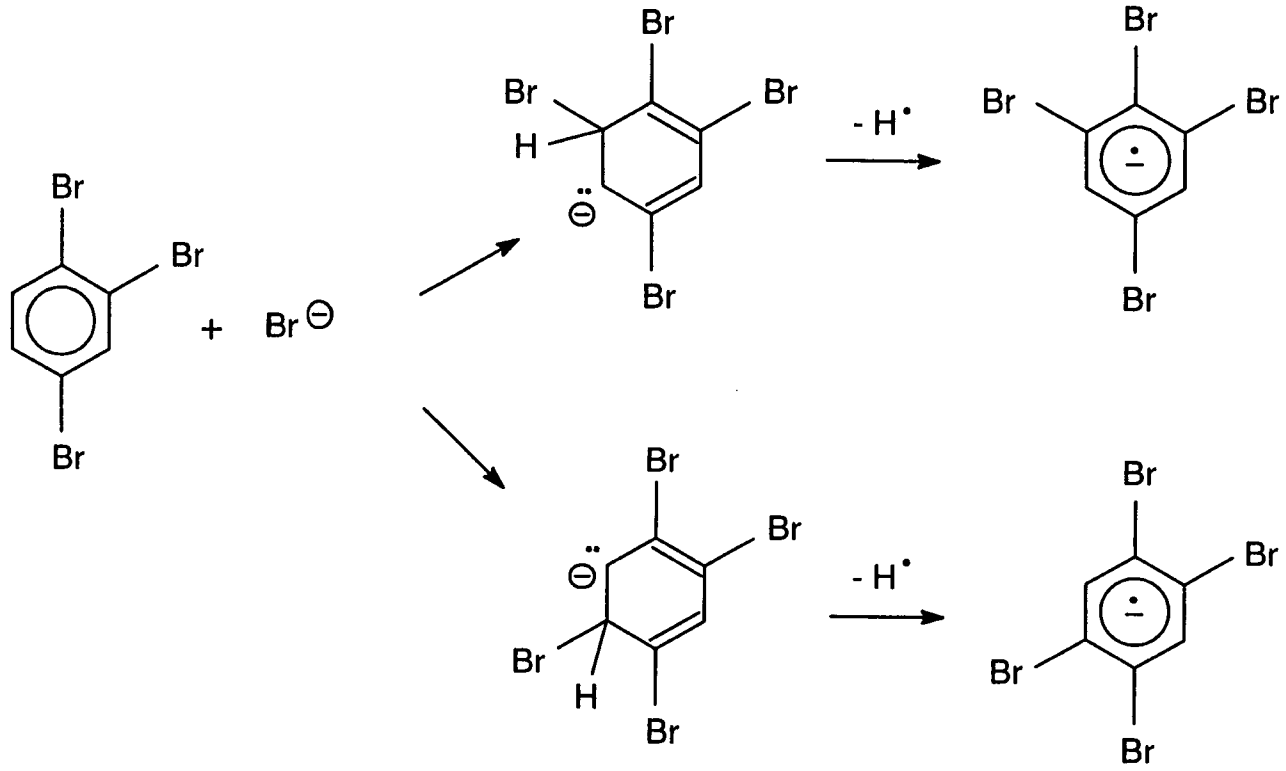

Scheme 5.3. Possible substitutions of bromide ion to 1,2,4-tribromobenzene.

Computational methods have been employed to predict the addition and what isomers are most likely to form. Semi-empirical AM1 and Gaussian 94[16] *ab initio* STO-3G (for tribromobenzenes only) geometry optimizations of the proposed reactants and products have been performed and are illustrated in Figures 5.6 and 5.7 for the dibromobenzene and tribromobenzene isomers, respectively. It was anticipated that the bromide addition to **135TrBB** would require an exceedingly large activation energy which would explain why the addition is not experimentally observed for this particular isomer. However, as depicted in Figure 5.7, this is not the case and in fact bromide addition to **135TrBB** is the most exothermic process. This contradiction is reitterated in the third scenario of bromide addition to ***m*DBB**, depicted in Figure 5.6. Here again the reaction is expected to be prevented due to sterics, but the calculations imply otherwise.

Conclusions

Negative chemical ionization mass spectrometry has been used to simulate the electron transfer reaction of donor assisted polybromobenzene photodebromination. In both cases an aryl radical anion is the precursor to C-Br bond fragmentation. The mode of the fragmentation was also determined by the NCIMS method. It demonstrates that fragmentation from a parent aryl radical anion is dominated by bromide ion bond fission and that fission resulting in a bromine atom, although very minimal, increases upon increased bromine substitution. In the course of this study it was also observed that all three dibromobenzene isomers and two of the tribromobenzene isomers, **123TrBB** and **124TrBB**, are susceptible to bromide ion addition within the mass spectrometer source

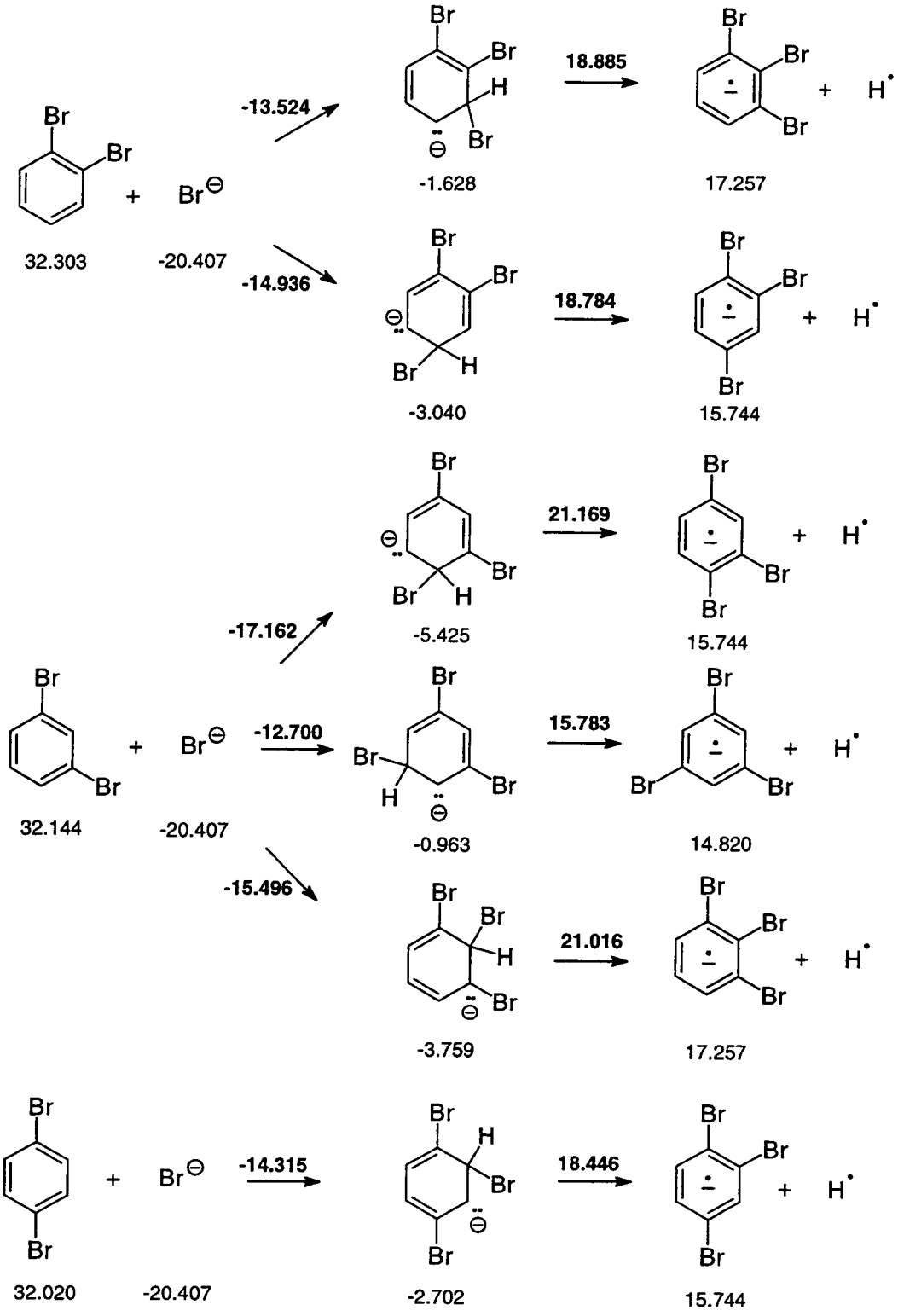

Figure 5.6. Semi-empirical AM1 prediction of the "additional bromine" process for the dibromobenzenes. Heats of formation and activation energies, which are bolded, are displayed in kcal/mol.

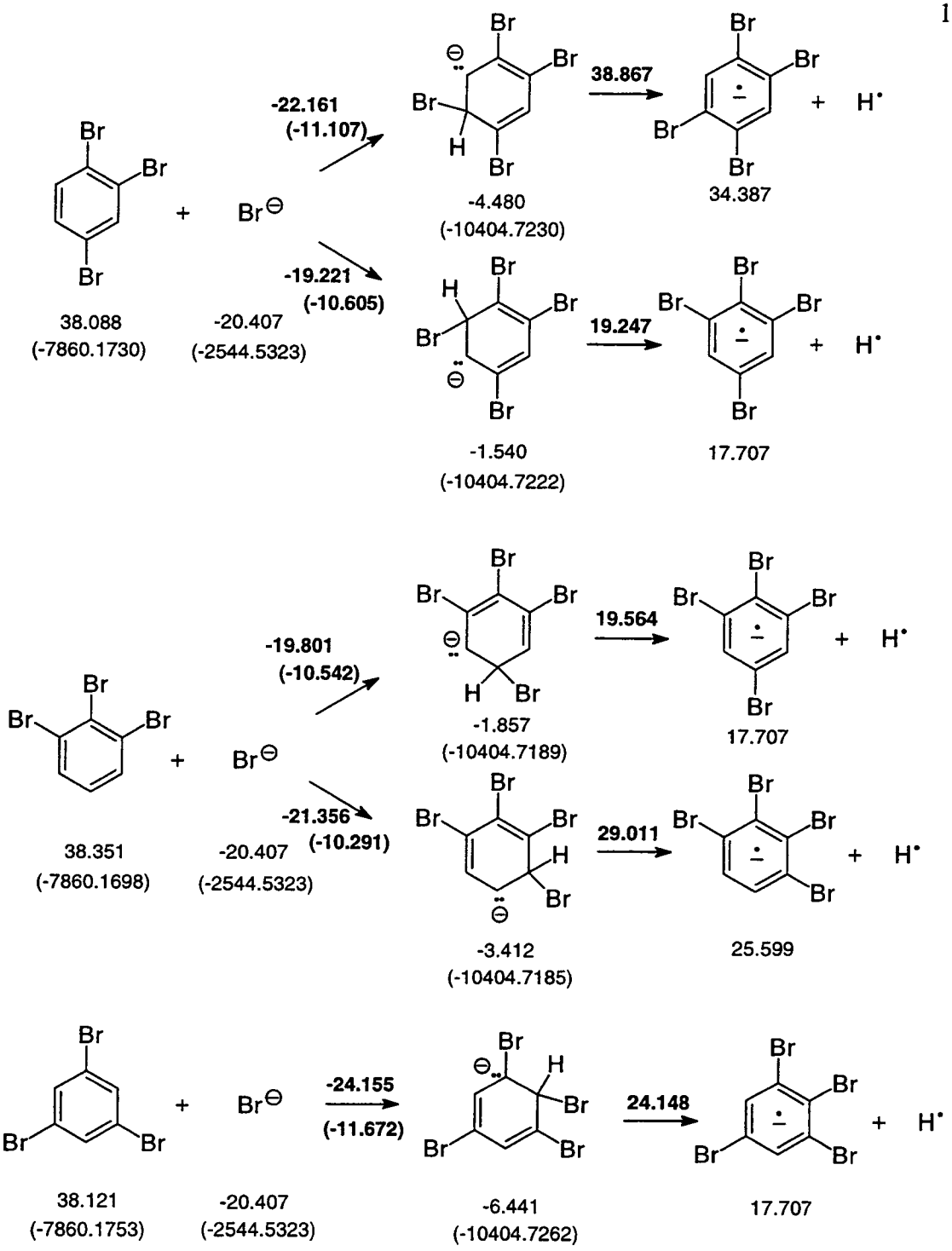

Figure 5.7. Semi-empirical AM1 and Gaussian 94 *ab initio* STO-3G predictions of the "additional bromine" process for the tribromobenzenes. Heats of formation from AM1 calculations are given in kcal/mol and energies from STO-3G calculations, in parentheses, are shown in Hartrees. Activation energies are bolded and displayed in kcal/mol.

under these NCIMS conditions. The process appears to be prevented due to steric factors when existing substituents are located in a *meta* orientation. A mechanism for this process has been proposed.

Unlike NCIMS, an electron monochromator is capable of scanning not only the mass to charge ratio, but also the energies of the negative ions that are formed. In lieu of this, electron monochromator experiments could be utilized to establish how many states of the parent radical anion are generated, and which one(s) are responsible for the corresponding bromide ion and aryl carbanion fragmentation modes. Future studies will be directed at these determinations.

Experimental

Materials:

1,2-Dibromobenzene (Aldrich, 98%), 1,3-dibromobenzene (Aldrich, 97%), 1,4-dibromobenzene (Aldrich, 98%), 1,2,4-tribromobenzene (Aldrich, 98%), 1,3,5-tribromobenzene (Fluka Chemika, 98%), 1,2,4,5-tetrabromobenzene (Aldrich, 97%), and hexabromobenzene (Aldrich, 98%) were used as received, while 1,2,3-Tribromobenzene and 1,2,3,5-tetrabromobenzene were synthesized and purified according to the procedures decribed previously.[17] Acetonitrile, ChromAR HPLC grade, was used as purchased from Mallinckrodt Chemical as it was found to be pure by GC analysis.

NCIMS Studies:

Each polybromobenzene was introduced into a Finnigan 4023 Mass Spectrometer with ionization module set to negative ion chemical ionization mode using methane (Matheson, ultra high purity, 99.97%) as the buffer gas by both probe insertion and a Varian 3400 Gas Chromatographic splitless injection interface. In the latter an Alltech Econo-Cap Carbowax capillary column of 30 m × 0.25 mm ID × 0.25 μm film was employed. Intensities were determined by taking a summation of the entire isotopic pattern of each negatively charged ion.

Acknowledgements

Special thanks to Don Griffin for contributing his time and expertise on the NCIMS system. Financial support for this work was granted by the National Institute of Environmental Health Sciences and the N. L. Tartar Research Foundation.

References

1. Watanabe, I.; Kashimoto, T.; Tatsukawa, R. *Bull. Environ. Contam. Toxicol.*, **1986**, *36*, 778-784.

2. Bieniek, D.; Bahadir, M.; Korte, F. *Heterocycles*, **1989**, *28*, 719-722.

3. Klusmeier, W.; Vogler, P.; Ohrbach, K.-H.; Weber, H.; Kettrup, A. *J. Anal. App. Pyrolysis*, **1988**, *13*, 277-285.

4. Freeman, P. K.; Hatlevig, S. A. *Topics in Current Chemistry*, **1993**, *168*, 48-91.

5. Couch, T. L. *Thesis*, **1996**, Oregon State University.

6. Freeman, P. K.; Ramnath, N. *J. Org. Chem.*, **1988**, *53*, 148-152.

7. Barofsky, D. F.; Deinzer, M. L. *Mass Spectrometry of Organic Molecules (AC 637/ CH 537)*, Fall **1992** Class Notes, Oregon State University.

8. Weast, R. C.; Lide, D. R.; Astle, M. J.; Beyer, W. H. *CRC Handbook of Chemistry and Physics*, 70th Ed., **1990**, CRC Press, Inc., Boca Raton, FL, pp. B-249.

9. Carey, F. A.; Sundberg, R. J. *Advanced Organic Chemistry. Part A: Structure and Mechanisms*, 3rd Ed., **1990**, Plenum Press, New York, NY, pp. 196-209.

10. Hammett, L. P. *Physical Organic Chemistry*, 2nd Ed., **1970**, McGraw-Hill Book Company, San Francisco, CA, pp. 367.

11. Couch, T. L. *Thesis*, **1996**, Oregon State University.

12. March, J. *Advanced Organic Chemistry: Reactions, Mechanisms, and Structure*, 3rd Ed., **1985**, John Wiley & Sons, Inc., New York, NY, pp. 244.

13. Approximated with σ_{ortho} of chlorine since σ_{meta} and σ_{para} values for chlorine and bromine are very similar. Jones, D. A. D.; Smith, G. G. *J. Org. Chem.*, **1964**, *29*, 3531.

14. Log (k_1/k_2) values obtained for the dibromobenzene isomers were not used in the determination of the slope because formation of the aryl carbanion is so small that it falls below the detection limit of the mass detector. Points shown demonstrate only their minima.

15. 1,2,3,4-Tetrabromobenzene was not available for study.

16. Frisch, M. J.; Trucks, G. W.; Schlegel, H. B.; Gill, P. M. W.; Johnson, B. G.; Robb, M. A.; Cheeseman, J. R.; Keith, T. A.; Petersson, G. A.; Montgomery, J. A.; Raghavachari, K.; Al-Laham, M. A.; Zakrzewski, V. G.; Ortiz, J. V.; Foresman, J. B.; Cioslowski, J.; Stefanov, B. B.; Nanayakkara, A.; Challacombe, M.; Peng, C. Y.; Ayala, P. Y.; Chen, W.; Wong, M. W.; Andres, J. L.; Replogle, E. S.; Gomperts, R.; Martin, R. L.; Fox, D. J.; Binkley, J. S.; Defrees, D. J.; Baker, J.; Stewart, J. P.; Head-Gordon, M.; Gonzalez, C.; Pople, J. A. *Gaussian, Inc.*, **1995**, Pittsburgh, PA.

17. Couch, T. L. *Thesis*, **1996**, Oregon State University, Chapter 2.

Chapter 6

Conclusion

The photodegradation of polybrominated aromatic compounds has been proposed as an alternative method of waste disposal. This technique would use the sun as an abundant energy resource and would prevent direct release of these persistent, toxic polybromoarenes into the environment through high temperature incineration. However, prior to any practical application a complete understanding of the photodegradation process must be obtained. This research has been dedicated to developing a detailed mechanistic description of the removal of bromine substituents from a series of brominated benzenes in order to attain this knowledge.

In Chapter 2, the direct photodebrominations of bromobenzene (**BB**), 1,2,4-tribromobenzene (**124TrBB**), and 1,2,3,5-tetrabromobenzene (**1235TBB**) were shown to result in the selective removal of bromine substituents located in *ortho* orientations. Stern-Volmer plots, prepared from both degassed and aerated photolysis experiments, indicated that excimer intermediates are solely responsible for the photodebrominations. Triplet quenching studies with fumaronitrile and isoprene suggest that the excimers are of singlet state origin. Radiative quantum yields also demonstrate the dominant singlet reactivity with high fluorescence quantum yields and low phosphorescence quantum yields. Singlet excimer intermediates were further verified by fluorescence quenching.

The addition of electron donors, triethylamine and sodium borohydride, were found to moderately increase the photolability of the **BB**, **124TrBB**, and **1235TBB** photodebrominations in Chapter 3. These donor assisted photodebrominations were

determined to be controlled by singlet exciplex intermediates rather than singlet excimers for **BB** and **124TrBB**. With **1235TBB** both the triethylamine and the sodium borohydride exciplexes are formed in accordance with a kinetically governed donor assisted photodebromination reaction. Regiochemical comparisons of the excimer and exciplex mediated products of **124TrBB** and **1235TBB** reveal that the intermediates are likely to have suprisingly similar charge distributions. The non-photochemical electron transfer reduction of **124TrBB** by 4,4'-di-*tert*-butylbiphenyl as an organolithium reagent, resulted in a regiochemical outcome consistent with that of the **124TrBB** donor assisted photodebrominations, indicating that the exciplexes are charge separated species.

The fact that these polybromobenzene compounds react through singlet intermediates, either excimer or exciplex, was surprising on the basis of the heavy atom effect. However, the computational method used in Chapter 4 demonstrated that although these compounds do contain numerous heavy atoms, they are prevented from the $S_1 \rightarrow T_n$ intersystem crossing transition by a lack of symmetry conservation. This *ab initio* CIS method was also used to predict the likelihood of efficient intersystem crossing and consequent triplet reactivity in a number of other polyhaloaromatic compounds.

In Chapter 5, negative chemical ionization mass spectrometry, NCIMS, was used to simulate and investigate the electron transfer reaction of donor assisted polybromobenzene photodebromination. In each case an arene radical anion is the precursor to C-Br bond fragmentation. Through NCIMS the mode of the fragmentation was determined to be dominated by bromide ion bond fission. Although the alternative bromine atom fission is very minimal, it was found to increase upon increased bromine

substitution. Based on these results, computational predictions of the regiochemical outcomes of donor assisted **124TrBB** and **1235TBB** photodebrominations were prepared in Chapter 3. From this comparison it was also concluded that the **1235TBB** exciplexes are also charge separated species, consisting in part of an arene radical anion.

To aid in the practical implementation of sunlight induced polybromoarene photodebromination, further experiments could be directed at a search for polybromobenzene ground state dimers and any ground state complexation between the polybromobenzenes and the triethylamine or sodium borohydride electron donors. If these ground state complexes were to exist, excited complexes may have formation rates that exceed the rate of diffusion, as might be expected based on some of the results obtained for this thesis. To complement this, actual measurements of the singlet lifetimes of these polybromobenzenes should also be completed by use of a femtosecond laser which was not accessible to this author. Modeling the singlet excimer and singlet exciplex intermediates may provide valuable information about their similarities and differences.

BIBLIOGRAPHY

Abraham, M. H.; Doherty, R. U.; Kamlet, M. J.; Harris, J. M.; Taft, R. W. *Ibid.*, **1987**, 1097-1101, 913-920.

Approximated with σ_{ortho} of chlorine since σ_{meta} and σ_{para} values for chlorine and bromine are very similar. Jones, D. A. D.; Smith, G. G. *J. Org. Chem.*, **1964**, *29*, 3531.

Barltrop, J. A.; Bradbury, D. *J. Am. Chem. Soc.*, **1973**, *95*, 5085-5086.

Barltrop, J. A.; Coyle, J. D. *Excited States in Organic Chemistry*, **1975**, John Wiley & Sons, Ltd., Great Britain, pp. 21-24, 101.

Barofsky, D. F.; Deinzer, M. L. *Mass Spectrometry of Organic Molecules (AC 637/ CH 537)*, Fall **1992** Class Notes, Oregon State University.

Benson, S. W. *Thermochemical Kinetics*, **1968**, Wiley, New York, NY, pp. 215.

Bieniek, D.; Bahadir, M.; Korte, F. *Heterocycles*, **1989**, *28*, 719-722.

Birks, J. B. *Photophysics of Aromatic Molecules*, **1970**, Wiley-Interscience, London, pp. 496.

Bunce, N. J.; Safe, S.; Ruzo, L. O. *J. Chem. Soc. Perkin I*, **1975**, 1607-1610.

Bunce, N. J.; Pilon, P.; Ruzo, L. O.; Sturch, D. J. *J. Org. Chem.*, **1976**, *41*, 3023-3025.

Bunce, N. J.; Ravanal, L. *J. Am. Chem. Soc.*, **1977**, *99*, 4150-4152.

Bunce, N. J.; Schoch, J-P.; Zerner, M. C. *J. Am. Chem. Soc.*, **1977**, *99*, 7986-7991.

Bunce, N. J. *J. Org. Chem.*, **1982**, *47*, 1948-1955.

Bunce, N. J.; Gallacher, J. C. *J. Org. Chem.*, **1982**, *47*, 1955-1958.

Bunce, N. J.; Hayes, P. J.; Lemke, M. E. *Can. J. Chem.*, **1983**, *61*, 1103-1104.

Bunce, N. J.; LaMarre, J.; Vaish, S. P. *Photochemistry and Photobiology*, **1984**, *39*, 531-533.

Buser, H. R. *Anal. Chem.*, **1986**, *58*, 2913-2919.

Caldwell, R. A.; Creed, D.; Ohta, H. *J. Am. Chem. Soc.*, **1975**, *97*, 3246-3247.

Caldwell, R. A.; Jacobs, L. D.; Furlani, T. R.; Nalley, E. A.; Laboy, J. *J. Am. Chem. Soc.*, **1992**, *114*, 1623-1625.

Calvert, J. G.; Pitts, J. N. *Photochemistry*, **1966**, John Wiley & Sons, New York, NY, pp. 781.

Carey, F. A.; Sundberg, R. J. *Advanced Organic Chemistry. Part A: Structure and Mechanisms*, 3rd Ed., **1990**, Plenum Press, New York, NY, pp. 186, 196-209, 288-289, 732.

Casey, M.; Leonard, J.; Lygo, B.; Proctor, G. *Advanced Practical Organic Chemistry*, **1990**, Chapman and Hall, pp. 166-176.

Clark, W. D. K.; Steel, C. *J. Am. Chem. Soc.*, **1971**, *93*, 6347.

Cotton, F. A. *Chemical Applications of Group Theory*, 3rd Ed., **1990**, John Wiley & Sons, Inc., New York, NY, pp. 110.

Couch, T. L. *Thesis*, **1996**, Oregon State University.

Coxon, J. M.; Halton, B. *Organic Photochemistry*, 2nd Ed., **1987**, Cambridge University Press, New York, NY, pp. 23-26.

Dalton, J. C.; Wriede, P. A.; Turro, N. J. *J. Am. Chem. Soc.*, **1970**, *92*, 1318-1326.

Davidson, R. S.; Goodin, J. W.; *Tetrahedron Letters*, **1981**, *22*, 163-166.

Demas, J. N.; Crosby, G. A. *J. Phys. Chem.*, **1971**, *75*, 991-1024.

Determined from 0-0 band of phosphorescence emission spectra obtained in absolute ethanol at 77°K.

Doyle, M. P.; Seigfried, B.; Dellaria, J. F. *J. Org. Chem.*, **1977**, *42*, 2426-2431.

Dreeskamp, H.; Zander, M. *Z. Naturforsch.*, **1973**, *28a*, 1743-1744.

Dreeskamp, H.; Koch, E.; Zander, M. *Chem. Phys. Letters*, **1975**, *31*, 251.

Epling, G. A.; Florio, E. *J. Chem. Soc. Chem. Commun.*, **1986**, *3*, 185-186.

Epling, G. A.; Florio, E. *Tetrahedron Letters*, **1986**, *27*, 675-678.

Experimentally determined in Chapter 5 of this thesis.

The fluorescence quantum yield of a 9.75×10^{-7} M 1,2,3,5-tetrabromobenzene solution in ethanol was measured to be 0.94 in Chapter 2 of this thesis.

For an opposing view, which presumes that the Hamiltonian operator is antisymmetric see the text of McGlynn et al. McGlynn, S. P.; Azumi, T.; Kinoshita, M. *Molecular Spectroscopy of the Triplet State*, **1969**, Prentice-Hall, Inc., Englewood Cliffs, NJ, pp. 201.

Foresman, J. B.; Head-Gordon, M.; Pople, J. A.; Frisch, M. J. *J. Phys. Chem.*, **1992**, *96*, 135-149.

Freedman, B. *Environmental Ecology: The Impacts of Pollution and Other Stresses on Ecosystem Structure and Function*, **1989**, Academic Press, Inc., New York, NY, pp.147-158.

Freeman, P. K; Hutchinson, L. L. *J. Org. Chem.*, **1980**, *45*, 1924-1930.

Freeman, P. K.; Ramnath, N. *J. Org. Chem.*, **1988**, *53*, 148-152.

Freeman, P. K.; Clapp, G. E.; Stevenson, B. K. *Tetrahedron Letters*, **1991**, *32*, 5705-5708.

Freeman, P. K.; Ramnath, N.; Richardson, A. D. *J. Org. Chem.*, **1991**, *56*, 3643-3646.

Freeman, P. K.; Ramnath, N. *J. Org. Chem.*, **1991**, *56*, 3646-3651.

Freeman, P. K.; Jang, J-S.; Ramnath, N. *J. Org. Chem.*, **1991**, *56*, 6072-6079.

Freeman, P. K.; Hatlevig, S. A. *Topics in Current Chemistry*, **1993**, *168*, 48-91.

Frisch, M. J.; Trucks, G. W.; Schlegel, H. B.; Gill, P. M. W.; Johnson, B. G.; Robb, M. A.; Cheeseman, J. R.; Keith, T. A.; Petersson, G. A.; Montgomery, J. A.; Raghavachari, K.; Al-Laham, M. A.; Zakrzewski, V. G.; Ortiz, J. V.; Foresman, J. B.; Cioslowski, J.; Stefanov, B. B.; Nanayakkara, A.; Challacombe, M.; Peng, C. Y.; Ayala, P. Y.; Chen, W.; Wong, M. W.; Andres, J. L.; Replogle, E. S.; Gomperts, R.; Martin, R. L.; Fox, D. J.; Binkley, J. S.; Defrees, D. J.; Baker, J.; Stewart, J. P.; Head-Gordon, M.; Gonzalez, C.; Pople, J. A. *Gaussian, Inc.*, **1995**, Pittsburgh, PA.

Fry, A. J.; Liu, R. S. H.; Hammond, G. S. *J. Am. Chem. Soc.*, **1966**, *88*, 4781-4782.

Gilbert, A.; Baggott, J. *Essentials of Molecular Photochemistry*, **1991**, Blackwell Scientific Publications, Boston, MA, pp. 32, 41-42.

Gordon, M.; Ware, W. R. *The Exciplex*, **1975**, Academic Press, Inc., New York, NY, pp. 7.

Hadad, C. M.; Foresman, J. B., Wiberg, K. B. *J. Phys. Chem.*, **1993**, *97*, 4293-4312.

Hamanoue, K.; Nakayama, T.; Ikenaga, K.; Ibuki, K.; Otani, A. *J. Photochem. Photobiol. A: Chem.*, **1993**, *69*, 305-311.

Hammett, L. P. *Physical Organic Chemistry*, 2nd Ed., **1970**, McGraw-Hill Book Company, San Francisco, CA, pp. 367.

Hammond, G. S.; Turro, N. J.; Leermakers, P. A. *J. Phys. Chem.*, **1962**, *66*, 1144-1147.

Hammond, G. S.; Liu, R. S. H. *J. Chem. Soc.,Chem. Commun.*, **1963**, *85*, 477-478.

Hammond, G. S.; Saltiel, J.; Lamola, A. A.; Turro, N. J.; Bradshaw, J. S.; Cowan, D. O.; Counsell, R. C.; Vogt, V.; Dalton, C. *J. Am. Chem. Soc.*, **1964**, *86*, 3197-3217.

Ingle, J. D. Jr.; Crouch, S. R. *Spectrochemical Analysis*, **1988**, Prentice-Hall, Inc., Englewood Cliffs, NJ, pp. 339.

Jang, J.-S. *Thesis*, **1990**, Oregon State University.

Karaman R.; Fry, J. *Tetrahedron Letters*, **1989**, *30*, 4935.

Karaman, R.; Kohlman, D.; Fry, J. *Tetrahedron Letters*, **1990**, *31*, 6155-6158.

Karaman, R.; He, G.; Blasko, A.; Bruice, T. *J. Org. Chem.*, **1993**, *58*, 438.

Kavarnos, G. J. *Fundamentals of Photoinduced Electron Transfer*, **1993**, VCH Publishers, Inc., New York, NY, pp. 53-61, 291, 314.

Kearvell, A.; Wilkinson, F. *Molecular Crystals*, **1968**, *4*, 69-81.

Klusmeier, W.; Vogler, P.; Ohrbach, K.-H.; Weber, H.; Kettrup, A. *J. Anal. App. Pyrolysis*, **1988**, *13*, 277-285.

Lamola, A. A.; Hammond, G. S. *J. Chem. Phys.*, **1965**, *43*, 2129-2135.

Levine, I. N. *Quantum Chemistry*, 4th Ed., **1991**, Prentice-Hall, Inc., Englewood Cliffs, NJ, pp. 14-16.

Libes, S. M. *An Introduction to Marine Biogeochemistry*, **1992**, John Wiley & Sons, Inc., New York, NY, pp. 599.

Log (k_1/k_2) values obtained for the dibromobenzene isomers were not used in the determination of the slope because formation of the aryl carbanion is so small that it falls below the detection limit of the mass detector. Points shown demonstrate only their minima.

March, J. *Advanced Organic Chemistry: Reactions, Mechanisms, and Structure*, 3rd Ed., **1985**, John Wiley & Sons, Inc., New York, NY, pp. 244.

Marchetti, A. P.; Kearns, D. R. *J. Am. Chem. Soc.*, **1967**, *89*, 768-777.

McClure, D. S. *J. Chem. Phys.*, **1949**, *17*, 905-913.

McMillen, D. F.; Golden, D. M. *Ann. Rev. Phys. Chem.*, **1982**, *33*, 493.

Michl, J. *J. Am. Chem. Soc.*, **1996**, *118*, 3568-3579.

Morris, J. V.; Mahaney, M. A.; Huber, J. R. *J. Phys. Chem.*, **1976**, *80*, 969-974.

Murov, S. L. *Handbook of Photochemistry*, **1973**, Marcel Dekker, Inc., New York, NY, pp. 4, 59.

Murov, S. L.; Carmichael, I.; Hug, G. L. *Handbook of Photochemistry*, 2nd Ed., **1993**, Marcel Dekker, Inc., New York, NY, pp. 208.

Ohashi, M.; Tsujimoto, K.; Seki, K. *J. Chem. Soc. Chem. Commun.*, **1973**, 384.

Originated from conversations with Dr. Christine Pastorek and Dr. T. Darrah Thomas.

Párkányi, C.; Lee, Y. J. *Tetrahedron Letters*, **1974**, *13*, 1115-1118.

Parker, C. A. *Photoluminescence of Solutions*, **1968**, Elsevier Publishing Co., New York, NY, pp. 275.

Parker, C. A.; Hatchard, C. G. *Chemical Physics*, **1962**, *87*, 664-676.

Performed in the laboratory of Dr. Joseph W. Nibler with Steve Mayer.

Perkin Elmer Model LS 50B Luminescence Spectrometer Owner's Manual, Chapter 8.

Rawson, D.; Meyers, A. I. *Tetrahedron Letters*, **1991**, *32*, 2095.

Safe, S.; Hutzinger, O. *J. Chem. Soc. Chem. Commun.*, **1971**, 446.

Safe, S.; Hutzinger, O. *J. Chem. Soc. Perkin I*, **1972**, 686.

Sandros, K. *Acta Chemi Scand.*, **1969**, *23*, 2815.

Soloveichik, O. M.; Ivanov, V. L.; Kuz'min, M. G. *High Energy Chem.*, **1989**, *23*, 281.

Takemura, T.; Yamada, Y.; Bada, H. *Chem. Phys.*, **1982**, *68*, 171-177.

1,2,3,4-Tetrabromobenzene was not available for study.

Tsujimoto, K.; Tasaka, S.; Ohashi, M. *J. Chem. Soc. Chem. Commun.*, **1975**, 758-759.

Turro, N. J. *Modern Molecular Photochemistry*, **1978**, The Benjamin / Cummings Publishing Company, Inc., Menlo Park, CA, pp. 86-91, 185, 186-187, 192.

Ware, W. R. *J. Phys. Chem.*, **1962**, *66*, 455-458.

Watanabe, I.; Kashimoto, T.; Tatsukawa, R. *Bull. Environ. Contam. Toxicol.*, **1986**, *36*, 778-784.

Watanabe, I.; Tatsukawa, R. *Bull. Environ. Contam. Toxicol.*, **1987**, *39*, 953-959.

Weast, R. C.; Lide, D. R.; Astle, M. J.; Beyer, W. H. *CRC Handbook of Chemistry and Physics*, 70th Ed., **1990**, CRC Press, Inc., Boca Raton, FL, pp. B-249.

Wilkinson, F.; Dubois, J. T. *J. Chem. Phys.*, **1963**, *39*, 377-383.

Zander, M. *Z. Anal. Chem.*, **1973**, *263*, 19-23.

Zimmerman, H. E.; Kutateladze, A. G. *J. Am. Chem. Soc.*, **1996**, *118*, 249-250.

Appendices

Appendix A

Kinetic Analysis of Complete Polybromobenzene Photodebromination Mechanism

According to Scheme 2.1, debrominated product formation is governed by equation A.1, where k_s and k_T are direct homolytic cleavage from the bromoarene (**ArBr**: representing **BB**, **124TrBB**, and **1235TBB**) singlet and triplet excited states, respectively, and k_r and k_{tr} are cleavage from the excimer intermediates, either singlet or triplet in origin.

$$\frac{d[products]}{dt} = k_s[ArBr^{*1}] + k_r[Excimer^{*1}] + k_T[ArBr^{*3}] + k_{tr}[Excimer^{*3}] \quad \textbf{(A.1)}$$

Disregarding k_T due to energetic requirements reduces equation A.1 to equation A.2.

$$\frac{d[products]}{dt} = k_s[ArBr^{*1}] + k_r[Excimer^{*1}] + k_{tr}[Excimer^{*3}] \quad \textbf{(A.2)}$$

Consider Case ①:

The rate of intersystem crossing, k_{isc}, is high which results in negligible singlet cleavage processes, k_s and k_{ex}. Product formation is then limited to cleavage from the triplet excimer intermediate.

$$\frac{d[products]}{dt} = k_{tr}[Excimer^{*3}] \quad \textbf{(A.3)}$$

The rate of formation of triplet excimer is determined by equation A.4.

$$\frac{d[Excimer^{*3}]}{dt} = k_{tex}[ArBr][ArBr^{*3}] - k_{tr}[Excimer^{*3}] - k_{te}[Excimer^{*3}] \quad \textbf{(A.4)}$$

The steady state approximation (SSA) states that a reactive intermediate's formation is equal to its destruction, or d[X]/dt = 0. Assuming the SSA, equation A.4 becomes equation A.5.

$$k_{tex}[ArBr][ArBr^{*3}] = k_{tr}[Excimer^{*3}] + k_{te}[Excimer^{*3}] \quad \textbf{(A.5)}$$

Solving equation A.5 for the concentration of triplet excimer results in equation A.6 which is dependent on the bromoarene triplet excited state.

$$[Excimer^{*3}] = \frac{k_{tex}[ArBr][ArBr^{*3}]}{k_{tr} + k_{te}} \quad \textbf{(A.6)}$$

The excited triplet state's formation rate is represented in equation A.7.

$$\frac{d[ArBr^{*3}]}{dt} = k_{isc}[ArBr^{*1}] - k_{td}[ArBr^{*3}] - k_{tex}[ArBr][ArBr^{*3}] \quad \textbf{(A.7)}$$

Equation A.8 assumes the SSA which when solved for the concentration of triplet state becomes equation A.9.

$$k_{isc}[ArBr^{*1}] = k_{td}[ArBr^{*3}] + k_{tex}[ArBr][ArBr^{*3}] \quad \textbf{(A.8)}$$

$$[ArBr^{*3}] = \frac{k_{isc}[ArBr^{*1}]}{k_{td} + k_{tex}[ArBr]} \quad \textbf{(A.9)}$$

The rate of formation of the singlet excited state is given in equation A.10. It is rearranged to equation A.11 by assuming the SSA and then solved for the singlet state concentration.

$$\frac{d[ArBr^{*1}]}{dt} = I - k_d[ArBr^{*1}] - k_{isc}[ArBr^{*1}] \quad \textbf{(A.10)}$$

$$I = k_d[ArBr^{*1}] + k_{isc}[ArBr^{*1}] \quad \textbf{(A.11)}$$

$$[ArBr^{*1}] = \frac{I}{k_d + k_{isc}} \quad \textbf{(A.12)}$$

Product formation, equation A.3, can then be simplified to equation A.15 by plugging in equation A.6, letting $F = k_{tr} / (k_{tr} + k_{te})$, plugging in equation A.9 and equation A.12, and setting $\phi_{isc} = k_{isc} / (k_d + k_{isc})$.

$$\frac{d[products]}{dt} = k_{tr}[Excimer^{*3}] = \frac{k_{tr}k_{tex}[ArBr][ArBr^{*3}]}{k_{tr} + k_{te}} \qquad \textbf{(A.13)}$$

$$= Fk_{tex}[ArBr][ArBr^{*3}] = \frac{Fk_{tex}[ArBr]k_{isc}[ArBr^{*1}]}{k_{td} + k_{tex}[ArBr]} = \frac{IFk_{tex}k_{isc}[ArBr]}{(k_d + k_{isc})(k_{td} + k_{tex}[ArBr])} \qquad \textbf{(A.14)}$$

$$\frac{d[products]}{dt} = \frac{IF\phi_{isc}k_{tex}[ArBr]}{k_{td} + k_{tex}[ArBr]} \qquad \textbf{(A.15)}$$

By definition the product quantum yield, $\Phi_{products}$ is equal to (d[products]/dt) / I.

$$\Phi_{products} = \frac{F\phi_{isc}k_{tex}[ArBr]}{k_{td} + k_{tex}[ArBr]} \qquad \textbf{(A.16)}$$

The reciprocal of which is the final equation for Case ①. Equation A.17 is the form that is used for data analysis where the calculated $1/\Phi_{prod}$ is plotted against 1/[ArBr].

$$\frac{1}{\Phi_{products}} = \frac{k_{td}}{F\phi_{isc}k_{tex}[ArBr]} + \frac{1}{F\phi_{isc}} \qquad \textbf{(A.17)}$$

Consider Case ②:

The rate of intersystem crossing, k_{isc}, is low resulting in negligible triplet cleavage, k_{tex}. Products are therefore only produced from singlet state processes.

$$\frac{d[products]}{dt} = k_s[ArBr^{*1}] + k_r[Excimer^{*1}] \qquad \textbf{(A.18)}$$

The singlet formation rate, represented in equation A.19, is used to predict the concentration of the excited singlet by employing the SSA.

$$\frac{d[ArBr^{*1}]}{dt} = I - k_d[ArBr^{*1}] - k_{isc}[ArBr^{*1}] - k_S[ArBr^{*1}] - k_{ex}[ArBr][ArBr^{*1}] \quad \textbf{(A.19)}$$

$$I = k_d[ArBr^{*1}] + k_{isc}[ArBr^{*1}] + k_S[ArBr^{*1}] + k_{ex}[ArBr][ArBr^{*1}] \quad \textbf{(A.20)}$$

$$[ArBr^{*1}] = \frac{I}{k_d + k_{isc} + k_S + k_{ex}[ArBr]} \quad \textbf{(A.21)}$$

The singlet excimer formation rate and the SSA are used to determine the concentration of the singlet excimer, shown in equation A.24.

$$\frac{d[Excimer^{*1}]}{dt} = k_{ex}[ArBr][ArBr^{*1}] - k_r[Excimer^{*1}] - k_e[Excimer^{*1}] \quad \textbf{(A.22)}$$

$$k_{ex}[ArBr][ArBr^{*1}] = k_r[Excimer^{*1}] + k_e[Excimer^{*1}] \quad \textbf{(A.23)}$$

$$[Excimer^{*1}] = \frac{k_{ex}[ArBr][ArBr^{*1}]}{k_r + k_e} \quad \textbf{(A.24)}$$

Production of products in Case ② is simplified by substituting equation A.21, equation A.24, and $F_s = k_r / (k_r + k_e)$ into equation A.18.

$$\frac{d[products]}{dt} = \frac{k_s I}{k_d + k_{isc} + k_S + k_{ex}[ArBr]} + \frac{k_r k_{ex}[ArBr] I}{(k_r + k_e)(k_d + k_{isc} + k_S + k_{ex}[ArBr])} \quad \textbf{(A.25)}$$

Then by definition,

$$\frac{d[products]}{dt} = \frac{k_s I + F_s k_{ex}[ArBr]I}{k_d + k_{isc} + k_S + k_{ex}[ArBr]} \quad \textbf{(A.26)}$$

$$\Phi_{products} = \frac{k_s + F_s k_{ex}[ArBr]}{k_d + k_{isc} + k_S + k_{ex}[ArBr]} \quad \textbf{(A.27)}$$

Taking the reciprocal of equation A.27 results in a non-linear form of $1/\Phi_{products}$ versus 1/[ArBr].

$$\frac{1}{\Phi_{products}} = \frac{k_d + k_{isc} + k_S + k_{ex}[ArBr]}{k_s + F_s k_{ex}[ArBr]} \quad \textbf{(A.28)}$$

If homolytic singlet cleavage is dominant, $k_s >> F_S\, k_{ex}\,[ArBr]$ and $(k_d + k_{isc} + k_S) >> k_{ex}[ArBr]$, equation A.28 would be reduced to equation A.29. The latter is independent of 1/[ArBr] and would result in a straight line where $1/\Phi_{products}$ is constant.

$$\frac{1}{\Phi_{products}} = \frac{k_d + k_{isc} + k_S}{k_S} \quad \textbf{(A.29)}$$

If, on the other hand, k_{ex} is dominant, equation A.28 simplifies to equation A.30 that does exhibit linearity between $1/\Phi_{products}$ and 1/[ArBr].

$$\frac{1}{\Phi_{products}} = \frac{k_d + k_{isc} + k_S + k_{ex}[ArBr]}{F_s k_{ex}[ArBr]} = \frac{k_d + k_{isc} + k_S}{F_s k_{ex}[ArBr]} + \frac{1}{F_s} \quad \textbf{(A.30)}$$

Consider Case ③:

The intersystem crossing rate is now intermediate and no simplifications arise. Product formation is therefore governed by equation A.2, repeated as equation A.31.

$$\frac{d[products]}{dt} = k_s[ArBr^{*1}] + k_r[Excimer^{*1}] + k_{tr}[Excimer^{*3}] \quad \textbf{(A.31)}$$

The concentration of triplet excimer is given in equation A.6, the triplet excited state concentration by equation A.9, singlet excited state concentration by equation A.21, and singlet excimer concentration by equation A.21. Together they are combined into equation A.31 to result in the complicated equation A.32 which is somewhat simplifed to equation A.33 by letting $\phi_{isc} = k_{isc} / (k_d + k_{isc} + k_S + k_{ex}[ArBr])$, and recalling that $F_s = k_r / (k_r + k_e)$ and $F = k_{tr} / (k_{tr} + k_{te})$.

$$\frac{d[products]}{dt} = \frac{k_s I}{k_d + k_{isc} + k_S + k_{ex}[ArBr]} + \frac{k_r k_{ex}[ArBr] I}{(k_r + k_e)(k_d + k_{isc} + k_S + k_{ex}[ArBr])}$$

$$+ \frac{k_{tr} k_{tex}[ArBr] k_{isc} I}{(k_{tr} + k_{te})(k_d + k_{isc} + k_S + k_{ex}[ArBr])(k_{td} + k_{tex}[ArBr])} \qquad \textbf{(A.32)}$$

$$\frac{d[products]}{dt} = \frac{k_s I}{k_d + k_{isc} + k_S + k_{ex}[ArBr]} + \frac{F_s k_{ex}[ArBr] I}{k_d + k_{isc} + k_S + k_{ex}[ArBr]} + \frac{F k_{tex}[ArBr] \phi_{isc} I}{k_{td} + k_{tex}[ArBr]}$$

$$= \frac{I(k_s + F_s k_{ex}[ArBr])}{k_d + k_{isc} + k_S + k_{ex}[ArBr]} + \frac{F k_{tex}[ArBr] \phi_{isc} I}{k_{td} + k_{tex}[ArBr]} \qquad \textbf{(A.33)}$$

By definition the product quantum yield for Case ③ is presented in equation A.34.

$$\Phi_{products} = \frac{(k_s + F_s k_{ex}[ArBr])(k_{td} + k_{tex}[ArBr]) + (F k_{tex} \phi_{isc}[ArBr])(k_d + k_{isc} + k_S + k_{ex}[ArBr])}{(k_{td} + k_{tex}[ArBr])(k_d + k_{isc} + k_S + k_{ex}[ArBr])} \qquad \textbf{(A.34)}$$

This is flipped to obtain equation A.35 which is obviously non-linear with respect to 1/[ArBr].

$$\frac{1}{\Phi_{products}} = \frac{(k_{td} + k_{tex}[ArBr])(k_d + k_{isc} + k_S + k_{ex}[ArBr])}{(k_s + F_s k_{ex}[ArBr])(k_{td} + k_{tex}[ArBr]) + (F k_{tex} \phi_{isc}[ArBr])(k_d + k_{isc} + k_S + k_{ex}[ArBr])} \qquad \textbf{(A.35)}$$

Appendix B

Kinetic Analysis of Polybromobenzene Photodebromination with Oxygen as theTriplet Quencher

According to Scheme 2.2, in the presence of a triplet quencher, photodebromination products are formed through either a singlet or a triplet state excimer intermediate, shown kinetically in equation B.1.

$$\frac{d[products]}{dt} = k_r[Excimer^{*1}] + k_{tr}[Excimer^{*3}] \quad \textbf{(B.1)}$$

The triplet excimer formation, governed by equation B.2, may be simplified by invoking the SSA and then solved for the concentration of the triplet excimer.

$$\frac{d[Excimer^{*3}]}{dt} = k_{tex}[ArBr][ArBr^{*3}] - k_{tr}[Excimer^{*3}] - k_{te}[Excimer^{*3}] \quad \textbf{(B.2)}$$

$$k_{tex}[ArBr][ArBr^{*3}] = k_{tr}[Excimer^{*3}] + k_{te}[Excimer^{*3}] \quad \textbf{(B.3)}$$

$$[Excimer^{*3}] = \frac{k_{tex}[ArBr][ArBr^{*3}]}{k_{tr} + k_{te}} \quad \textbf{(B.4)}$$

Since equation B.4 is dependent on the concentration of the triplet excited state, an expression for this concentration must also be determined. The formation of the excited state is given in equation B.5. It may be simplified and rearranged to equation B.7 using the SSA.

$$\frac{d[ArBr^{*3}]}{dt} = k_{isc}[ArBr^{*1}] - k_{td}[ArBr^{*3}] - k_{tex}[ArBr][ArBr^{*3}] - k_q[Q][ArBr^{*3}] \quad \textbf{(B.5)}$$

$$k_{isc}[ArBr^{*1}] = k_{td}[ArBr^{*3}] + k_{tex}[ArBr][ArBr^{*3}] + k_q[Q][ArBr^{*3}] \quad \textbf{(B.6)}$$

$$[ArBr^{*3}] = \frac{k_{isc}[ArBr^{*1}]}{k_{td} + k_{tex}[ArBr] + k_q[Q]} \quad \textbf{(B.7)}$$

Now an expression for the singlet excited state concentration is necessary. Its formation is simplified with the SSA which is then solved for concentration resulting in equation B.10.

$$\frac{d[ArBr^{*1}]}{dt} = I - k_d[ArBr^{*1}] - k_{isc}[ArBr^{*1}] - k_{ex}[ArBr][ArBr^{*1}] \quad \textbf{(B.8)}$$

$$I = k_d[ArBr^{*1}] + k_{isc}[ArBr^{*1}] + k_{ex}[ArBr][ArBr^{*1}] \quad \textbf{(B.9)}$$

$$[ArBr^{*1}] = \frac{I}{k_d + k_{isc} + k_{ex}[ArBr]} \quad \textbf{(B.10)}$$

From equation B.1, product formation is partially determined by the concentration of singlet excimer intermediate, which may be represented as equation B.13. The singlet excited state term of which has already been determined, equation B.10.

$$\frac{d[Excimer^{*1}]}{dt} = k_{ex}[ArBr][ArBr^{*1}] - k_r[Excimer^{*1}] - k_e[Excimer^{*1}] \quad \textbf{(B.11)}$$

$$k_{ex}[ArBr][ArBr^{*1}] = k_r[Excimer^{*1}] + k_e[Excimer^{*1}] \quad \textbf{(B.12)}$$

Assume the SSA:

$$[Excimer^{*1}] = \frac{k_{ex}[ArBr][ArBr^{*1}]}{k_r + k_e} \quad \textbf{(B.13)}$$

The total formation of products, equation B.1, is then reduced to equation B.14 by plugging in equations B.4 and equation B.13.

$$\frac{d[products]}{dt} = \frac{k_r k_{ex}[ArBr][ArBr^{*1}]}{k_r + k_e} + \frac{k_{tr} k_{tex}[ArBr][ArBr^{*3}]}{k_{tr} + k_{te}} \quad \textbf{(B.14)}$$

Further simplification is achieved by plugging in Equations B.7 and Equation B.10 and letting $F = k_{tr} / (k_{tr} + k_{te})$ and $F_s = k_r / (k_r + k_e)$.

$$\frac{d[products]}{dt} = \frac{F_s k_{ex}[ArBr] I}{k_d + k_{isc} + k_{ex}[ArBr]} + \frac{F k_{tex}[ArBr] k_{isc} I}{(k_d + k_{isc} + k_{ex}[ArBr])(k_{td} + k_{tex}[ArBr] + k_q[Q])} \quad \textbf{(B.15)}$$

Finally, let $\phi_{isc} = k_{isc} / (k_d + k_{isc} + k_{ex}[ArBr])$.

$$\frac{d[products]}{dt} = \frac{F_s k_{ex}[ArBr] I}{k_d + k_{isc} + k_{ex}[ArBr]} + \frac{F k_{tex}[ArBr] \phi_{isc} I}{k_{td} + k_{tex}[ArBr] + k_q[Q]} \quad \textbf{(B.16)}$$

By definition, the product quantum yield, $\Phi_{products}$, is the formation of products over the intensity of absorbed radiation. Thus, Equation B.16 may be restated as Equation B.17.

$$\Phi_{products} = \frac{F_s k_{ex}[ArBr]}{k_d + k_{isc} + k_{ex}[ArBr]} + \frac{F k_{tex}[ArBr] \phi_{isc}}{k_{td} + k_{tex}[ArBr] + k_q[Q]} \quad \textbf{(B.17)}$$

Nondegassed Photolysis:

In nondegassed acetonitrile solution, which has an oxygen content of 9.1×10^{-3} M and a diffusion rate, k_{diff}, of 1.9×10^{10} $M^{-1}s^{-1}$,[1] oxygen quenching dominates the triplet reaction pathway. This is due to the extraordinarily large diffusion coefficient of oxygen that results in an oxygen quenching rate, k_q, of 2.4×10^{11} $M^{-1}s^{-1}$ for singlets.[2] Assuming

this value for triplet quenching as well, even when the formation of the triplet excimer is diffusion controlled equation B.18 is true by at least an order of magnitude.

$$k_q[O_2] \; > \; k_{td} + k_{tex}[ArBr] \qquad \textbf{(B.18)}$$

With triplet decay rates, k_{td}, derived from actual triplet lifetimes and the highest aryl bromide concentration employed in photolysis experiments, the right hand side of the inequality was determined for each polybromobenzene, Table B.1. The left hand side is consistently 2.2×10^9. Because of the dominance of oxygen triplet quenching in the photodebromination, equation B.17 reduces to equation B.19.

$$\Phi_{products} = \frac{F_s k_{ex}[ArBr]}{k_d + k_{isc} + k_{ex}[ArBr]} + \frac{F k_{tex}[ArBr]\phi_{isc}}{k_q[Q]} \qquad \textbf{(B.19)}$$

Since the denominator, $k_q[Q]$, of the second term of equation B.19 is much larger than the numerator (F and ϕ_{isc} are both effeciences bounded by 0 and 1), the entire second term will approach zero and may be excluded. The product quantum yield of the photodebromination in nondegassed acetonitrile solutions is therefore, governed by equation B.20.

$$\Phi_{products} = \frac{F_s k_{ex}[ArBr]}{k_d + k_{isc} + k_{ex}[ArBr]} \qquad \textbf{(B.20)}$$

Taking the reciprocal and algebraically simplifying results in equation B.21. A plot of the inverse product quantum yield against the inverse polybromobenzene concentration is then a test to validate the singlet excimer formation and a method of measuring its rate.

$$\frac{1}{\Phi_{products}} = \frac{k_d + k_{isc}}{F_s k_{ex}[ArBr]} + \frac{1}{F_s} \qquad \textbf{(B.21)}$$

Degassed Photolysis:

All photolysis samples are degassed on a vacuum line via the freeze-pump-thaw method to a pressure of at least 5×10^{-5} torr. Assuming ideal gas behavior, this corresponds to an oxygen concentration of 3×10^{-9} M at 25°C. Under these conditions, oxygen quenching is negligible and does not contribute to the triplet reaction pathway because the inequality represented in equation B.22 is valid.

$$k_q[O_2] \ll k_{td} + k_{tex}[ArBr] \qquad \textbf{(B.22)}$$

Here the left hand side, $k_q [O_2]$, will be 720, obviously much less than the right hand side given in Table B.1. Therefore, in degassed photolysis experiments, equation B.17 simplifies to equation B.23, which allows the competition between singlet and triplet excimer intermediates for the production of debromination products.

$$\Phi_{products} = \frac{F_s k_{ex}[ArBr]}{k_d + k_{isc} + k_{ex}[ArBr]} + \frac{F k_{tex}[ArBr]\phi_{isc}}{k_{td} + k_{tex}[ArBr]} \qquad \textbf{(B.23)}$$

Table B.1. Calculations for the validation of the inequalities used to demonstrate the effect of oxygen triplet quenching rates in aerated and degassed photolysis conditions.

Aryl Bromide	k_{td} (s^{-1})	**[ArBr]** (mM)	$k_{td} + k_{tex}$ **[ArBr]**	
			Nondegassed[A]	*Degassed*[B]
BB	8.40×10^4	3.98 to 23.8	4.5×10^8	7.6×10^7
124TrBB	7.25×10^4	1.68 to 10.1	1.9×10^8	3.2×10^7
1235TBB	1.75×10^5	1.28 to 8.23	1.6×10^8	2.5×10^7

[A] Using limiting case of **ArBr**: when concentration is the highest.
[B] Using limiting case of **ArBr**: when concentration is the lowest.

References

1. Murov, S. L.; Carmichael, I.; Hug, G. L. *Handbook of Photochemistry*, 2nd Ed., **1993**, Marcel Dekker, Inc., New York, pp. 208.

2. Ware, W. R. *J. Phys. Chem.*, **1962**, 66, 455-458.

Appendix C

Kinetic Analysis of Chemical Triplet Quenching Mechanism

According to Scheme 2.2 and from Appendix B, the product quantum yield, $\Phi_{products}$, of the photodebromination of polybromobenzenes in the presence of a triplet quencher, Q, is governed by equation C.1.

$$\Phi_{products} = \frac{F_s k_{ex}[ArBr]}{k_d + k_{isc} + k_{ex}[ArBr]} + \frac{F k_{tex}[ArBr]\phi_{isc}}{k_{td} + k_{tex}[ArBr] + k_q[Q]} \qquad \textbf{(C.1)}$$

When the quencher is not present the product quantum yield $\Phi^0_{products}$ simplifies to equation C.2.

$$\Phi^0_{products} = \frac{F_s k_{ex}[ArBr]}{k_d + k_{isc} + k_{ex}[ArBr]} + \frac{F k_{tex}[ArBr]\phi_{isc}}{k_{td} + k_{tex}[ArBr]} \qquad \textbf{(C.2)}$$

Relating $\Phi^0_{products}$ to $\Phi_{products}$ results in the non-linear expression given in equation C.3.

$$\frac{\Phi^0_{products}}{\Phi_{products}} = \frac{\dfrac{F_s k_{ex}[ArBr]}{k_d + k_{isc} + k_{ex}[ArBr]} + \dfrac{F k_{tex}[ArBr]\phi_{isc}}{k_{td} + k_{tex}[ArBr]}}{\dfrac{F_s k_{ex}[ArBr]}{k_d + k_{isc} + k_{ex}[ArBr]} + \dfrac{F k_{tex}[ArBr]\phi_{isc}}{k_{td} + k_{tex}[ArBr] + k_q[Q]}} \qquad \textbf{(C.3)}$$

If products are formed only through a triplet state process, the first term of both the numberator and denominator of equation C.3 drop out, resulting in equation C.4.

$$\frac{\Phi^0_{products}}{\Phi_{products}} = \frac{\dfrac{F k_{tex}[ArBr]\phi_{isc}}{k_{td} + k_{tex}[ArBr]}}{\dfrac{F k_{tex}[ArBr]\phi_{isc}}{k_{td} + k_{tex}[ArBr] + k_q[Q]}} \qquad \textbf{(C.4)}$$

Simplification of equation C.4 to equation C.5 leads to a product quantum yield ratio, $\Phi^0_{products}/\Phi_{products}$, that is linearly dependent on the concentration of quencher.

$$\frac{\Phi^0_{products}}{\Phi_{products}} = \frac{k_{td} + k_{tex}[ArBr] + k_q[Q]}{k_{td} + k_{tex}[ArBr]} = 1 + \frac{k_q[Q]}{k_{td} + k_{tex}[ArBr]} \qquad \textbf{(C.5)}$$

If products are not formed from a triplet state, and instead originate from a singlet excited state, the second term of the numerator and denominator of equation C.3 drop out. Equation C.6 demonstrates that in this situation the product quantum yield ratio is completely independent of the quencher concentration.

$$\frac{\Phi^0_{products}}{\Phi_{products}} = \frac{\dfrac{F_s k_{ex}[ArBr]}{k_d + k_{isc} + k_{ex}[ArBr]}}{\dfrac{F_s k_{ex}[ArBr]}{k_d + k_{isc} + k_{ex}[ArBr]}} = 1 \qquad \textbf{(C.6)}$$

Appendix D

Kinetic Analysis of Complete Exciplex Mechanism

According to Scheme 3.1, the photodebromination of **BB**, **124TrBB**, and **1235TBB** (jointly respresented as ArBr) in the presence of an electron donor and a triplet quencher will result in debrominated products from a singlet exciplex, a singlet excimer, or a triplet exciplex, as shown in equation D.1, where k_{pr}, k_r, and k_{tpr} are the corresponding formation rates.

$$\frac{d[products]}{dt} = k_{pr}[Exciplex^{*1}] + k_r[Excimer^{*1}] + k_{tpr}[Exciplex^{*3}] \quad \textbf{(D.1)}$$

The formation of the singlet exciplex, is written as equation D.2.

$$\frac{d[Exciplex^{*1}]}{dt} = k_{plex}[D][ArBr^{*1}] - k_{pr}[Exciplex^{*1}] - k_{pe}[Exciplex^{*1}] \quad \textbf{(D.2)}$$

Applying the steady state approximation, SSA, results in equation D.3 which is solved for the concentration of the singlet exciplex in equation D.4.

$$k_{plex}[D][ArBr^{*1}] = k_{pr}[Exciplex^{*1}] + k_{pe}[Exciplex^{*1}] \quad \textbf{(D.3)}$$

$$[Exciplex^{*1}] = \frac{k_{plex}[D][ArBr^{*1}]}{k_{pr} + k_{pe}} \quad \textbf{(D.4)}$$

The formation of the singlet excimer is written as equation D.5, which may be rearranged to the concentration of singlet excimer by applying SSA, equation D.7.

$$\frac{d[Excimer^{*1}]}{dt} = k_{ex}[ArBr][ArBr^{*1}] - k_e[Excimer^{*1}] - k_r[Excimer^{*1}] \quad \textbf{(D.5)}$$

$$k_{ex}[ArBr][ArBr^{*1}] = k_e[Excimer^{*1}] + k_r[Excimer^{*1}] \quad \textbf{(D.6)}$$

$$[Excimer^{*1}] = \frac{k_{ex}[ArBr][ArBr^{*1}]}{k_r + k_e} \quad \textbf{(D.7)}$$

Triplet exciplex formation is governed by equation D.8. It may be simplified by the SSA and rearranged to give equation D.10.

$$\frac{d[Exciplex^{*3}]}{dt} = k_{tplex}[D][ArBr^{*3}] - k_{tpe}[Exciplex^{*3}] - k_{tpr}[Exciplex^{*3}] \quad \textbf{(D.8)}$$

$$k_{tplex}[D][ArBr^{*3}] = k_{tpe}[Exciplex^{*3}] + k_{tpr}[Exciplex^{*3}] \quad \textbf{(D.9)}$$

$$[Exciplex^{*3}] = \frac{k_{tplex}[D][ArBr^{*3}]}{k_{tpe} + k_{tpr}} \quad \textbf{(D.10)}$$

Equations must also be derived for the concentration of the excited triplet and the excited singlet, equations D.13 and D.16, respectively, using the same procedure.

$$\frac{d[ArBr^{*3}]}{dt} = k_{isc}[ArBr^{*1}] - k_{td}[ArBr^{*3}] - k_q[Q][ArBr^{*3}] - k_{tplex}[D][ArBr^{*3}] \quad \textbf{(D.11)}$$

$$k_{isc}[ArBr^{*1}] = k_{td}[ArBr^{*3}] + k_q[Q][ArBr^{*3}] + k_{tplex}[D][ArBr^{*3}] \quad \textbf{(D.12)}$$

$$[ArBr^{*3}] = \frac{k_{isc}[ArBr^{*1}]}{k_{td} + k_q[Q] + k_{tplex}[D]} \quad \textbf{(D.13)}$$

And,

$$\frac{d[ArBr^{*1}]}{dt} = I - k_{isc}[ArBr^{*1}] - k_d[ArBr^{*1}] - k_{plex}[D][ArBr^{*1}] - k_{ex}[ArBr][ArBr^{*1}] \quad \textbf{(D.14)}$$

$$I = k_{isc}[ArBr^{*1}] + k_d[ArBr^{*1}] + k_{plex}[D][ArBr^{*1}] + k_{ex}[ArBr][ArBr^{*1}] \quad \textbf{(D.15)}$$

$$[ArBr^{*1}] = \frac{I}{k_{isc} + k_d + k_{plex}[D] + k_{ex}[ArBr]} \quad \textbf{(D.16)}$$

The formation of products, can now be expanded by substituting equations D.4, D.7, and D.10 into equation D.1, giving D.17.

$$\frac{d[products]}{dt} = \frac{k_{pr}k_{plex}[D][ArBr^{*1}]}{k_{pr} + k_{pe}} + \frac{k_r k_{ex}[ArBr][ArBr^{*1}]}{k_r + k_e} + \frac{k_{tpr}k_{tplex}[D][ArBr^{*3}]}{k_{tpr} + k_{tpe}} \quad \textbf{(D.17)}$$

Setting $F_p = k_{pr} / (k_{pr} + k_{pe})$, $F = k_r / (k_r + k_e)$, and $F_{tp} = k_{tpr} / (k_{tpr} + k_{tpe})$ and substituting equations D.13 and D.16 into equation D.17 will further expand it into equation D.18.

$$\frac{d[products]}{dt} = \frac{F_p k_{plex}[D]I}{k_{isc} + k_d + k_{plex}[D] + k_{ex}[ArBr]} + \frac{F k_{ex}[ArBr]I}{k_{isc} + k_d + k_{plex}[D] + k_{ex}[ArBr]}$$

$$+ \frac{F_{tp}k_{isc}k_{tplex}[D]I}{(k_{isc} + k_d + k_{plex}[D] + k_{ex}[ArBr])(k_{td} + k_q[Q] + k_{tplex}[D])} \quad \textbf{(D.18)}$$

Using the definition of product quantum yield, $\Phi_{products}$, as the rate of formation of products over the intensity of absorbed radiation, I, an expression for $\Phi_{products}$ is developed, equation D.19.

$$\Phi_{products} = \frac{F_p k_{plex}[D]}{k_{isc} + k_d + k_{plex}[D] + k_{ex}[ArBr]} + \frac{F k_{ex}[ArBr]}{k_{isc} + k_d + k_{plex}[D] + k_{ex}[ArBr]}$$

$$+ \frac{F_{tp} k_{isc} k_{tplex}[D]}{(k_{isc} + k_d + k_{plex}[D] + k_{ex}[ArBr])(k_{td} + k_q[Q] + k_{tplex}[D])} \quad \textbf{(D.19)}$$

Degassed Photolysis:

If the photodebromination is carried out under degassed conditions, oxygen quenching is negligible and $k_q[Q]$ will fall out. Equation D.19 is then inverted and simplified to give equation D.20.

$$\frac{1}{\Phi_{products}} = \frac{(k_{isc} + k_d + k_{plex}[D] + k_{ex}[ArBr])(k_{td} + k_{tplex}[D])}{(F_p k_{plex}[D] + F k_{ex}[ArBr])(k_{td} + k_{tplex}[D]) + F_{tp} k_{isc} k_{tplex}[D]} \quad \textbf{(D.20)}$$

When there is *no contribution from the singlet excimer*, the second term of equation D.19 drops out, resulting in equation D.21 which demonstrates a competition between singlet and triplet exciplexes.

$$\Phi_{products} = \frac{F_p k_{plex}[D]}{k_{isc} + k_d + k_{plex}[D]} + \frac{F_{tp} k_{isc} k_{tplex}[D]}{(k_{isc} + k_d + k_{plex}[D])(k_{td} + k_{tplex}[D])} \quad \textbf{(D.21)}$$

In Stern-Volmer format, equation D.21 is given as equation D.22.

$$\frac{1}{\Phi_{products}} = \frac{(k_{isc} + k_d + k_{plex}[D])(k_{td} + k_{tplex}[D])}{(F_p k_{plex}[D])(k_{td} + k_{tplex}[D]) + F_{tp} k_{isc} k_{tplex}[D]} \quad \textbf{(D.22)}$$

Modifications of this can be prepared by assuming either a singlet or a triplet exciplex, equations D.23 and D.24, respectively. In the latter, ϕ_{isc} is the efficiency of intersystem crossing.

$$\frac{1}{\Phi_{products}} = \frac{k_{isc} + k_d}{F_p k_{plex}[D]} + \frac{1}{F_p} \quad \textbf{(D.23)}$$

Aerated Photolysis:

If the reaction were done under aerated conditions, no triplet exciplex formation would occur because of the high efficiency of oxygen quenching. Thus, equation D.19 simplifies to equation D.25.

$$\frac{1}{\Phi_{products}} = \frac{k_{td}}{F_{tp}\phi_{isc}k_{tplex}[D]} + \frac{1}{F_{tp}\phi_{isc}} \qquad \textbf{(D.24)}$$

$$\Phi_{products} = \frac{F_p k_{plex}[D] + Fk_{ex}[ArBr]}{k_{isc} + k_d + k_{plex}[D] + k_{ex}[ArBr]} \qquad \textbf{(D.25)}$$

A stern-volmer representation of the aerated, singlet complex competition is given by equation D.26.

$$\frac{1}{\Phi_{products}} = \frac{k_{isc} + k_d + k_{plex}[D] + k_{ex}[ArBr]}{F_p k_{plex}[D] + Fk_{ex}[ArBr]} \qquad \textbf{(D.26)}$$

Equation D.26 can be broken down into two sections, that of the pure exciplex contribution, equation D.27, and that of the pure excimer contribution, equation D.28.

$$\frac{1}{\Phi_{products}} = \frac{k_{isc} + k_d}{F_p k_{plex}[D]} + \frac{1}{F_p} \qquad \textbf{(D.27)}$$

$$\frac{1}{\Phi_{products}} = \frac{k_{isc} + k_d}{Fk_{ex}[ArBr]} + \frac{1}{F} \qquad \textbf{(D.28)}$$

Note, that although equation D.28 is linear if plotted against 1/[ArBr], it is not dependent on 1/[D], and therefore will result in a flat horizontal line when plotted against the latter.